Regulation of meiotic prophase checkpoint function by the AAA+ ATPase Pch2 and the HORMA protein Hop1

Inaugural-Dissertation

zur

Erlangung des Doktorgrades

Dr. rer. nat.

Der Fakultät für Biologie

an der

Universität Duisburg-Essen

vorgelegt von

Vivek B. Raina

aus Jammu, Jammu and Kashmir, Indien

durchgeführt am

Max Planck Institut für molekulare Physiologie

Abteilung für mechanistische Zellbiologie

AG Vader

Oktober 2020

Die der vorliegenden Arbeit zugrunde liegenden Experimente wurden am Max Planck Institut für molekulare Physiologie in der Abteilung für mechanistische Zellbiologie durchgeführt.

1. Gutachter: Prof. Dr. Andrea Musacchio
2. Gutachter: Prof. Dr. Doris Hellerschmied-Jelinek

Vorsitzender des Prüfungsausschusses: Prof. Dr. Dominik Boos

Tag der mündlichen Prüfung: 25th November 2020

DOI: 10.17185/duepublico/73479
URN: urn:nbn:de:hbz:464-20201202-090452-5

I dedicate this doctoral work to

Late Shri Aman Thakur

who as a high school biology teacher instilled me with the sense of curiosity,

and inspired me to pursue a career in basic sciences

Publications

In the context of this doctoral work, the following articles were published:

- **Vivek B. Raina**, Gerben Vader. 2020.
  "Homeostatic control of meiotic prophase checkpoint function by Pch2 and Hop1." *Current Biology doi: 10.1016/j.cub.2020.08.064*

- María Ascensión Villar-Fernández, Richard Cardoso da Silva, Magdalena Firlej, Dongqing Pan, Elisabeth Weir, Annika Sarembe, **Vivek B. Raina**, Tanja Bange, John R. Weir, Gerben Vader. 2020.
  "Biochemical and functional characterization of a meiosis-specific Pch2/ORC AAA+ assembly." *Life Science Alliance doi: 10.26508/lsa.201900630*

Contents

List of Figures

List of Tables

List of Abbreviations

AAA+ ATPase	ATPases associated with diverse cellular activities
APC/C	Anaphase promoting complex/cyclosome
APS	Ammonium persulfate
ATP	Adenosine triphosphate
CDK	Cyclin-dependent kinases
C-Hop1	Closed-Hop1
C-Mad2	Closed-Mad2
CIN	Chromosomal instability
dNTP	Deoxynucleotides
DNA	Deoxyribonucleic acid
DTT	Dithiothreitol
DSB	Double strand break
DAPI	4′,6-diamidino-2-phenylindole
EDTA	Ethylenediaminetetraaceticacid
FITC	Fluorescein isothiocyanate
GFP	Green fluorescent protein
LB	Luria-Bertani
LiAc	Lithium acetate
MCC	Mitotic Checkpoint Complex
O-Mad2	Open-Mad2
PBS	Phosphate-buffered saline
PC	Polycomplex
PCR	Polymerase chain reaction
PEG	Polyethlene glycol
pH3-T11	Phosphorylated Histone H3 at Threonine 11
SAC	Spindle Assembly Checkpoint
SC	Synaptonemal complex
SIC	Synapsis initiation complex
SUMO	Small Uniquitin-like Modifier
TEMED	Tetramethylethylenediamine
TCA	Trichloroacetic acid
U-Hop1	Unbuckled-Hop1

Chapter 1
Introduction

The orderly segregation of chromosomes during cell division ensures faithful inheritance of genetic information. Somatic cells undergo mitotic division, producing genetically identical daughter cells; whereas germ cells undergo meiotic division, creating gametes with half the number of chromosomes as compared to the parental cell. The reduction in the ploidy of cells requires the presence of additional regulatory mechanisms, aberrations which results in erroneous chromosomal segregation. In human females, nearly one-third of all gametes carry an incorrect number of chromosomes (Hassold and Hunt 2001). The incorrect segregation of chromosomes, referred to as aneuploidy, is the major cause of infertility, miscarriages, and other developmental defects. To protect cells from such aneuploidy, surveillance mechanisms, termed checkpoints, are in place to respond to different lesions during both mitosis and meiosis. In contrast to mitosis, where years of intensive research has shaped our understanding about the general basis of surveillance mechanisms, the mechanistic knowledge of surveillance pathways during the meiotic program is not very well understood.

1.1 Budding yeast: a model organism to study meiosis

The budding yeast, *Saccharomyces cerevisiae*, has been extensively used as a model organism to study the cell cycle, chromosome segregation, DNA damage, and recombination. Its ability to rapidly undergo meiosis upon nutrient starvation in a synchronous manner, along with the ease with which genetic manipulations can be carried out makes it an ideal system to study meiotic processes. Furthermore, the availability of a wide range of genetic tools, such as inducible expression systems makes budding yeast a suitable model organism. More importantly, most of the processes are highly conserved from yeast to mammals. With all this in mind, I employed budding yeast as the model system to perform all the experiments for this doctoral work.

1.2 Cell cycle

Faithful transmission of the duplicated genome to daughter cells forms the basis of growth and organismal development. It is achieved by eukaryotic cell cycle which, via a highly regulated set of events, facilitates temporal uncoupling of cellular growth, genome replication and segregation of the duplicated genome (Alberts et al. 2015). Duplication of the genome takes place during S-phase whereas M-phase is when segregation of the duplicated chromosomes occurs. The S phase and M phase are separated by phases (G1 and G2) of cellular growth necessary for progression into the next cell cycle stage (Alberts et al. 2015). Accurate regulation of cell phases ensures the transition from one phase to another occurs only at a correct time and order. Serine/Threonine Cyclin-Dependent Kinases (CDK) form the central component of this regulation. The activation of Cdk's depend on its binding with proteins called cyclins. Different cyclins are made during different cell cycle stages which leads to the formation of specific Cyclin/Cdk complex triggering different cell cycle events (Coudreuse and Nurse 2010; Norbury and Nurse 1992; Loog and Morgan 2005). Cell cycle checkpoints operate at the transition points monitoring the set of requirements necessary for progression into the next stage (Hartwell and Weinert 1989). If the necessary set of requirements are not met, transition into the subsequent phase is delayed via negative feedback signals to the cell cycle machinery, providing time for the previous phase to be completed correctly (Morgan 2012).

1.3 Meiotic cell division

Meiosis forms the basis of sexual reproduction. During meiotic cell division, the chromosome content of cells is reduced by half. This is achieved by two consecutive rounds of cell division which are preceded by a single round of DNA replication. During the first round of division maternal and paternal chromosomes, called homologous chromosomes or homologs, are segregated. This is followed by a second round of division where copies of DNA generated during replication, i.e. sister chromatids, are separated (Kleckner 1996).

To ensure faithful segregation of genetic material, chromosome pairs need to be connected to each other. During DNA replication, sister chromatids are topologically embraced by a ring-shaped multi-protein complex called cohesin (Haering et al. 2008; Uhlmann and Nasmyth 1998). However, this is not the case for

the pair of homologous chromosomes where no such connection exists a priori. The majority of processes before the segregation of homologous chromosomes are dedicated towards establishing a linkage between them. This is achieved via two highly controlled and interdependent sequences of events, namely recombination and synaptonemal complex polymerization, taking place during prophase preceding the first meiotic division. The recombination cascade starts with programmed DNA damage followed by intricate chromosomal choreography culminating in the crossover formation which provides the physical linkage between the homologs (Page and Hawley 2003). Appropriate crossover formation is hugely dependent on synapsis, i.e. polymerization of the synaptonemal complex, which brings two homologous chromosomes in close proximity (Zickler and Kleckner 2015) (Figure 1.1). Defects in either synaptonemal complex polymerization or recombination events result in unfaithful segregation of chromosomes.

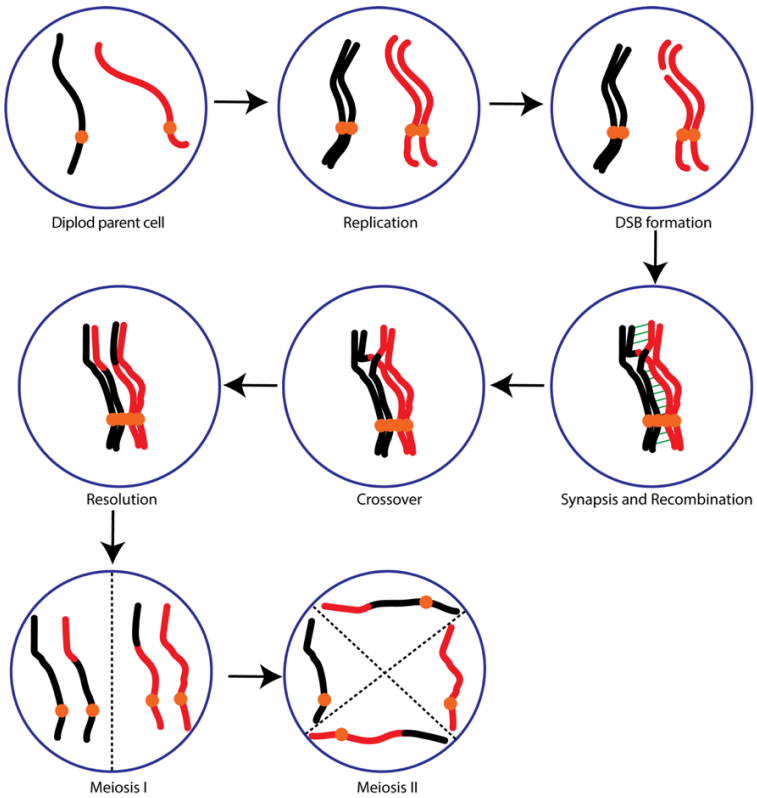

Figure 1.1: **Overview of the meiotic cell division**
Cartoon representation of a cell at different stages undergoing meiosis. After replication of the parental genetic material, double-strand break (DSB) formation takes place. Repair of these breaks i.e. recombination, results in the physical linkage of the homologs in the form of a crossover. Synaptonemal complex polymerization i.e. synapsis facilitates the processes of recombination. After resolution of the crossover, which results in exchange of genetic material, chromosomes are divided into daughter cells. Homologous chromosomes segregate during meiosis I followed by the segregation of sister chromosomes during meiosis II.

1.4 Synaptonemal complex

During the course of meiotic prophase, chromosomes undergo dense condensation and by mid-meiotic, pachytene stage the condensed homologous chromosomes are also completely aligned in a lengthwise manner. The alignment takes place by virtue of the formation of a structurally conserved, highly proteinaceous structure called Synaptonemal Complex (SC) (Moses 1969). In organisms like budding yeast and mice, initiation of the SC assembly is dependent on the programmed double-strand break (DSB) formation (Giroux, Dresser, and Tiano 1989; Baudat et al. 2000; Romanienko and Camerini-Otero 2000); whereas, in organisms like worms and fruit flies, it is independent of the formation of DSBs (Dernburg et al. 1998; McKim et al. 1998; MacQueen et al. 2002; Vazquez, Belmont, and Sedat 2002). The SC polymerizes at the interface of two homologs along their entire length in a process called synapsis. Synapsis juxtaposes the two homologs in close proximity to each other facilitating the process of crossover recombination between the homologous chromosomes. The crossover recombination then results in the formation of chiasmata, a direct physical attachment between the homologs. As cells exit meiotic prophase SC is disassembled, with only the crossover holding the two homologs together during chromosome segregation at meiosis I. Mutations affecting the SC assembly severely reduces the efficacy of crossovers, resulting in chromosome mis-segregations at meiosis I (Gladstone et al. 2009; Miyamoto et al. 2003; Judis et al. 2004)

1.4.1 The Structure of SC

The general structure of SC is conserved across organisms. There are three different sub-structures within SC: two parallel lateral elements connected by transverse filaments and a central element (Page and Hawley 2003). The Lateral element runs along the entire length of homologous chromosomes and contains cohesin proteins along with meiosis-specific proteins Red1 and Hop1 (Klein et al. 1999; Smith and Roeder 1997; Hollingsworth, Goetsch, and Byers 1990). The lateral element creates the axis from which loops of DNA emanate giving rise to the tethered loop-axis structure of meiotic chromatin necessary for the efficient DSB formation (Blat et al. 2002; Keeney 2001; Panizza et al. 2011). The region between the two homologs contains both the transverse filament and the central element. The transverse filament

is a set of perpendicularly oriented proteins connecting the two lateral elements. Central element proteins are present at the center of the SC and help in the proper assembly of the SC by stabilizing the structure. In budding yeast, the presence of Zip1, a large coiled-coil domain-containing protein, is the hallmark of transverse filaments (Sym, Engebrecht, and Roeder 1993). Zip1 forms homodimers with the C-terminal of the protein positioned towards the lateral element and the N-terminal positioned towards the central element (Dong and Roeder 2000). Central element proteins like Gmc2 and Ecm11 are believed to stabilize the N-terminal interactions by forming stable homodimers (Humphryes et al. 2013; Leung et al. 2015). The formation of a proper lateral element is a pre-requisite for the efficient assembly of transverse filament and hence for SC maturation (Hollingsworth, Goetsch, and Byers 1990; Rockmill and Roeder 1990). The formation and maturation of SC is a highly dynamic process.

1.4.2 Dynamics of SC polymerization

The dynamics of SC assembly can be divided into three separate events, namely, initiation, extension and maintenance followed by disassembly.

1.4.2A Initiation of SC

Before SC polymerization, chromosomes must find and pair with their homologs to prevent SC initiation between non-homologous chromosomes. In budding yeast, initial pairing takes place by a highly dynamic, homology-independent process called centromere coupling. During centromere coupling, centromeres continually associate and disassociate until chromosomes begin to pair in a homologous manner by loading the transverse filament protein Zip1 at centromeres (Tsubouchi and Roeder 2005; Zickler and Kleckner 2015). In addition to the centromeres, the initiation of SC assembly also takes place at non-centromeric regions in a DSB-dependent manner (Agarwal and Roeder 2000; Chua and Roeder 1998; Sym, Engebrecht, and Roeder 1993). The distinction of SC initiation at different locations is made possible because of differences in the role of meiotic proteins involved in this process. The small ubiquitin-like modifier (SUMO) E3-ligase Zip3 and proline isomerase Fpr3 restrict the Zip1 polymerization at the centromeres (Macqueen and Roeder 2009). The initiation of the SC at non-centromeric regions takes place at DSB sites that are presumed to be sites for crossover recombination. At these sites, Zip3 plays a role in promoting the formation of SC. The signal emanating from recombination initiation triggers

localization of synapsis initiation complex (SIC) proteins like Zip2, Zip4, Spo16, Msh4, Msh5. These proteins promote the assembly of SC by negatively regulating the SC restrictive behavior of Zip3 (Börner, Kleckner, and Hunter 2004).

1.4.2B Extension and maintenance of SC

Once SC assembly has been initiated, synapsis takes place along the entire length of the homologous chromosomes. This helps in maintaining the homologs in close proximity until the crossover is formed. The extension of SC utilizes a positive feedback system whereby the N-terminal of Zip1 is able to activate the SUMOylation of Gmc2-Ecm11, two central element components, by Siz1 and Siz2 (SUMO E3 ligases) (Humphryes et al. 2013; Leung et al. 2015). The assembly of Gmc2 and Ecm11 is dependent on the fully assembled SIC. PolySUMOylation of Ecm11 facilitates recruitment of more Zip1. The additional recruitment of Zip1 causes more recruitment of Gmc2-Ecm11 thereby creating a positive feedback system (Humphryes et al. 2013; Leung et al. 2015). This eventually leads to fully synapsed chromosomes where the SC must be maintained until the formation of crossover (Figure 1.2). Once fully established, SC remains highly dynamic with a constant turnover of the SC components along the synapsed regions (Voelkel-Meiman et al. 2012). The SC is able to grow and maintain a stable structure because the rate of incorporation of SC components is higher than the rate of their disassociation (Voelkel-Meiman et al. 2012). The SC is maintained until the completion of recombination events after which it starts to disassemble.

1.4.2C Disassembly of SC

The disassembly of SC needs to be precisely coordinated with the completion of recombination events. Once SC is disassembled, it is the crossover that tethers the homologs together allowing for their faithful segregation. This precise control of SC disassembly is controlled by cell-cycle specific kinases like Cdc5 and Ipl1 whose expression are in turn regulated by specific transcription factors like Ndt80 (Jordan et al. 2009; Sourirajan and Lichten 2008).

1.4.3 Extrachromosomal SC aggregates: Polycomplex

Polycomplexes (PC) are large extra-chromosomal aggregates of SC-related material observed during the pachytene stage of meiosis. Abnormalities in either DSB

formation, chromosome synapsis and/or recombination gives rise to the formation of a PC (Hughes and Hawley 2020; Sym and Roeder 1995). Although PCs are generally associated with abnormal chromosome metabolism during meiotic prophase, they are also observed during normal meiosis. Strains showing a prophase block because of the deletion of either *CDC5*, *NDT80* or *SPO10* also show the presence of a PC (Simchen et al. 1981; Horesh, Simchen, and Friedmann 1979; Bhuiyan, Dahlfors, and Schmekel 2003; Kundu and Moens 1982). The SC is assembled at the interface of two homologs, in contrast to PCs which are generally observed in DNA-free regions. However, both of them are composed of the same building blocks and share structural properties. Zip1 is the main component of both SC and the PC (Sym, Engebrecht, and Roeder 1993; Sym and Roeder 1995). Many of the SC-central element proteins like Gmc2, Ecm11 also localize to the PC structures (Humphryes et al. 2013). In fact,

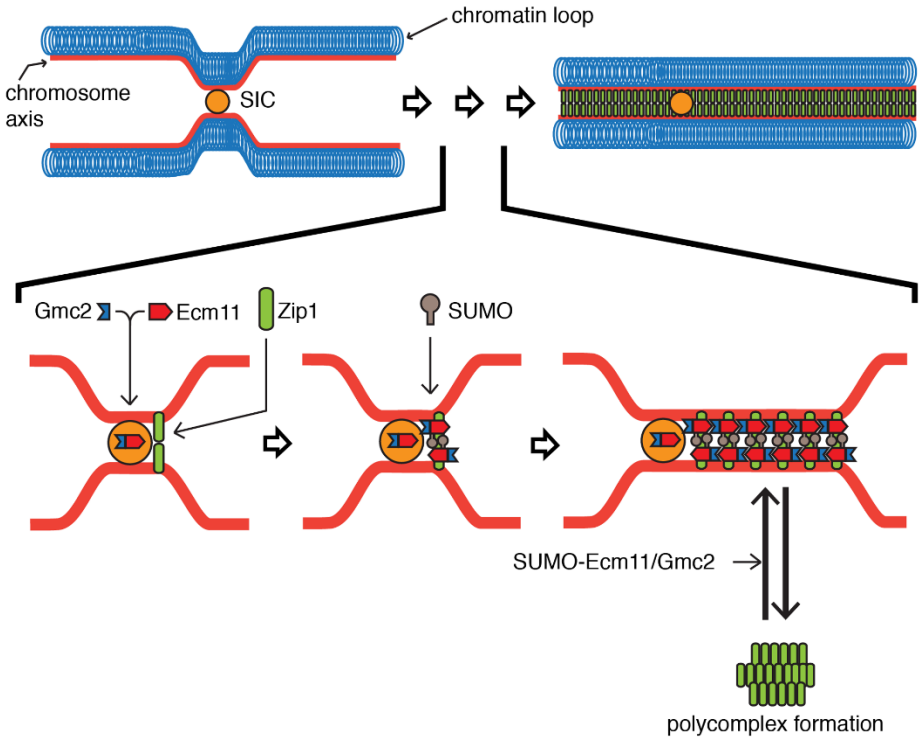

Figure 1.2: **Model of Synaptonemal complex polymerization**
Synaptonemal complex is scaffolded onto a properly formed chromosomal axis. Polymerization is initiated from synapsis initiation complex (SIC) sites where Zip1, Gmc2 and Ecm11 localize. After Ecm11 is SUMOylated, it recruits additional Zip1 creating a positive feedback system resulting in the assembly of synaptonemal complex along the entire length of chromosomes. The same regulation of Ecm11 SUMOylation is necessary for the formation of Polycomplex as well. Image adapted from (Humphryes et al. 2013)

Ecm11 and Gmc2 are essential for the formation of PC even in the face of recombination defects suggesting a connection between the SC and the PC (Figure 1.2). Furthermore, SIC proteins like Zip2, Zip3 and Zip4 also associate with PC (Voelkel-Meiman et al. 2019; Chua and Roeder 1998; Shinohara et al. 2015; Hughes and Hawley 2020). Apart from protein composition, SC and PC also share structural similarities. Like the higher-order structure of SC, PCs have a tripartite structure with SC proteins arranged in a railroad track like organization. PC can be thought of as several stacks of SC stuck parallel to each other. Overexpression of Zip1 also leads to the formation of PC (Sym and Roeder 1995; Dong and Roeder 2000). The formation of PCs in a Zip1 overexpression condition might reflect a scenario where the excessive Zip1 levels results in anomalous formation of PCs. How the formation and extensions of these structures are regulated in unperturbed cells and also under overexpression conditions is not very well understood. Unknown proteins or post-translational modifications that are involved in the regulation of proper SC formation and keep the formation of PCs in check might play a role in this process.

1.5 Crossover recombination: the physical linkage

Crossover formation involves the exchange of genetic material between the two homologs. Crossovers are a result of recombination-based repair of programmed DSBs. Spo11 is a meiosis-specific topoisomerase-like enzyme which forms the catalytic core of a sophisticated machinery responsible for generation of DSBs (Keeney and Kleckner 1995; Keeney, Giroux, and Kleckner 1997; Szostak et al. 1983; Cao, Alani, and Kleckner 1990; Sun et al. 1989). Spo11 remains covalently attached to the 5’-terminus of DNA and is eventually released by endonucleolytic activity of Sae2 endonuclease (Keeney and Kleckner 1995; Farah, Cromie, and Smith 2009; Cao, Alani, and Kleckner 1990). This is then followed by 5’-3’ resection of DNA facilitated by Exo1 and Sae2 proteins leaving behind 3’-single-stranded tail of DNA (Sun et al. 1989; Zakharyevich et al. 2010). Rad51 and Dmc1, members of the RecA family of recombinases, facilitates the strand invasion (Bishop et al. 1992; Chen, Yang, and Pavletich 2008; San Filippo, Sung, and Klein 2008). Rad51 plays a critical role in recombination during both mitosis and meiosis. In contrast, Dmc1 is expressed specifically during meiosis (Bishop et al. 1992). The primary purpose of these proteins is to enable the homology search by the resected single-stranded DNA. Rad51 and Dmc1 decorate the 3’-tail of the resected DNA to form a nucleoprotein filament which

invades the DNA to form a nascent D-loop, eventually resulting in the formation of a single-end invasion. The other strand of DNA is then stabilized to help mature single-end invasion. This leads to the formation of a double-Holliday junction which is ultimately resolved into a crossover (Schwacha and Kleckner 1995; Storlazzi et al. 1995). The strand invasion intermediates that are not stabilized are displaced from the homolog and are repaired as non-crossovers (Figure 1.3) (Allers and Lichten 2001; Hunter and Kleckner 2001).

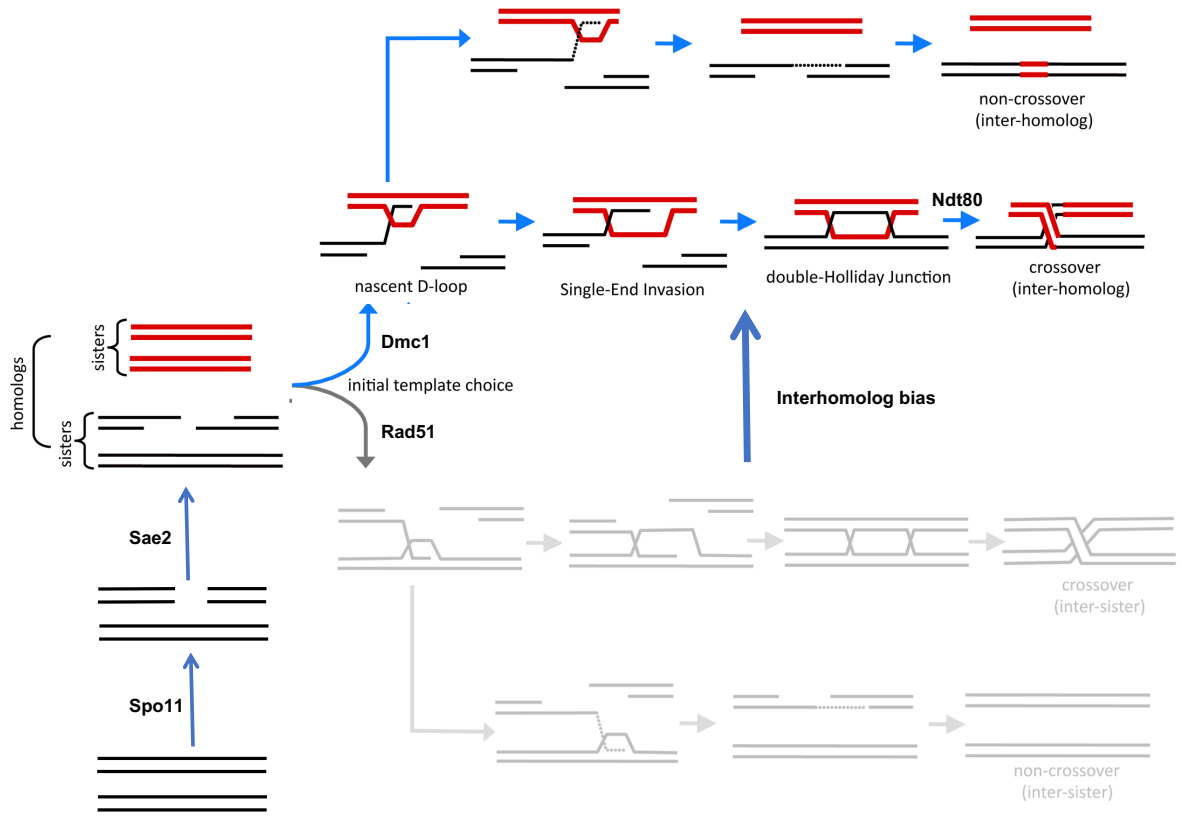

Figure 1.3: **Homologous recombination during meiotic prophase**
After replication Spo11-mediated DSB formation takes place. In a Sae2-dependent manner, 5'-3' resection of DNA initiates leading to the formation of 3'-tail of DNA. The initial template choice for the repair is mediated by two recombinases: Dmc1 and Rad51. Dmc1 helps in using the homolog as a template whereas Rad51 facilitates the use of sister chromatid as the template. During meiosis there is an active bias towards the use of homolog as the repair template. Dmc1 helps in homology search and forms the nascent D-loop. If the D-loop is stabilized, it forms a single end invasion which eventually leads to the formation of a crossover. However, if the stabilization of the D-loop is not optimal the DSB lesion is repaired by forming a non-crossover. The resolution of double Holliday junctions to crossover is also associated with the expression of transcription factor Ndt80. Image modified from (Lao and Hunter 2010)

DSBs can be repaired using a template belonging to either sister or homologous chromosome (Goldfarb and Lichten 2010). However, during meiosis, an active bias exists towards the use of homolog as the template. There are multiple mechanisms that ensure interhomolog recombination is the preferred repair pathway. Dmc1 catalyzes the interhomolog recombination while Rad51 promotes Dmc1 filament assembly but facilitates inter-sister recombination (Figure 1.3) (Neale and Keeney 2006; Brown and Bishop 2014). The differences in roles played by Rad51 and Dmc1 are a result of the different subset of accessory factors used. The Hop2/Mnd1 protein complex interacts with Dmc1 whereas Hed1 binds specifically to Rad51 (Tsubouchi and Roeder 2002, 2006). Rad54 is an accessory factor that is known to stimulate the recombinase activity of Rad51. Interaction of Hed1 with Rad51 blocks the interaction of Rad51 with Rad54 thereby suppressing its activity (Busygina et al. 2008). Additionally, Dmc1 can stabilize mismatched base triplets while scanning for homology, whereas Rad51 cannot (Lee et al. 2017; Lee et al. 2015; Borgogno et al. 2016). These properties reflect an intrinsic difference between the two recombinases. Besides the recombinase-dependent selection of repair pathway, the kinases Mec1/Tel1 also play a role in the regulation of repair pathway choice. Mec1/Tel1 dependent phosphorylation of Hop1, along with other proteins like Pch2 and Rad17 play a role in establishing a bias created towards using homolog as the repair template instead of sister chromatid (Ho and Burgess 2011).

In summary, an active bias towards the use of homolog as the repair template exists during meiosis. The formation of an obligatory inter-homolog crossover is dependent on the interaction of Rad51 and Dmc1 with their co-factors. These interactions result in suppressing the activity of Rad51 and allows Dmc1 to dominate, resulting in an inter-homolog repair of DSBs. Additionally, the bias towards homolog for repair is also created in part by the activity of Mec1/Tel1 kinases and by proteins like Pch2 and Rad17.

1.6 Surveillance mechanisms during cell division

Surveillance mechanisms, also known as checkpoints, monitor the coordinated progression through the cell division program. They play an integral part in ensuring orderly execution of cellular events by creating interdependent relationships between different events of the cellular progression. A checkpoint generally halts the cell cycle

progression until the execution of the previous event has taken place in a proper manner (Hartwell and Weinert 1989). For example, an active checkpoint provides time for the cell to complete events like chromosome biorientation, recombination, synapsis among others to complete before committing to the next steps. Cell cycle checkpoints operate during both mitotic and meiotic cell division programs to maintain genome integrity. The first checkpoint operates during late G1 phase, at which stage cells unidirectionally commit to DNA replication and entry into cell cycle (Hartwell 1974)**.**The next checkpoint, operating during G2 phase, monitors the state of DNA replication (Jeggo and Löbrich 2007). The last checkpoint known as Spindle Assembly Checkpoint (SAC) operates during the chromosomal segregation event in M phase. SAC ensures the proper segregation of sister chromosomes during cell division (Musacchio 2015). Because of the presence of an additional round of chromosome segregation event during meiosis, there are additional surveillance mechanisms that operate during meiotic prophase (Subramanian and Hochwagen 2014). These checkpoints monitor DSB repair and synapsis ensuring proper segregation of chromosomes during meiosis I. Checkpoints play a very important role in proper cell cycle progression, here I will be focusing on describing the meiotic prophase checkpoint and spindle assembly checkpoint in more detail in the following sections.

1.6.1 Checkpoints during meiotic prophase

As mentioned earlier, for faithful segregation of chromosomes during meiotic division, proper execution of critical events like recombination and synapsis is indispensable. Surveillance mechanisms, or checkpoints, exist during meiotic prophase which monitor stepwise execution of both recombination and synapsis. The generation of programmed DSBs is essential for the initiation of these events. The DNA damage-response kinases Tel1 and Mec1 (mammalian ATM and ATR orthologs respectively) are activated by the DNA substrates generated in response to Spo11-mediated DSBs (Subramanian and Hochwagen 2014; Carballo and Cha 2007). Tel1 is activated by the blunt DNA at DSB sites whereas Mec1 is activated by the single-stranded 3'-tail left after 5'-3' resection of DNA (Shiotani and Zou 2009; Zou and Elledge 2003). Active Tel1/Mec1 phosphorylate the chromosome axis protein Hop1 in its SCD region (SQ/TQ Cluster Domain) enabling Hop1 to act as an adaptor for Mek1 activation (Figure 1.4) (Carballo et al. 2008; Cheng et al. 2013). The Forkhead-associated domain of Mek1 then interacts with the phosphorylated Hop1, resulting in

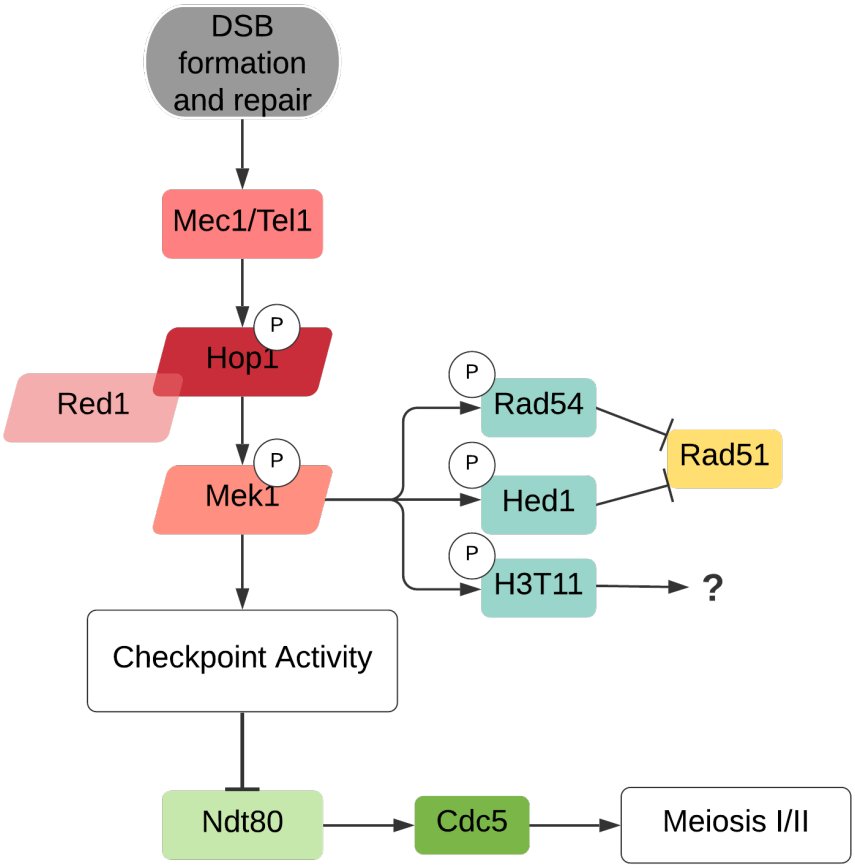

Figure 1.4: **Checkpoint signaling cascade during meiotic prophase**
DSB formation and subsequent processing results in the activation of Tel1 and Mec1 kinases. These kinases phosphorylate the axis protein Hop1 which then acts as an anchor to facilitate the phosphorylation of effector kinase Mek1. Active Mek1 results in checkpoint activity by inhibiting Ndt80 dependent transcriptional activity of multiple genes, one of which is Cdc5. Active Mek1 also helps creating interhomolog bias by phosphorylating a number a substrate like Rad54 and Hed1 which inhibit Rad51 function. Histone H3-Thr11 is also a substrate of Mek1.

the chromosomal recruitment of Mek1. On the chromosomes, Mek1 is activated in part by (trans) autophosphorylation of Thr327 present in its activation loop (Niu et al. 2007). However, for full activation of Mek1, multiple genetically separable phosphorylation events take place. Activated Mek1 creates a positive feedback system by stabilizing the phosphorylation of Hop1 (Niu et al. 2007; Niu et al. 2005; Carballo et al. 2008; Penedos et al. 2015). The activation of Mek1 results in reinforcing the preferential use of homolog instead of sister chromatid as a repair template during recombination (i.e. inter-homolog bias) The interhomolog bias is created in part by phosphorylation of Rad54, a binding partner of Rad51 (see above). The phosphorylation of Rad54 by Mek1 attenuates its interaction with Rad51, resulting in Dmc1 to predominate the

strand exchange activity (Niu et al. 2009). In addition to phosphorylation of Rad54, activated Mek1 also directly phosphorylates Hed1 at Thr40 residue, which leads to a stabilization of the protein (Figure 1.4). The stabilization of Hed1 promotes negative regulation of Rad51 strand exchange activity, further strengthening the role of Dmc1 in mediating inter-homolog recombination (Callender et al. 2016). Thus, Mek1 via its kinase activity on multiple substrates ensures the creation of inter-homolog bias for DSB repair.

Activation of Mek1, a sign of active checkpoint signaling, is also responsible for delay or arrest of meiotic progression. Active Mek1 targets the cell cycle machinery by phosphorylating and activating CDK-inhibitory kinase Swe1. Active Mek1 also leads to the inhibition of Ndt80 activity. Ndt80 is a transcription factor whose activity leads to the expression of a set of middle sporulation-specific genes, including *CLB1* (cyclin) gene. Transcriptional downregulation of *CLB1* along with the inhibitory phosphorylation of Cdc28 by Swe1, restricts the Clb1-Cdc28 (Cyclin/CDK) activity, thereby preventing cells from exiting meiotic prophase (Tung, Hong, and Roeder 2000) (Acosta, Ontoso, and San-Segundo 2011). Another important target of Ndt80 is the prophase-exit promoting budding yeast polo-like kinase, Cdc5 (Sourirajan and Lichten 2008) (Figure 1.4). The use of an allele that expresses *CDC5* during mitosis but not during meiosis (*cdc5-mn*, meiotic null) revealed that Cdc5 expression also plays a role in the exit from checkpoint. *cdc5-mn* mutants show reduced crossover, defective resolution of recombination products and persistence of SC (Sourirajan and Lichten 2008). Thus, active checkpoint during meiotic prophase, via inhibition of Ndt80, results in the downregulation of *CDC5* and *CLB* genes, which together with the inactivation of Cdc28 leads to the delay/arrest in the meiotic progression.

Apart from Rad54, Mek1 itself, Hed1 and Ndt80, Mek1 also directly phosphorylates Histone H3 at Threonine 11 (H3-T11) in response to DSB generated signaling (Kniewel et al. 2017). Although, the phosphorylation of H3-T11 by Mek1 is dispensable for its meiotic function, it is often used as a marker for activated Mek1 and ongoing checkpoint signaling during meiotic prophase.

To summarize, activation of Mek1, in response to DSBs, is the most critical component for creating homolog bias and in maintaining the checkpoint activity leading

to a delay/arrest during meiotic prophase. As such, Mek1 is the effector kinase of checkpoint activity during meiotic prophase.

1.6.2 Spindle assembly checkpoint

The Spindle Assembly Checkpoint (SAC) operates during chromosome segregation event in eukaryotic cells. The SAC prevents the passage of cells into the final stages of cell division until the chromosomes are properly attached and a state of chromosome bi-orientation on the spindle is achieved. It delays the metaphase-to-anaphase transition on recognizing the presence of kinetochores (a complex assembly of proteins on the centromere of each chromosome that mediates chromosome attachment to microtubules) harboring unattached microtubule-binding sites (Rieder et al. 1995; Dick and Gerlich 2013). Active SAC catalyzes the assembly of an inhibitory effector complex called mitotic checkpoint complex (MCC). MCC is composed of core SAC proteins: Mad2, Mad3 (BubR1 in mammals), Bub3 and Cdc20. The main target of MCC is a vital E3-ubiquitin ligase called Anaphase promoting complex/cyclosome (APC/C). MCC blocks the activity of APC/C and helps prevents mitotic exit (Musacchio 2015; Lara-Gonzalez, Westhorpe, and Taylor 2012). As proper bi-polar microtubule-kinetochore attachments take place and the chromosomes attain the state of bi-orientation, MCC is disassembled. This allows APC/C to act on two of its crucial substrates, Cyclin B and Securin (Figure 1.5) (Glotzer, Murray, and Kirschner 1991; Yamamoto, Guacci, and Koshland 1996). APC/C mediated rapid degradation of cyclin B dissolves the cyclin B/Cdk1 complex, resulting in the inactivation of Cdk1 and a subsequent exit from mitosis. Simultaneously, APC/C also mediates the degradation of securin, liberating separase from the inhibition of securin. Separase cleaves the kleisin subunit of cohesin, resulting in the opening of the cohesin ring. This leads to the loss of sister chromatid cohesion and results in the onset of anaphase (Funabiki et al. 1996; Holloway et al. 1993; Uhlmann, Lottspeich, and Nasmyth 1999; Uhlmann et al. 2000). Thus, the ultimate function of SAC is to keep the activity of APC/C in check to prevent the loss of sister chromatid cohesion and inhibit the premature entry of cells into anaphase.

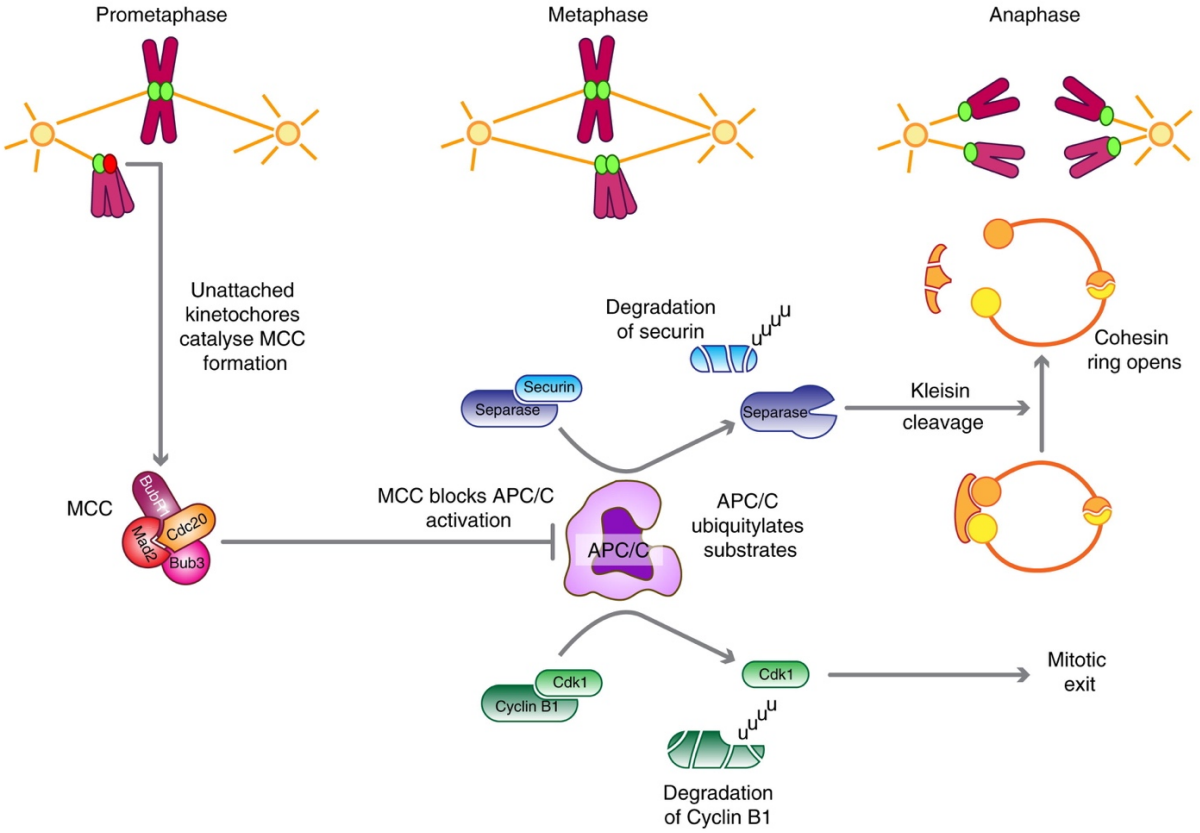

Figure 1.5: **Molecular machinery involved in the Spindle Assembly Checkpoint** Unattached kinetochores result in the formation of MCC consisting of Mad2, Cdc20, BubR1 and Bub3. The main function of MCC is to block the activation of ubiquitin ligase APC/C until chromosome bi-orientation is achieved. Upon chromosome bi-orientation, MCC is disassembled allowing APC/C to release separase from the inhibitory activity of securin, thereby allowing separase to cleave the cohesin ring keeping the sister chromatids together. APC/C activation also results in the degradation of Cyclin B1, leading to the inactivation of Cdk1 and subsequent exit from mitosis. Image adapted from (Lara-Gonzalez, Westhorpe, and Taylor 2012)

1.7 Interplay of AAA+ ATPase and HORMA domain proteins

1.7.1 AAA+ ATPase

AAA+ ATPases, an acronym for ATPases Associated with various cellular Activities, are a functionally diverse group of proteins which can bind to and hydrolyze ATP to bring about conformational changes in a wide range of substrates (Hanson and Whiteheart 2005).

The hallmark of AAA+ ATPases is the structurally conserved, ~200-250 amino acids long AAA+ domain structural core which is formed by a three-tiered *α-β-α*

sandwich (Iyer et al. 2004). Each AAA+ domain consists of a Walker-A and Walker-B motif critical for binding and hydrolyzing ATP, respectively. The consensus sequence for a Walker-A motif is GXXXXGK[T/S], where X is any amino acid and the C-terminal residue is either threonine or serine (Hanson and Whiteheart 2005). The Walker-B motif is characterized by the sequence hhhhDE, where h represents any hydrophobic residue and the C-terminal residues are aspartate and glutamate (Hanson and Whiteheart 2005). The conserved aspartate and glutamate residues are important for catalyzing ATP-hydrolysis. The aspartate residue helps in coordinating the Mg^{2+} required for ATP-hydrolysis whereas the glutamate residue forms the catalytic base from where the nucleophilic attack on the γ-phosphate is initiated during ATP hydrolysis. Mutation of the glutamate residue in the Walker-B motif therefore prevents ATP-hydrolysis while still allowing its binding. For this reason, glutamate to glutamine or alanine mutation has been used to create a “substrate trap” to dissect the roles of ATP binding and ATP hydrolysis in AAA+ protein activities (Weibezahn et al. 2003).

AAA+ ATPases are known to oligomerize via its ATPase domains. With the exception of a few, most of the AAA+ ATPases are known to oligomerize into a closed barrel-like hexameric ring with an open central channel (Wang et al. 2001). These oligomeric assemblies are thought to be the active state of such ATPases. One of the characteristics of forming these barrel-shaped complexes is the presence of ATP-binding pockets at the interface of different subunits. This typical arrangement enables the coordination between the binding and hydrolysis of ATP. The dynamics of ATP binding and hydrolysis results in the propagation of structural changes within different subunits. This coordination is provided, most importantly, by a conserved arginine finger present in one of the AAA+ domain, contributing to the ATP-binding pocket of the neighboring subunit by contacting the γ-phosphate of the bound ATP (Ogura, Whiteheart, and Wilkinson 2004). The synchronized behavior makes the AAA+ assembly work in a concerted manner thus forming a processive machine. The conformational changes brought about by the binding and/or hydrolysis of ATP is then relayed onto its substrate, in most cases, via a non-catalytic N-terminal domain.

AAA+ ATPases are known to perform a vast variety of essential functions to cell physiology including, but not limited to, initiation of DNA replication, maintaining robustness of cell cycle checkpoints, control of protein homeostasis and ribosomal

DNA stability. The functional diversity of AAA+ ATPases is provided by their ability to interact with many different substrates via their N-terminal extensions (Tucker and Sallai 2007). Cdc48, also known as p97, is one of the best characterized AAA+ ATPase. Cdc48 is implicated to play a role in various cellular processes including, but not limited to, ubiquitin fusion degradation (UFD) pathway, endoplasmic reticulum-associated degradation (ERAD) pathway, DNA repair etc. (Mullally, Chernova, and Wilkinson 2006; Jarosch et al. 2002; Ye, Meyer, and Rapoport 2001; Braun et al. 2002; Meyer and Weihl 2014). The domain architecture of Cdc48 includes an N-terminal region followed by two AAA+ ATPase domains and finally an unstructured C-terminal region. The Cdc48 homomers come together to form a functional double hexamer that enables it to use ATP hydrolysis in a coordinated manner to generate mechanical force to disassemble protein complexes or unfold proteins(Nishikori et al. 2011). There are multiple other AAA+ ATPases discovered which are involved in a myriad of cellular processes and mechanistically function in a manner similar to that of Cdc48. One such AAA+ ATPase is Pch2/TRIP13.

1.7.1A Pch2/TRIP13: the well-known AAA+ ATPase

Pachytene checkpoint 2 (Pch2), and its mammalian homolog TRIP13, is a AAA+ ATPase known to regulate processes like meiotic DNA recombination, chromosomal axis formation, meiotic prophase checkpoint among others (Vader 2015). Homologs of *PCH2* have been identified in worms, fruit flies, plants and mammals. In budding yeast, it is a meiosis-specific protein but its homologs (PCH-2 in *C.elegans* and TRIP13 in mammals) are known to play roles during both mitotic and meiotic processes (Vader 2015). Pch2 was initially discovered in budding yeast in a screen for mutants that could bypass the arrest caused due to synapsis defects (San-Segundo and Roeder 1999). Since then, checkpoint associated roles have also been described in other organisms. In *C.elegans*, pch-2 is needed for apoptosis of oocytes that experience defective SC polymerization (Bhalla and Dernburg 2005). Similarly, in *D. melanogaster*, *pch2* is required for a delay in oocyte selection caused by the mutations in crossover-promoting factors (Joyce and McKim 2009; Bhalla and Dernburg 2005). Disruption of TRIP13 leads to fertility defects in both male and female mice. Male mice display small gonads whereas female mice have very few or no follicles, a result of the oocyte elimination (Roig et al. 2010; Li and Schimenti 2007). Apart from meiosis, the role of Pch2/TRIP13 is also implicated in regulating mitotic processes especially in the regulation of SAC during cell division (Tipton et al. 2012;

Musacchio 2015). TRIP13 is one of the genes thought to give rise to chromosomal instability (CIN) in human tumors (Yost et al. 2017). Structurally, like most other AAA+ ATPase, Pch2/TRIP13 oligomerizes into functional hexameric assemblies (Chen et al. 2014; Ye et al. 2015). Apart from the ATPase domain, Pch2/TRIP13 contains an N-terminal region which helps in the substrate specificity. Most, if not all, of the regulatory functions of Pch2/TRIP13 are carried out by modulating HORMA domain-containing client proteins (Vader 2015). As such, HORMA domain-containing proteins act as clients for AAA+ ATPases to execute their function during various signaling cascades.

1.7.2 HORMA domain-containing proteins

The HORMA domain was first identified in *S.cerevisiae* in three functionally unrelated proteins, namely, Hop1, Rev7 and Mad2 by virtue of sequence similarity (Aravind and Koonin 1998). Hop1 is a meiosis-specific protein known to bind chromosomes during early meiosis and controls different aspects of recombination and chromosome segregation (Hollingsworth, Goetsch, and Byers 1990; Sale 2013). Rev7 is a subunit of translesion DNA polymerase ζ known to play a role in recombination pathways during mitotic DNA DSB break repair (Sale 2013). Mad2 is, structurally and functionally, the best-understood HORMA domain-containing protein. It is a key regulator of the spindle assembly checkpoint (Mapelli and Musacchio 2007). Since the initial discovery of HORMA domain in *S.cerevisiae*, proteins containing this domain have been identified in many other eukaryotic organisms. Strikingly, HORMA domain-containing proteins are not restricted only to eukaryotes. Recently, a HORMA domain-containing protein was identified in bacterial signaling operon, suggesting the evolutionary conservation of this domain (Ye et al. 2020). HORMA domains are known to form functional protein assemblies and play a role in diverse signaling pathways. Apart from the above-mentioned pathways, HORMA domain-containing proteins are also associated with the initiation of autophagy (Rosenberg and Corbett 2015).

Structural studies of HORMA domain-containing proteins have revealed that apart from sharing sequence similarities, these domains share structural properties as well. The hallmark of a HORMA domain is the presence of two functionally different regions: the N-terminal “core” region and the C-terminal “safety belt” region (Aravind and Koonin 1998). HORMA domains can exist in two different conformations depending on how the safety belt region packs itself against the core region. Packing

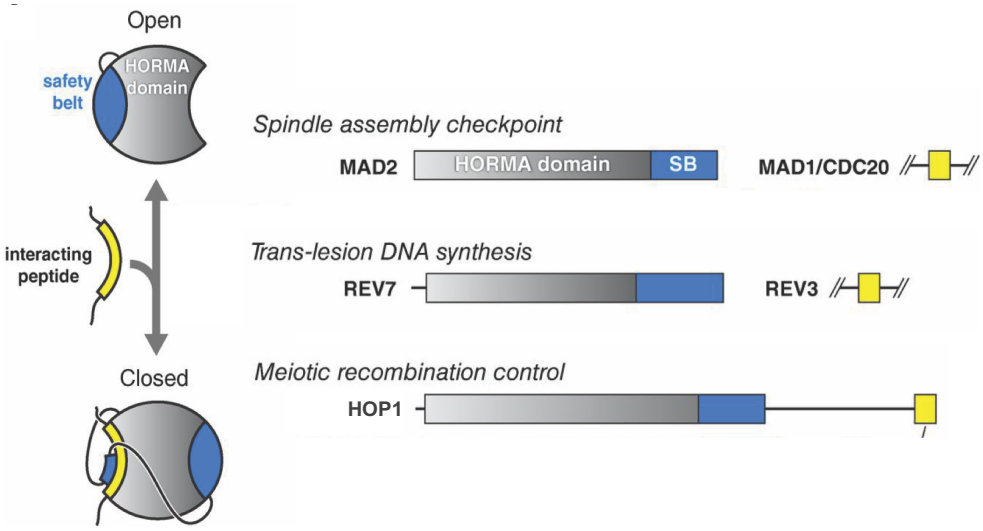

Figure 1.6: **Different conformations and architecture of HORMA domain-containing proteins**
Cartoon representation of two different conformations a HORMA domain can adopt. The two conformations are distinguished by how the safety belt region (shown in blue) wraps itself around the core region (shown in gray). Upon binding of closure motif/interaction peptide (shown in yellow), the HORMA domain achieves a closed conformation. In open conformation, the HORMA domain cannot bind with the closure motif. Closure motifs can be present within the protein, like in Hop1; or it can be present in the interacting partners like Mad1 and Cdc20 for Mad2, and Rev3 for Rev7. Image modified from (Rosenberg and Corbett 2015)

of the safety belt region is coupled to the binding of the core region with a short peptide interaction motif known as “closure motif”. When the core region interacts with a closure motif, the safety belt wraps itself around the core region, a conformation termed as “closed”. On the other hand, when the safety belt occupies the closure motif interaction site, a conformation termed as “open”, the core region is unable to bind to the closure motif (Figure 1.6) (Aravind and Koonin 1998; Rosenberg and Corbett 2015). With respect to a signaling event, the open conformation of a HORMA protein is considered to be the latent state whereas the closed or unbuckled conformation is considered to be the active state. This sets up a framework whereby HORMA domain proteins, by adopting two topologically different conformations, can result in contrasting outcomes of the signaling. However, not all the HORMA domain proteins, for example, Rev7, are known to exist in open and closed conformations. As of now, Rev7 has only been observed in a closed conformation. A closure motif can be present within the protein itself (for example in Hop1) or it can be present in the interacting partner of the protein (for example in Cdc20 and Mad1 for Mad2, and; in Rev3 for Rev7) (Figure 1.6).

The topological linkage of HORMA domain to the closure motif of its binding partner gives rise to functional protein complex assembly. Thus, HORMA domain proteins by virtue of its interaction with closure motif-containing interaction partners, can adopt two distinct conformations and play contrasting roles via assembly and disassembly of protein complexes.

1.7.2A Hop1: meiotic HORMA domain-containing protein

Hop1, like the majority of other HORMA domain-containing proteins, can adopt two different conformations (West, Komives, and Corbett 2018; Rosenberg and Corbett 2015). The open conformation of Hop1 is slightly different than the well-characterized open conformation of Mad2. In this conformation, termed “Unbuckled” Hop1 (U-Hop1), the safety belt region is disengaged from the HORMA domain core region and is thought to exist in an extended state (West, Komives, and Corbett 2018). Also, unlike Mad2, Hop1 is known to contain its own closure motif (Figure 1.6). Red1, a chromosomal axial protein responsible for the chromosomal localization of Hop1, also contains a closure motif with which Hop1 can associate (West, Komives, and Corbett 2018; Niu et al. 2005). Hop1 can bind to both its own closure motif as well as to the closure motif of its interacting partner, Red1. The current model of chromosomal axis organization proposes that Hop1 initially interacts with a closure motif in chromosomally associated Red1 freeing up its own closure motif in the process. This is followed by additional recruitment of Hop1 to oligomerize in a head-to-tail manner, mimicking “beads on a string” pattern (West, Komives, and Corbett 2018; Rosenberg and Corbett 2015).

Hop1 is essential for the proper assembly of SC and absence of Hop1 results in the appearance of PC structures (Carballo et al. 2008; Hollingsworth and Byers 1989; Hollingsworth, Goetsch, and Byers 1990). Hop1 plays a role in the signaling of meiotic prophase checkpoint. The lack of Hop1 in cells results in the decrease of spore viability, reflecting the importance of Hop1 in chromosome segregation events (Hollingsworth and Byers 1989; Hollingsworth, Goetsch, and Byers 1990). Hop1 is a highly conserved protein with its mammalian homologs, HORMAD1 and HORMAD2, playing very similar roles of axis formation and checkpoint regulation in mice (Wojtasz et al. 2009). The chromosomal localization of Hop1, and HORMAD proteins in mammals, is negatively regulated by Pch2, and TRIP13 respectively . The interplay of

AAA+ ATPase and HORMA domain-containing proteins across species indicates the functional conservation of AAA+ HORMA module. As such, HORMA domain-containing proteins are modulated by AAA+ ATPases resulting in AAA+ HORMA module playing a role in a variety of diverse signaling cascades across different species.

1.7.3 AAA+ HORMA proteins during mitotic Spindle assembly checkpoint

A dysregulated SAC might result in chromosome missegregation and lead to the production of aneuploid cells, hallmark of birth defects and multiple cancers. Hence proper regulation of SAC is of utmost importance. AAA+ ATPases and HORMA domain-containing proteins combine to play a critical role in regulating the SAC. Pch2 homologs in *C.elegans* (PCH-2) and mammals (TRIP13) are known to regulate SAC by modulating HORMA domain-containing protein Mad2 (Nelson et al. 2015; Alfieri, Chang, and Barford 2018; Musacchio 2015). It is to note that budding yeast Pch2 has not yet been implied to play a role in SAC regulation.

Mad2, similar to Hop1, can exist in two different conformations: an “open” conformation (O-Mad2) or a “closed” conformation (C-Mad2) (Sironi et al. 2002; Sironi et al. 2001; Luo et al. 2004). A closed conformation of Mad2 is achieved upon binding to either Mad1 or Cdc20, both of which contain a similar Mad2-interaction motif (closure motif). A critical step in signaling of the SAC is the catalytic assembly of Mad2 and Cdc20 subcomplex. According to the “Mad2-template model”, O-Mad2 is recruited to the unattached kinetochores where more stably associated Mad1/C-Mad2 act as the template to convert O-Mad2 to C-Mad2. C-Mad2 is then able to capture Cdc20 forming the Cdc20/C-Mad2 subcomplex that subsequently forms the MCC by association with constitutive BubR1/Bub3 subcomplex (Figure 1.7) (Musacchio and Salmon 2007).

Whereas it is critical to activate SAC by MCC formation, it is equally crucial to silence the SAC signaling, upon chromosome bi-orientation, for ensuring cell cycle progression. One of the ways to achieve silencing of the SAC signal is through disassembly of MCC. The AAA+ ATPase TRIP13 promotes the conformational conversion of Mad2 from C-Mad2 to O-Mad2 (Ye et al. 2017; Ye et al. 2015). This induced conformational change likely contributes to the extraction of Mad2 from the

MCC and leads to the disassembly of MCC. It is to note that other mechanisms involving the action of phosphatases that counteract mitotic kinase activity and removal of checkpoint proteins from kinetochores also act simultaneously to silence the SAC signaling.

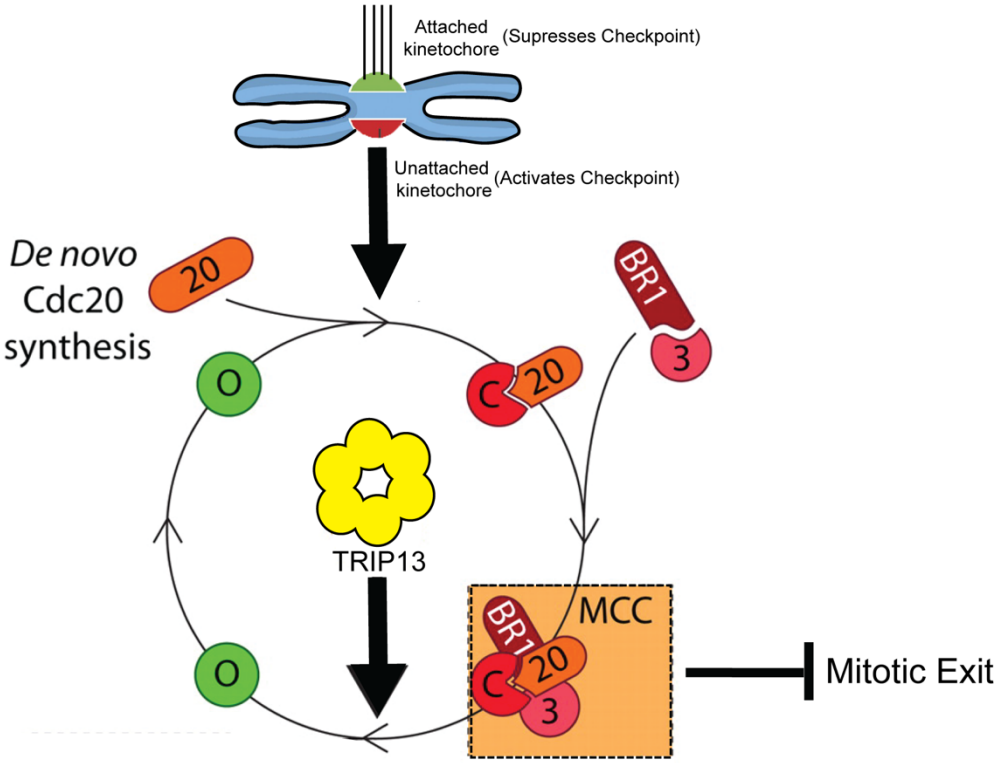

Figure 1.7: **Dual role of TRIP13 during Spindle assembly checkpoint**
The Mad1-Mad2 complex serves as the template to bring in O-Mad2 (depicted as O in green) which is then converted into C-Mad2 (shown as C in red) by its interaction with Cdc20 (shown as 20 in orange). The C-Mad2-Cdc20 complex then interacts with BubR1 (shown as BR1) and Bub3 (shown as 3) to form the MCC. TRIP13 helps to disassemble this complex thus helping silencing the SAC. On the other hand, disassembly of MCC releases O-Mad2 which can then be used for conversion back to C-Mad2 by interacting with Cdc20 and form MCC again. Thus, the action of TRIP13 on MCC results in both activation and silencing of SAC. Some of the proteins are omitted for clarity. Image modified from (Westhorpe et al. 2011)

Considering that TRIP13 plays a role in the disassembly of MCC, one would expect an extended SAC signaling in its absence. But paradoxically, deficiency of TRIP13 leads to an inability of cells to activate the checkpoint even in the presence of spindle disrupting agents (Ma and Poon 2016; Yost et al. 2017). This observation was reconciled by a proposal that O-Mad2, formed after extraction of C-Mad2 from MCC by TRIP13, is recycled back to form additional MCC (Eytan et al. 2014; Varetti et al.

2011; Musacchio 2015). This proposal was supported by experiments involving a degron-mediated TRIP13-degradation system to temporally control the TRIP13 expression (Ma and Poon 2018). Thus, by replenishing the levels of O-Mad2 required for its *de novo* incorporation in the MCC, TRIP13 also helps in the activation of the SAC (Figure 1.6). This shows that TRIP13 not only plays a role in the inactivation of SAC, but also in its activation. The dynamic assembly and disassembly of MCC, by virtue of the interplay between AAA+ ATPase TRIP13 and HORMA domain-containing Mad2, is critical for maintaining for the responsiveness of SAC signaling (Varetti et al. 2011; Musacchio and Ciliberto 2012).

1.7.4 AAA+ HORMA proteins during meiotic prophase checkpoint

As mentioned in section 1.6.1A, Pch2 is a meiosis-specific AAA+ ATPase whose expression starts during early G2/Prophase, reaches the maximum peak around the pachytene stage and then steadily declines as cells progress into meiosis (San-Segundo and Roeder 1999). It was first identified as a checkpoint protein involved in maintaining the checkpoint arrest/delay caused due to the absence of Zip1, a central component of the synaptonemal complex (San-Segundo and Roeder 1999). It is to note that depending on the budding yeast strain, deletion of *ZIP1* can either result in a delay of meiotic progression (strains of SK1 background) or a near-complete arrest at the pachytene stage (strains of BR background). The alleviation of *zip1Δ* induced checkpoint delay/arrest by *pch2Δ* results in decreased spore viability indicating defects in chromosome segregation during meiosis I (San-Segundo and Roeder 1999). Pch2 has received a lot of attention, in recent times, because of its involvement in a number of other regulatory processes like chromosome axis modulation, crossover control, meiotic recombination, Interhomolog bias, suppression of DSBs, among other functions taking place during meiotic prophase (Vader 2015). It is now becoming clearer that all these regulatory roles of Pch2 are dependent on its interplay with a single client protein: Hop1 (Vader 2015). Pch2 and Hop1 form a AAA+ HORMA module and regulate the aforementioned chromosomal processes.

Cytologically, Pch2 localizes to individual chromosomes and to the nucleolar area (Subramanian et al. 2016). The nucleolar region in budding yeast consists of ~150-200 tandem repeats of 9.1 kb ribosomal DNA. Pch2 is recruited to synapsed chromosomes in a Zip1-dependent manner (Subramanian et al. 2016; San-Segundo

and Roeder 1999). Studies from our lab have shown that this recruitment is also partially dependent on Orc1 (a member of origin recognition complex) and active transcription (Cardoso da Silva, Villar-Fernández, and Vader 2020; Villar-Fernández et al. 2020). However, the exact molecular mechanisms governing this recruitment is not very well understood. The chromosomal recruitment of Pch2 enables the active removal of Hop1 from chromosomal axis (Herruzo et al. 2016; San-Segundo and Roeder 1999). Pch2 can directly interact with Hop1 and can remove assemblies of Hop1 from DNA *in-vitro* (Chen et al. 2014). During early meiosis, Hop1 and Zip1 start to load onto chromosomes in a foci-like manner which takes the shape of a more domain-like organization with differential hyperabundances along the chromosomes during pachynema. Interestingly, in the absence of Pch2, Hop1 and Zip1 largely colocalize on the chromosomes (Joshi et al. 2009; Borner, Barot, and Kleckner 2008). However, if and how Pch2 regulates the synaptonemal complex polymerization is still not completely understood.

In budding yeast, the boundaries of nucleolar region are susceptible to DSBs. The recruitment of Pch2 to the nucleolar region is associated with its role in protecting the nucleolar boundaries from Spo11-mediated DSBs (Vader et al. 2011). The nucleolar region is devoid of SC polymerization, thus distinguishing it from the rest of chromosomal regions. The recruitment of Pch2 to nucleolar region is thus not dependent on synapsis; instead, it depends on Orc1, with whom Pch2 forms a complex, and Sir2 (Vader et al. 2011; Villar-Fernández et al. 2020). These proteins help in recruiting Pch2 to these sites, where Pch2 acts on its client: Hop1. Absence of either Orc1 or Pch2 leads to the appearance of Hop1 in the nucleolar area which correlates with the formation of DSBs at these sites (Vader et al. 2011).

Pch2 also plays a role in establishing interhomolog bias as cells lacking Pch2 are observed to show an increase in the inter-sister repair (Joshi et al. 2015; Ho and Burgess 2011). It is proposed that Pch2, along with Tel1, is important for establishing interhomolog bias during early meiosis when the levels of DSBs are low (Joshi et al. 2015; Ho and Burgess 2011). However, once DSBs cross a threshold level, the Mec1-dependent pathway gets activated too. Hence, Pch2 and Tel1 are important for establishing interhomolog bias under limiting DSB levels. A percentage of Pch2 foci also colocalize with Zip3, a member of Synapsis initiation complex (SIC) (Joshi et al. 2009). Zip3 sites on chromosomes correspond to future crossover sites. Pch2 here is

thought to play a role in maintaining crossover interference (making sure that two crossovers are not genetically close to each other). For roles that Pch2 play in either establishing interhomolog bias or crossover interference, Xrs2, a member of MRX (Mre11, Rad50 and Xrs2) complex is considered to play the role as a co-factor (Ho and Burgess 2011). However, the client for Pch2 remains the same: Hop1.

As mentioned earlier, Pch2 was initially discovered as a checkpoint factor, but further research uncovered paradoxical roles for Pch2 in the meiotic prophase checkpoint function. Deletion of *PCH2* in an otherwise wild type background delays meiotic progression. The absence of Pch2 leads to a lack of removal of Hop1 from the chromosome axis. Hop1 plays a central role in relaying the checkpoint signaling operating during prophase (Wu, Ho, and Burgess 2010; Chuang, Cheng, and Wang 2012; Subramanian et al. 2016). Thus, the increase in the abundance of Hop1 on chromosomes, in absence of Pch2, is considered to be the reason for this delay. In contrast, deletion of *PCH2* in *zip1Δ* cells leads to an alleviation of the delay in meiotic progression caused due to the absence of Zip1 (Herruzo et al. 2016; San-Segundo and Roeder 1999; Subramanian et al. 2016; Ho and Burgess 2011). Additionally, deletion of *PCH2* does not lead to the alleviation of checkpoint arrest caused due to the absence of Dmc1 recombinase (i.e. Pch2 does not have any effect on arrest caused due to *dmc1Δ*) (Ho and Burgess 2011; Wu and Burgess 2006; Hochwagen et al. 2005). The difference in response of Pch2 to different lesions during meiotic prophase has led to the proposal that two different checkpoints exist: one that responds to defects in recombination and one that responds to defects in synapsis, with Pch2 playing a role exclusively in the synapsis checkpoint (Wu and Burgess 2006). However, both the synapsis and recombination checkpoints are dependent on DSB formation and are known to be relayed through the activity of Hop1 and eventually activity of Mek1 (Wu, Ho, and Burgess 2010; Chuang, Cheng, and Wang 2012; Subramanian et al. 2016). Since Pch2 is known to execute almost all of its known functions by acting on a single client protein: Hop1, it is not completely understood why Pch2 would specifically act only in one pathway and not on the other. The rationale proposed for Pch2's role in synapsis checkpoint is that its absence allows the DSBs to be repaired using the sister chromatid as the template in a Rad51 recombinase dependent manner (Herruzo et al. 2016; Farmer et al. 2012). This preference of inter-sister repair pathway allows the cells to repair DSBs via sister chromatids as a template

rather than homologous chromosomes. This is believed to be the explanation for faster meiotic progression in *zipΔ pch2Δ* double deletes as compared to *zipΔ* deletion alone (Herruzo et al. 2016). To summarize, depending on the lesions responsible for the activation of meiotic prophase checkpoint, Pch2 can play different roles (Figure 1.8). Its absence can result in either delay of the meiotic progression, alleviation of the checkpoint and accordingly, faster meiotic progression or have no role in the meiotic progression at all.

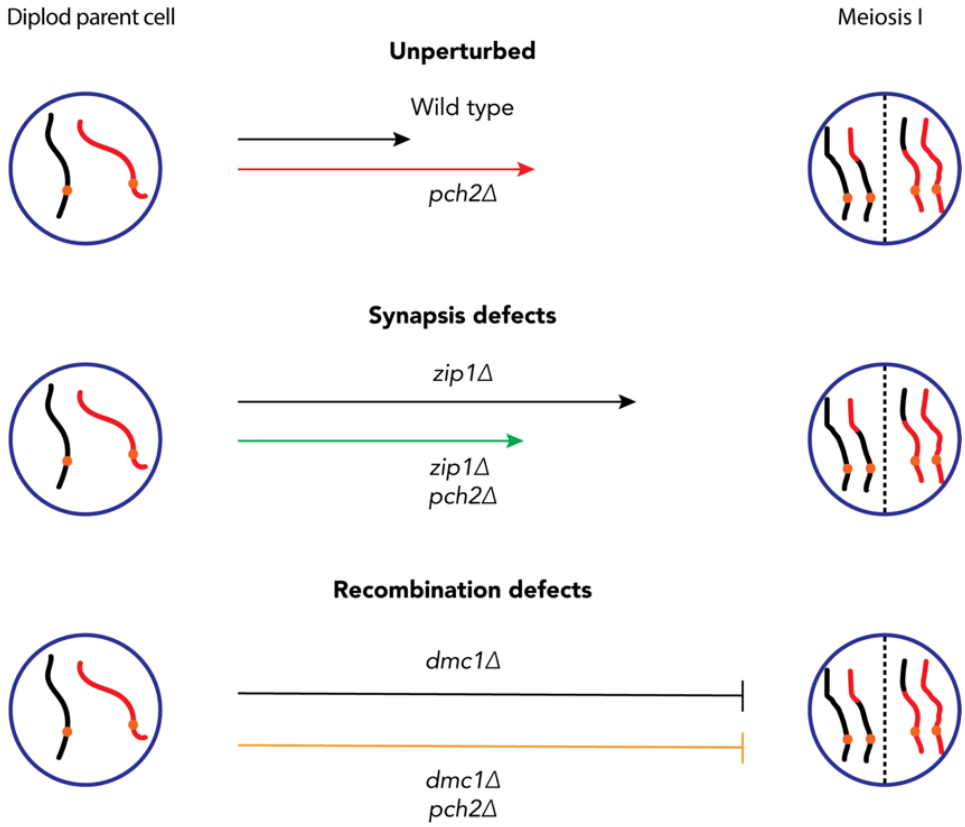

Figure 1.8: **Paradoxical roles of Pch2 in cellular progression during meiotic prophase**
Image showing different consequences of deletion of *PCH2* in different conditions on meiotic progression. The length of the arrow represents the time spent in meiotic prophase (arrows are not in scale among each other). Under unperturbed conditions, *pch2Δ* delays the meiotic progression. On the contrary, *pch2Δ* results in the alleviation of the meiotic delay caused due to synapsis defects (like *zip1Δ*). Additionally, deletion of *PCH2* has no effects on the arrest of meiotic progression caused due to recombination defects (like *dmc1Δ*).

1.8 Objectives

Pch2 and Hop1 form a AAA+ HORMA module, which acts as the master regulator of meiotic processes taking place during prophase. The interplay between Pch2 and Hop1 is responsible for regulating DSBs, establishing interhomolog bias, crossover control, synaptonemal complex polymerization, regulating checkpoint activity among others (Vader 2015). Chromosomal axis formation, which encompass Hop1, is important for synaptonemal complex polymerization. Pch2, in turn, regulates the chromosomal abundance of Hop1. This raises a question as to whether Pch2 also plays a role in regulating the SC polymerization. Hop1 is a central player in the meiotic checkpoint network. Phosphorylation of Hop1 by Mec1/Tel1 kinases are important for the activation of effector kinase Mek1 (Carballo et al. 2008; Acosta, Ontoso, and San-Segundo 2011; Chuang, Cheng, and Wang 2012; Niu et al. 2005; Niu et al. 2009; Wu, Ho, and Burgess 2010). Hop1 is able to transduce the checkpoint signal emanating from both synapsis and recombination defects (Wu and Burgess 2006; Wu, Ho, and Burgess 2010). However, Pch2 is thought to play a role in relaying the signal originating only from synapsis defects.

With the overarching objective of expanding the understanding of Pch2-Hop1 AAA+ HORMA module during the meiotic processes, I aimed to decipher:

- How the interplay between Pch2 and Hop1 regulate the synaptonemal complex polymerization,
- Why and how, Pch2 is able to differentiate between synapsis and recombination defects, and finally
- How Pch2 and Hop1 regulate the meiotic checkpoint network.

The ultimate goal of this doctoral work is to establish a unified model which could explain the seemingly paradoxical roles of Pch2 during meiotic prophase checkpoint.

Chapter 2
Material And Methods

2.1 Materials

2.1.1 Consumables and chemicals

Unless otherwise mentioned, chemicals and reagents were purchased from Applied Biosystems, Biorad, Difco, Invitrogen, Merck, New England Biolabs, Promega, Roth, Roche, Serva, Sigma and VWR. For all methods described, sterile solutions, deionized sterile water and sterile flasks were used. Important consumables and chemicals used in this work are listed in Table 2.1

Table 2.1: Important consumables and chemicals

Chemicals, enzymes and reagents	***Supplier***
Alpha factor	In-house
BglII and AscI restriction enzymes	New England BioLabs
Citric acid	Sigma-Aldrich
cOmplete Mini, EDTA-free protease inhibitor	Roche
D-Sorbitol	Sigma-Aldrich
ECL prime/select Western Blotting detection reagent	GE Healthcare
Formaldehyde, methanol free	Polysciences
Glusulase	Perkin-Elmer
Glycerol	Gerbu Biotechnik
Lithium acetate dihydrate	Sigma-Aldrich
Magnesium chloride	J.T. Baker Chemicals
Methanol	Sigma-Aldrich
Milk powder blocking grade	Carl Roth
Midori Green advanced DNA stain	Nippon Genetics
PTFE printed 30-well glass slide	Electron Microscopy Sciences
Poly-L-Lysine (0.01%)	Sigma-Aldrich
Proteinase K	VWR
Photo-Flo 200	Kodak

Chemicals, enzymes and reagents	***Supplier***
Potassium acetate	Carl Roth
RNase A	Sigma-Aldrich
Sheared Salmon sperm DNA	Thermo-Fischer
Sodium azide	Sigma-Aldrich
SYTOX Green nucleic acid stain	Life technologies
TaKaRa Ex Taq®	TaKaRa Bio
Trichloroacetic acid	Sigma-Aldrich
Tris	Carl-Roth
Tween-20	Applichem
Vectashield mounting medium with 4',6-Diamidine-2'-phenylindole dihydrochloride (DAPI)	Vector Laboratories
Zymolyase-100T	Amsbio
[α-^{32}P]-dCTP	Perkin-Elmer
β-Estradiol	Sigma-Aldrich

2.1.2 Commercial kits

Commercial kits used in this study are listed in Table 2.2

Table 2.2: Commercial kits

Commercial kits	***Supplier***
QIAquick Gel Extraction Kit	Qiagen
QIAprep Spin Miniprep Kit	Qiagen
Wizard® SV Gel and PCR Clean-Up system	Promega

2.1.3 Antibodies

The primary and secondary antibodies used in this study are listed in Table 2.3 and Table 2.4 respectively.

Table 2.3: Primary Antibodies

Antigen	***Origin***	***Dilution***		***Supplier***
		WB	***IF***	
Flag M2	Mouse (Monoclonal)	1:1000	---	Sigma-Aldrich
Hop1	Rabbit	1:10000	1:200	*(Cardoso da Silva, Villar-Fernández, and Vader 2020)*
Phospho Histone H3 Threonine-11	Rabbit (Polyclonal)	1:1000	---	Abcam
Cdc5 (4F10)	Mouse (Monoclonal)	1:1000	---	Médimabs
Zip1	Goat	---	1:100	Santa Cruz Biotechnologies
GFP (clones 7.1 and 13.1)	Mouse (Monoclonal)	---	1:50	Sigma-Aldrich
GFP	Rabbit	1:5000	---	Made in house
Gmc2	Mouse	---	1:200	(Voelkel-Meiman et al. 2019)
Pgk1	Mouse (Monoclonal)	1:5000	---	Invitrogen
Alpha-Tubulin (YOL1/34)	Rat (Monoclonal)	---	1:100	Santa Cruz Biotechnologies
Histone H3	Rabbit polyclonal	1:1000	---	Invitrogen

Table 2.4: Secondary Antibodies

Antigen	***Origin***	***Dilution***	***Supplier***
HRP-conjugated α-mouse	Sheep	1:10000	GE/Amersham
HRP-conjugated α-rabbit	Donkey	1:10000	GE/Amersham
Alexa 488-conjugated α-mouse	Donkey	1:250	Bethyl Laboratories Inc
FITC-conjugated α-rat	Donkey	1:200	Jackson ImmunoResearch

Antigen	*Origin*	*Dilution*	*Supplier*
Alexa 488-conjugated α-goat	Donkey	1:500	Bethyl Laboratories Inc
Texas Red (594) dye-conjugated α-rabbit	Donkey	1:500	Bethyl Laboratories Inc

2.1.4 Media, buffers and solutions

All types of media, buffers and solutions used are listed with the corresponding method.

2.1.5 Yeast strains

All yeast strains used in this study are of SK1 background and their genotypes are listed in Table 8.1 (Appendices).

2.1.6 Oligonucleotides

Synthetic oligonucleotides were used for Polymerase Chain Reaction (PCR)-based epitope tagging of genes, confirmation of markers associated with genes, creating genes with different promoters and nested PCR for southern blot experiments. All oligonucleotides were supplied by Sigma-Aldrich. A list of synthetic oligonucleotides used in this study are listed in Table 2.5.

Table 2.5: Oligonucleotides

Name	*Sequence (5'-3')*
GV3, forward *PCH2*-check	gcc cgt agc cga aat gac tcc
GV9, forward *DMC1*-check	gat att ctt ccc tgg aag cgc
GV10, reverse *DMC1*-check	ata tgg cgt tag gta atg ctc
GV147, *YCR047C* probe F-out	ttg ttt tcg ccg ctg atc
GV148, *YCR047C* probe R-out	gaa gtt ggg caca at atc
GV149, *YCR047C* probe F-nested	gga att ccg aga gaa tcg act tgc taa
GV150, *YCR047C* probe R-nested	gga att cca gcc acc agt ggg ctt ttc
GV999, reverse *PCH2* check	gc gcc tcc gtt ggt gga tcc
GV2428, forward *pFA6a-F2-HA-MSH4*	aaa tta aaa gaa ata aac tcc gac ttc atc gaa aat ttt gaa gaa cgg atc ccc ggg tta att aa

Name	***Sequence (5'-3')***
GV2429, reverse *pFA6a-R1-HA-MSH4*	aca gaa ata atg gat tat agt ttt aag cta agc gga aaa gcc aaa gaa ttc gag ctc gtt taa ac
GV2446, forward *MSH4*-check	cca taa acc aaa tga aga g
GV2447, reverse *MSH4*-check	cta tct act gag acc atg tg
GV2510, forward *pGAL1-3X-FLAG-PCH2* tagging	tca taa aaa tat tct gat ctc aaa ctg aag aca taa aat aag gat gaa ttc gag ctc gtt taa ac
GV2511, reverse *pGAL1-3X-FLAG-PCH2* tagging	aac cct cag aga tga tcc tcg cac ttg tag gtc aac tat gta gct tcc acc ccc gcc tcc

2.1.7 Online tools and softwares

For database search regarding gene and protein sequence, online services were provided by the *Saccharomyces Genome Database* (http://www.yeastgenome.org/). The software listed in Table 2.6 were used for analysis of data and for preparing figures.

Table 2.6: Softwares

Software	***Version***	***Supplier***
Illustrator CC 2019	23.1.1	Adobe
Photoshop CC 2019	20.0.6	Adobe
Image Lab	5.2.1 build 11	Bio-Rad Laboratories
FIJI/ImageJ	2.0.0-rc-69/1.52p	National Institutes of Health
Excel	16.16.26	Microsoft
Word	16.16.25	Microsoft
Prism 8	8.3.0	GraphPad Software
SoftWorX	6.1.1	GE Healthcare Life Sciences
Imaris	7.3.4	Oxford instruments
FlowJo	10.2	FlowJo LLC

2.2 Microbiological methods

2.2.1 Cultivation and storage of yeast strains

Depending on the experimental procedure, yeast strains were cultivated on solid or liquid media under non-selective conditions. Liquid media used in this work are detailed in Table 2.7. For preparation of solid media, liquid media was supplemented with 2% (w/v) agar. Cells grown on solid media were incubated in HerathermTM incubators (Thermo Fisher Scientific) at 30^{o}C. Cells grown in pre-sporulation (BYTA) and sporulation media (SPO) were provided adequate aeration by making sure the total volume of flask was at least 10 times the volume of media. All liquid yeast cultures were grown either on an InnovaTM 2000 (New Brunswick Scientific) platform shaker or on a Multitron® shaker (Infors HT) at 30^{o}C with shaking at 180 rpm.

For selection of yeast strains containing antibiotic resistance markers, G418 (geneticine disulfate) or NAT (nourseothricin) was added to YPD media at 300 and 100 mg/mL respectively and supplemented with 2% agar. For selection of auxotrophic yeast strains, minimal (MIN) media was supplemented either with amino acids such as arginine, histidine, leucine, lysine, tryptophan, or with nucleotide precursors such as uracil and adenine.

For long term storage of yeast strains, cells were grown on a YPG-agar overnight at 30°C and resuspended in 1 mL of sterile 15% glycerol in a screw cap microcentrifuge tube. The content of the tube was thoroughly mixed and immediately frozen at -80°C. YPG-agar plates, containing non-fermentable carbon as the source media, are used to ensure the proper maintenance of mitochondria.

The frequently used liquid media for growing yeast cultures along with their composition are listed in Table 2.7.

Table 2.7: Liquid media for yeast cultures

Media	***Composition***	***Final concentration***
Yeast peptone dextrose (YPD)	Bactopeptone Yeast extract L-Tryptophan D-Glucose	2% (w/v) 1% (w/v) 0.015% (w/v) 2% or 4 % (w/v)
Yeast peptone glycerol (YPG)	Bactopeptone Yeast extract L-Tryptophan Glycerol	2% (w/v) 1% (w/v) 0.015% (w/v) 3% (v/v)
Pre-sporulation Buffered-YTA (BYTA)	Yeast extract Bactotryptone Potassium acetate Potassium phthalate	1% (w/v) 2% (w/v) 1% (w/v) 50mM
Sporulation (SPO)	Potassium acetate Acetic acid	0.3% (w/v) 5% (v/v)
Minimal (MIN)	Difco yeast nitrogen without AA and AS Ammonium sulfate Inositol D-Glucose	0.15% (w/v) 0.5% (w/v) 2 mM 2% (w/v)

2.2.2 Polymerase Chain Reaction

Polymerase Chain Reaction (PCR) is used to amplify fragments of DNA. This technique relies on the thermostable polymerase and requires DNA primers for the amplification of the region of interest. In this study, PCR was used to amplify DNA templates for transformation of *Saccharomyces cerevisiae* in order to perform genetic micromanipulations. The temperature for primer annealing and time for elongation steps were adjusted according to the primer composition and template length, respectively. A standard PCR mix for a total reaction volume of 50μL and a standard thermal cycling program for PCR are shown in Table 2.8 and Table 2.9 respectively.

Table 2.8: PCR mix (50μL total volume)

Component	***Volume***
60-100ng DNA template	1μL
20μM forward primer	2.5μL
20μM reverse primer	2.5μL
10mM dNTPs	4μL
10x ExTaq buffer	5μL
TaKaRa Ex Taq polymerase	0.4μL
Deionized water	34.6μL

Table 2.9: Thermal cycling program for PCR

Reaction step	***Temp (°C)***	***Time (s)***
1. Initial Denaturation	94	120
2. Denaturation	94	60
3. Primer annealing	55	30
4. Elongation	72	60 (Loop back to step 2 for 30 cycles)
5. Final Elongation	72	120
6. Hold	4	∞

2.2.3 Agarose Gel Electrophoresis

The method of agarose gel electrophoresis is employed to separate nucleic acid molecules depending on their molecular size. Upon application of electric current across the agarose gel, the negatively charged DNA molecules migrate towards the anode with lower sized DNA molecules migrating faster. The separated DNA fragments are visualized under ultraviolet light using fluorescent DNA intercalating dye. In this doctoral work, most of the gel electrophoresis was carried out using 1% (w/v) agarose gels, except when purification by gel extraction was done, for which 0.8% (w/v) agarose gels were used. Agarose gels were prepared by dissolving agarose in 1x TAE buffer and adding Midori Green advanced DNA stain (Nippon Genetics) at 1:25000 dilution. Prior to loading the samples on the gel, they were mixed with DNA loading dye. Electrophoresis was carried out in Agarose gel system (Carl Roth) at 100V

with 1x TAE as the electrolyte. Composition of buffers used in agarose gel electrophoresis is provided in Table 2.10.

Table 2.10: Solutions for agarose gel electrophoresis

Name	***Composition***
TAE (50x)	50mM Tris, 57.1mL glacial acetic acid, 500mM EDTA pH 8, fill up to 1L with H_2O
DNA loading dye (6x)	0.4% (w/v) Orange G, 30% (v/v) glycerol, 10mM Tris- HCl, 25mM EDTA

2..2.4 DNA Extraction from gels

Extraction of DNA from the agarose gels was carried out using the Gel Extraction and PCR purification kit as per manufacturer's instructions (Table 2.2).

2.2.5 Transformation of competent bacterial cells

50μL of chemically competent *E. Coli* OmniMax cells (provided by Department of Protein Facility, Max Planck Institute of Molecular Physiology, Dortmund) was thawed on ice and 100ng of DNA added. The suspension was gently mixed and incubated on ice for 30min. Cells were then heat-shocked at 42°C for 45 sec and immediately kept on ice for 2 mins. 300μL of liquid Luria-Bertani (LB) media was added and kept at 37°C for 40mins at constant shaking. The transformation mix was then platted onto a LB-agar plate containing appropriate antibiotic selection. The composition of LB-media and LB-agar is provided in Table 2.11.

Table 2.11: Media for bacterial growth

Name	***Composition***
LB-medium	10 g/L Bacto-tryptone, 5 g/L yeast extract, 10 g/L NaCl Autoclaved, pH 7.4
LB-agar	LB-medium + 1.5% (w/v) Bacto Agar

2.2.6 Plasmid isolation from bacterial cells

Plasmid isolation from bacterial cells was performed using the mini-prep plasmid isolation kit (Table 2.2.) according to manufacturer's instructions.

2.2.7 Genomic DNA isolation, digestion and Southern Blotting

10mL of meiotic cultures were collected at desired time points, centrifuged at 3000rpm for 3 minutes and stored at -20°C. All the samples were processed together after collection of the last time point. Pellets were resuspended in spheroplasting buffer supplemented with β-mercaptoethanol and 250µg/mL Zymolyase 100T and spheroplasted for 45 minutes at 37°C. Lysis of spheroplasts was done by addition of 100µL of lysing buffer and incubation at 65°C for 2 hours. Lysates were centrifuged at 14000 rpm for 20 minutes at 4°C, and supernatant was then added to 750µL of 100% ethanol. The precipitate was centrifuged at 14000 rpm for 20 minutes at 4°C and the pellet was resuspended in 750µL TE containing 50µg/mL of RNase A (Sigma Aldrich) by incubation at 37°C for 30 minutes followed by incubation at 4°C for 14 hours. Next day, 500µL of phenol/chloroform/isopropanol (25:24:1; Carl Roth) was added to the samples and gently mixed by inverting the microfuge tubes 60 times. The mixture was centrifuged at 14000 rpm for 10 minutes at 4°C and 600µL of the upper transparent phase, which contains DNA, was added to 750µL of isopropanol. The suspension was centrifuged at 14000 rpm for 10 minutes at 4°C, washed with 70% ethanol and centrifuged again at the same conditions to recover DNA. DNA was resuspended in 125µL TE.

30µL of 10x NEB buffer (homemade without BSA) and 232.5µL of water were added to 35µL of genomic DNA and digested by incubation at 37°C for 4 hours after addition of 2.5µL of HindIII restriction enzyme (NEB). Digested DNA was subjected to precipitation by addition of 25µL 3M NaOAc, pH 5.5 and 650µL ethanol and incubating the mixture at -20°C for 30 minutes. Precipitated DNA was centrifuged at 14000 rpm for 10 minutes at 4°C and the pellet was resuspended in 15µL TE.

Prior to agarose gel electrophoresis, 5µL of loading buffer was added to resuspended DNA. The gel electrophoresis was performed in an Owl A2-BP large gel system (Thermo Fisher Scientific) on a 0.6% SeaKem LE agarose (Lonza) gel for 16 hours at 70V with TBE buffer as electrolyte. The gel was stained in an Ethidium bromide bath for 30 minutes at room temperature and DNA visualized by UV light. The agarose gel was then incubated with 0.25M HCl for 40 minutes with gentle shaking followed by denaturation of DNA by incubation with 0.4M NaOH for 35 minutes. On an inverted gel tray in the Owl A2-BP large gel system, 20x35 cm of Whatman filter paper

was placed and the wick was wetted with 0.4M NaOH. Two gel-sized pieces of Whatman paper soaked in NaOH were then placed on the wick followed by placing the gel and a HybondXL membrane (GE Healthcare) pre-soaked in water on top. Two more Whatman papers were placed on the membrane and surrounded by Parafilm on the edges. 20 paper towels were placed on top and the whole apparatus was left overnight to achieve sufficient transfer of DNA. Next morning, the membrane was washed in 50mM sodium phosphate buffer, pH 7.2 for 30 minutes. Membranes were pre-hybridized with 20mL of hybridization solution and 300µL of denatured salmon sperm DNA for at least 30 minutes at 65°C in an HB-1000 hybridization oven (Analytik). DNA probe *YCR047C* (Chromosome III; 209361-210030), amplified from genomic DNA by nested PCR with primers GV147/GV148 and GV149/GV150, was labelled with [α-^{32}P]-dCTP (Perkin Elmer) using the Prime-It RmT Random Primer labeling Kit (Agilent technologies). Labelled probes, after purification using illustra ProbeQuant G-50 Micro column (GE Healthcare), were denatured for 10 minutes at 95°C and subsequently cooled to 4°C. Denatured probe was hybridized with the membrane at 65°C for 14 hours. This was followed by the wash of membrane once with 120mL low stringency SSC buffer for 15 minutes and once with 120mL of high stringency SSC buffer for 30 minutes at 65°C. Typhoon TRIO imager (GE Healthcare) was used to quantitate the hybridization signal and DNA double-strand breaks were quantified using Fiji/ImageJ software. Composition of buffers used in this assay is provided in Table 2.12.

Table 2.12: Buffer compositions for DNA isolation, digestion and Southern blotting

Name	***Composition***
Spheroplasting Buffer	1M Sorbitol, 42mM K_2HPO_4, 8mM KH_2PO_4, 5mM EDTA
Lysing Buffer	0.5M Tris pH 8, 0.25M EDTA, 3 %SDS
TE	10mM Tris pH 8, 1 mM EDTA
Hybridization solution	0.25mM Sodium Phosphate pH 7.2, 0.25M NaCl, 1mM EDTA, 7 % SDS, 5% Dextran Sulphate
Low stringency SSC buffer	0.3M NaCl, 30mM Sodium citrate, 0.1 % SDS
High stringency SSC buffer	15mM NaCl, 1.5mM Sodium citrate, 0.1 % SDS

2.2.8 Construction of yeast strains

2.2.8A Yeast DNA transformation

Prior to DNA transformation, yeast cells were made competent for transformation by treating them with Lithium acetate (LiAc). In this method, cells were prepared and suspended in a LiAc solution, along with the DNA to be transformed and an excess of carrier DNA. Polyethylene glycol (PEG) was added and the yeast cells then incubated at 30°C, followed by a heat-shock at 42°C that allows the DNA to enter the cells.

A yeast pre-culture was prepared by inoculating 50mL of liquid YPD media with desired yeast strain growing on a YPD plate. The pre-culture was grown overnight to saturation at 30°C at 180rpm shaking in a Multitron® shaker (Infors HT). Next morning, cells were diluted 1:50 in fresh liquid YPD media. Yeast culture was grown till OD_{600} reached 0.6-0.8 (for ~4 hours) and cells harvested by centrifugation at 3500 rpm for 5 minutes at room temperature. Supernatant was removed and cells were washed two times with 500µL LiAc-Sorbitol solution (1M LiAc,1M Sorbitol). Cells were then resuspended in 500µL LiAc-Sorbitol solution. The transformation mix was set up in a microfuge tube by adding 20µL of DNA, 15µL of Salmon sperm DNA (after heating at 95°C for 5 minutes and cooling on ice), 280µL of 50% PEG4000, and 100µL of cell suspension. The transformation mix was vortexed well and incubated at room temperature for 45 minutes with constant rotation. 40µL of DMSO was added to each sample and incubated at 42°C for 15 minutes. If the transformation construct contained drug resistance markers then 1mL of YPD was added to cells and incubated at 30°C for 2 hours with constant shaking. For auxotrophic markers, samples were immediately centrifuged at 3500 rpm for 5 minutes at room temperature, resuspended in 300µL YPD and plated on desired agar plates.

2.2.8B Deletion mutants and epitope tagging by homologous recombination

PCR-based strategy was employed to create all deletion mutants and for epitope tagging of endogenous genes (Longtine et al. 1998; Knop et al. 1999). For this method, PCR products were used to transform competent yeast cells. To allow homologous recombination with the endogenous locus of a gene, PCR products were generated using primers that contain sequences for amplification of special cassettes (including the marker gene) as well as sequences complementary to the gene of

interest. For gene deletions, the forward primer contains 45bp of the promoter sequence 5' of the start codon (ATG) of the respective gene, while the reverse primer includes 45bp of the terminator sequence 3' of the stop codon. For C-terminal epitope tagging of a gene, a forward primer containing 45bp 5' of the stop codon were used instead. PCR products were purified and concentrated after amplification using ethanol precipitation, and competent yeast cells transformed and plated on selection plates. The correct recombination was confirmed by diagnostic PCR using specific oligonucleotides (Table 2.5) for gene deletions and Western blot for epitope tagging.

2.2.8C Construction of an inducible *FLAG-PCH2* strain

The *GAL1*-promoter drives robust gene expression when bound by Gal4 transcription factor. The *GAL1*-promoter was used to create the inducible system of expression of N-terminally *FLAG*-tagged *PCH2*. The *GAL4* was fused to a domain of the estrogen receptor (ER), which sequesters the Gal4-ER protein in the cytoplasm. β-estradiol binds to the ER domain of Gal4-ER and facilitates its translocation from the cytoplasm to the nucleus (Benjamin et al. 2003; Louvion, Havaux-Copf, and Picard 1993)

For estradiol-dependent induction of *PCH2*, a *pGAL1*-promoter fusion with *3XFLAG-6XGLY-PCH2* was made as follows: a construct containing *pGAL1* along with a 3xFLAG epitope and 6x Glycine linker flanked with BglII and AscI (*BglII-pGAL-3xFLAG-6xGLY-AscI*; pGV867) restriction sites were custom synthesized into pUC57 plasmid by *Genewiz Inc*. The construct was recloned into a pFA6a-based precursor plasmid carrying *HIS3MX* (*pFA6a-His3MX6-PGAL1-3XFLAG-6GLY*; pGV876) Standard PCR-based one step promoter replacement strategy was employed using this construct as the template and primers (GV2510) and (GV2511).

2.2.8D Mating of haploid *S. cerevisiae* strains

Diploid yeast strains were generated by mating two haploid strains of the opposite mating type (*MATa* and *MATα*) on the YPD-agar plates. Cells from the two haploids were scraped with a sterile toothpick from a YPD plate, with more cells from the *MATa* mating-type than *MATα*. Next day, the mating mixture was streaked onto a YPD-plate containing well-spread *α*-factor (10 µg/ml). After two days at 30°C, single

shiny colonies were picked and patched onto a YPD-agar plate and grown overnight at 30°C. Diploid strains were selected from haploid cells by replica plating onto minimal (MIN) agar plates. Yeast cells were replica-plated onto MIN plates and MIN plates with 600µL of *MATa*/*MATα* yeast cells (tester strains) suspended in liquid YPD media evenly spread. Plates were grown overnight at 30°C. This approach is based on the ability of the tester strains (which contain a single auxotrophic marker) to complement the nutritional requirements of strains of the opposite mating type. This nutritional deficiency is complemented by the uncharacterized strains, which cannot grow on MIN plates due to auxotrophy. Diploid strains are distinguished by their inability of growing in any of the MIN / MIN plus tester strain plates (unless the resultant diploid strain contained all the markers that confer prototrophy).

2.2.8E Determination of mating type

Tester strain of known mating type containing single auxotrophic requirement, not present in other strain, was employed to know the mating type of uncharacterized strains. The genetic deficiency in the tester strain prevents it from growing on MIN plates. To know the mating type of an uncharacterized strain, a small amount of tester strain was resuspended in 200µL of YPD and evenly spread on a MIN plate. Uncharacterized strains were replica plated on it. Since uncharacterized strains themselves contained one or more auxotrophic mutations, only diploids resulting of mating between opposite mating types could grow on MIN plates. Growth on plates supplemented with *MATa* tester strain indicated that the uncharacterized strain was of *MATα* mating type, and vice versa.

2.2.9 Growth conditions for synchronous meiosis

For yeast growth, cells were always incubated at 30°C, unless otherwise mentioned. For synchronous entry of cells into meiosis, desired yeast strains were first patched on YPG-agar plates from glycerol stocks and grown overnight in a Heratherm incubator (Thermo Scientific). Cells were then transferred from YPG-agar to YPD-agar plates and again grown overnight. On the following day, liquid YPD media was inoculated with cells growing on YPD-agar plate and cells grown till saturation, generally for 24 hours at constant shaking at 180rpm. Cells were then diluted to OD_{600} of 0.3 in pre-sporulation BYTA media and grown for 16-18 hours with constant shaking of 180rpm in a Multitron incubator (Infors HT). Cells corresponding to OD_{600} of 1.9 were

then centrifuged, washed twice with water and resuspended in sporulation (SPO) media. Meiotic samples were collected at desired time points. The point of resuspension in SPO media was considered time t=0.

For experiments with estradiol dependent induction of *FLAG-PCH2*, β-estradiol to a final concentration of 1μM was added to the meiotic SPO culture at the desired time point to induce the expression of the protein.

2.2.10 Dissection of tetrads

Dissection of tetrads was done to obtain yeast strains with desired genotypes or to perform spore viability tests. Tetrads were obtained 24 hours after the induction of meiosis in SPO media. Samples for dissection were prepared by collecting 150μL of meiotic culture and adding an equal volume of Zymolyase 100T (10mg/mL) followed by incubation at 37°C for 20-30 minutes. 500μL of water was added to the sample and 60μL of diluted culture was then placed in a line at the center of YPD-agar plate. Yeast strains were dissected using a dissection microscope (Nikon Eclipse Ci, Schuett-biotec). The YPD-agar plated were then incubated at 30°C for growth of the dissected spores.

2.3 Biochemical techniques

2.3.1 Sodium dodecyl sulphate polyacrylamide gel electrophoresis (SDS-PAGE)

SDS-PAGE is a method used to quantitively analyze protein mixtures. In this method, SDS containing loading buffer is added to the samples. SDS denatures proteins and confers a net negative charge by binding uniformly along the length of the polypeptide chain. Prior to loading samples in the polyacrylamide gels, the samples are heated at 95°C for 5 mins. Heating the samples disrupts higher-order protein structures thereby facilitating the uniform binding of SDS. The samples are then subjected to the application of an electric field across the polyacrylamide gel. This causes the negatively charged polypeptides to move towards the anode and hence allows the separation of the proteins according to their molecular weight. Electrophoresis was performed in an electrophoresis chamber (Bio-Rad) at 100-120V in 1x SDS-running buffer for 1.5-2 hours. The choice of the polyacrylamide

concentration to be used depends on the molecular weight of the protein to be analyzed. SDS-PAGE resolved proteins were used for further analyses by western blotting. For most experiments in this doctoral work, 10% (v/v) gels were prepared except when expression of Histone H3 or phospho-Histone H3 Threonine-11 was checked. In these cases, 15% (v/v) gels were used. The recipe for preparation of 5mL and 10 mL of stacking and resolving gels, respectively, is provided in Table 2.13 and composition of buffers used in SDS-PAGE is provided in Table 2.14.

Table 2.13: Composition of SDS-PAGE gels

Component	***Resolving gel (10%)***	***Resolving gel (15%)***	***Stacking gel (5%)***
Water	4mL	2.3 mL	3.4 mL
30% acrylamide/ 0.8% Bisacrylamide mix	3.3mL	5 mL	0.83 mL
1.5M Tris pH 8.8	2.5mL	2.5 mL	-----
1M Tris pH6.8	-----	-----	0.63 mL
10% SDS	0.1mL	0.1 mL	0.05 mL
10% ammonium persulfate (APS)	0.1 mL	0.1 mL	0.05 mL
Tetramethylethylenediamine (TEMED)	0.004 mL	0.004 mL	0.005 mL

Table 2.14: Buffer compositions for SDS-PAGE

Name	***Composition***
SDS running buffer	25mM Tris-HCl, 192mM Glycine, 0.1% SDS (w/v)
SDS loading buffer (5x)	5mM EDTA, 60mM Tris-HCl pH6.8, 250mM DTT, 15% (w/v) SDS, 30%(v/v) glycerol, 0.1%(w/v) bromophenol blue

2.3.2 Western Blotting

Western blotting is performed to detect the presence of specific proteins within a mixture. The negatively charged proteins from SDS-polyacrylamide gel are transferred to a positively charged nitrocellulose membrane (BioTraceNT nitrocellulose

membrane; Pall corporation) by the application of an electric current across the western blot transfer apparatus (Mini-PROTEAN II Cell, BioRad). The wet transfer was performed at 350mA at 4^{o}C for 90 minutes in western transfer buffer.

After completion of the transfer of proteins, the nitrocellulose membrane was blocked using 5% (w/v) skimmed milk in Phosphate Buffered Saline 0.1% Tween (PBS-T) for 45 minutes at room temperature on a rocking platform See-saw SSL4 (Stuart See-saw rockers, Cole Parmer). For the immunoblot of proteins using phosphorylation-specific antibodies, 5% (w/v) bovine serum albumin (BSA) in Tris buffered Saline 0.1% Tween (TBS-T) was used. Blocking of the membrane was followed with an incubation using the appropriate dilution of the primary antibody in 5% (w/v) milk or 5% (w/v) BSA overnight at 4^{o}C. The membrane was then subjected to 3 washes of 15 minutes each with either PBS-T or TBS-T to remove remaining traces of primary antibody. This was followed by incubation of the membrane with the appropriate dilution of the horseradish peroxidase (HRP)-conjugated secondary antibody. The membrane was again washed for 20 minutes with either PBS-T or TBS-T for 3 times. Chemiluminescence with ECL Prime or ECL Select Western Blotting Detection Reagent (GE Healthcare) was used according to manufacturer's instructions to detect the protein signal on the membrane. Images were acquired using ChemiDoc MP Imaging System (BioRad). Composition of buffers used for western blotting procedure is shown in Table 2.15.

Table 2.15: Buffer compositions for Western Blotting

Name	***Composition***
Western transfer buffer	25mM Tris, 190mM Glycin, 10%(v/v) Methanol
Phosphate Buffered Saline	137mM NaCl, 2.7mM KCl, 10mM Na_2HPO_4, 2mM KH_2PO_4
Tris Buffered Saline	25mM Tris-HCl pH 7.4, 137mM NaCl, 2.7mM KCl

2.3.3 Chromatin fractionation assay

Chromatin fractionation assay was employed to differentiate between the chromosomal and non-chromosomal pool of proteins by performing standard western blotting technique. For performing this assay, 100mL of meiotic culture was collected at the desired time points and cells were harvested by centrifugation at 3000rpm for 3

minutes. Cell pellets were washed once in Buffer A and then resuspended in 1mL of buffer B. Zymolyase T100 was added to a final concentration of 1mg/mL and cells were spheroplasted for 30 minutes at 37°C. Spheroplasted cells were collected by centrifugation at 2000 rpm for 5 minutes and washed once with 1.2M Sorbitol. Cells were then resuspended in 250μL buffer C and incubated on ice for 5 minutes. At this point, 50μL of total lysate was collected, and remaining suspension was centrifuged at 14000 rpm for 20 minutes at 4°C. The supernatant, corresponding to the soluble fraction, was collected and the pellet was washed twice with 300μL of buffer C. Pellet was resuspended in 200μL buffer C; this suspension corresponded to the chromatin fraction. All the fractions were precipitated by adding 10% trichloroacetic acid and incubating on ice for 30 minutes. Precipitated protein samples were centrifuged at 14000rpm for 15 minutes at 4°C and washed with 1mL ice-cold 100% Acetone. Pellets were resuspended in resuspension buffer and analyzed by SDS-PAGE followed by western blotting. The composition of all the buffers used in this protocol is listed in Table 2.16.

Table 2.16: Buffer compositions for chromatin fractionation assay

Name	***Composition***
Buffer A	150mM NaCl, 50mM NaF, 10mM EDTA, 1mM NaN3
Buffer B	100mM Pipes pH6.9, 1mM EGTA, 1mM $MgCl_2$, 1.2M Sorbitol
Buffer C	25mM MOPS pH7.2, 15mM $MgCl_2$, 15mM EGTA, 1.2M Sorbitol, 0.5% Triton X-100, 1mM dithiothreitol, 60mM β-glycerophosphate, With freshly added: 0.2 mM Na_3VO_4, 1mM PMSF, 1 Complete Mini EDTA-free (Roche) pil/10 ml, Protease Inhibitor-Mix HP Plus (Serva), and 1 PhoSTOP (Sigma-Aldrich) pil/10 ml
Resuspension buffer	7M Urea, 2% SDS, 50mM Tris pH7.5

2.3.4 Trichloroacetic acid precipitation of native yeast extracts

For preparation of total cell extracts, 3mL of meiotic samples were collected at the indicated time points and cells harvested by centrifugation at 3000rpm for 5 mins

in a tabletop centrifuge (Centrifuge 5810R, Eppendorf, Hamburg, Germany). Cells were then immediately frozen at -20°C and all samples were processed together after collecting the last time point. Cell pellets were treated with 5mL of ice-cold 5% trichloroacetic acid (TCA) and incubated on ice for 10 min followed by centrifugation for 3 min at 4 °C, 3000 rpm. Cells were washed with 1 ml of ice-cold acetone and the pellet was air-dried overnight in the hood. Completely dried pellets were resuspended in 200μL Tris-DTT buffer (Tris pH 7.4, 50mM EDTA, 5mM dithiothreitol) and lysed using glass beads on a FastPrep-24 5G (MP Biomedicals). 50μL of 5X-SDS loading buffer was added and samples boiled at 98°C for 5 mins. Samples were then subjected to standard SDS-PAGE, and western blotting techniques, followed by incubation of samples with antibodies.

2.3.5 Co-Immunoprecipitation from native yeast extracts

Co-immunoprecipitation (Co-IP) experiment was performed to investigate protein-protein interaction. At the desired time point, 100mL of meiotic culture was collected and cells harvested by centrifugation at 3000 rpm for 3 minutes. Cells were washed with ice-cold water and pellets were either snap-frozen in liquid nitrogen for later use or processed immediately. Pellet was resuspended in 200μL Co-IP lysis buffer supplemented with protease inhibitors, and cells broken with acid-washed glass beads (Sigma Aldrich) using bead beater (FastPrep24, MP Biomedicals) two times for 60 seconds at speed 6. Samples were cooled on ice for 5 minutes in between the two runs. The lysate was centrifuged at 500 rpm for 1minute at 4°C and supernatant transferred to a fresh microfuge tube. Chromatin in the lysate was sheared by sonication two times by constant pulses of 15 seconds each using Branson Sonifier 450 at setting 2. The sonicated lysate was subjected to high-speed centrifugation at 15000 rpm for 20 mins at 4°C. Supernatant was then transferred to a new microfuge tube and 50μL of the supernatant collected as input. The remaining suspension was incubated with 1μL of α-HA antibody for 3 hours with continuous rotation at 4°C. After antibody incubation, 25μL of washed magnetic Dynabeads protein G (Invitrogen) were added to the lysate and incubated for three hours with constant rotation at 4^0C. The beads were then spun down at 1000rpm for 2 minutes at 4°C and washed three times with 500μL lysis buffer. Beads were resuspended in 50μL of 5X SDS-loading buffer (Table 2.16). The input samples were subjected to TCA precipitation by addition of 10% TCA, followed with a wash with ice-cold 100% acetone. The pellet was

resuspended in 50µL resuspension buffer (Table 2.16). Samples were then subjected to SDS-PAGE, followed by western blotting.

Table 2.17: Lysis Buffer composition for Co-IP assay

Name	***Composition***
Co-IP lysis buffer	50mM Tris-HCl pH 7.4, 150mM NaCl, 1% Triton X-100, 1mM EDTA with freshly added: 1mM PMSF, 1 Complete Mini EDTA-free (Roche) pil/10ml, and Protease Inhibitor-Mix HP Plus (Serva)

2.4 Cell biological techniques

2.4.1 Flow cytometry

The method of flow cytometry was employed to assess the DNA content and infer the synchronized cell cycle progression of the meiotic cultures. In this method, 150µL of the meiotic culture was collected generally at 0, 3 and 4 hours post-induction of meiosis and fixed for at least 2 hours by addition of 350µL of 100% ethanol. Fixed samples were centrifuged at 7000 rpm for 2 min and cells incubated with 500µL 50mM sodium citrate with 0.7µL RNase A (30mg/mL; Sigma-Aldrich) for a minimum of 2 hours at 50^{o}C. 10µL of Proteinase K (20mg/mL; VWR) was added and cells incubated at 50^{o}C for a minimum of 2 hours again. DNA was stained by adding 500µL of 50mM sodium citrate containing 0.2µL of SYTOX Green (Life technologies). Prior to analysis on the BD Accuri C6 flow cytometer (BD Biosciences), samples were subjected to sonication for 10 seconds at the lowest output on a Branson sonifier 450 to disrupt cell clumps. The FlowJo software was used to analyze the DNA histograms.

2.4.2 Surface spreading of chromosomes and immunofluorescence

To investigate the chromosomal localization of proteins, meiotic chromosomes were surface spread on glass slide and the desired proteins visualized by performing indirect immunofluorescence. At desired time points, 2mL of meiotic culture was collected, 1% sodium azide added and stored on ice. All samples were processed together after collection of the last time point. The meiotic culture was centrifuged at 2200 rpm for 2 minutes and cells were treated with 500µL of 200mM Tris pH7.5 containing 20mM dithiothreitol (DTT) for 2 min at room temperature. Cells were then

subjected to spheroplasting for 20 minutes at 30°C using spheroplasting buffer. The spheroplasts were then gently washed with 1mL ice-cold MES-Sorbitol solution by inverting the microfuge tube multiple times. After two washes, cells were resuspended in 55µL of the MES-Sorbitol solution. 20µL of the resuspended spheroplasts was placed on ethanol cleaned and air-dried glass slides. 40µL of the fixing solution was added to the cells on slide, and 80µL of 1% Lipsol was immediately added to it. The contents were gently mixed. After one minute, 80µL of the fixing solution was added and the contents on the slide were spread using a clean glass rod to mechanically spread the chromosomes. The samples were kept overnight in a flow hood to dry and then either stored at −20 °C for future use or processed immediately for immunofluorescence. To perform immunofluorescence, slides were gently washed with 0.4% (v/v) Photoflo (Kodak) diluted in PBS for 3 minutes followed by a wash with PBS for 5 minutes in Coplin jars. The samples were then blocked with 5% (w/v) BSA in PBS for 15 minutes at room temperature. Incubation with desired primary antibodies at appropriate dilution was performed overnight in a humidified chamber at 4°C. The slides were then washed two times with gentle shaking for 10 minutes each with PBS. This was followed by incubation of the samples with fluorescent-conjugated secondary antibody at appropriate dilution for 3 hours at room temperature. The slides were washed twice and mounted with glass coverslips using 20µl of Vectashield mounting media containing DAPI (Vector Laboratories). For both, primary and secondary antibody incubations, parafilm was used instead of coverslips. The composition of all the solutions used in chromosome spread assay is shown in Table 2.18.

Table 2.18: Buffer compositions for meiotic chromosome spreads

Name	***Composition***
Spheroplasting buffer	1M Sorbitol, 2% potassium acetate, 0.13µg/µL zymolyase
MES-Sorbitol solution	1M Sorbitol, 0.1M MES pH6.4, 1mM EDTA, 0.5mM $MgCl_2$
Fixing solution	3% paraformaldehyde, 3.4% sucrose

2.4.3 Whole-cell immunofluorescence

Whole-cell immunofluorescence was performed to investigate the entry of cells into meiosis I by visualizing the spindle morphology at different time points during meiotic progression. For performing immunofluorescence, 300 µL of meiotic culture

was collected at the desired time points and treated with 1% sodium azide. All samples were processed together after collection of the last time point. Cells were harvested by centrifugation at 3000rpm for 3 minutes and fixed overnight by resuspension in fixing solution. Next day, cells were washed 3 times with 0.1M K_2HPO_4, pH6.4 and resuspended in 1mL 1.2M sorbitol-citrate solution. Cells were centrifuged and resuspended in 200µL of 1.2M sorbitol-citrate solution. 20µL of glusulase (Perkin Elmer) and 6µL of Zymolyase were added to it and cells were spheroplasted for 2 hours at 30 °C with gentle rotation. After spheroplasting, cells were washed once with 1.2M sorbitol-citrate solution and resuspended in 30µL of the same. In the meantime, wells of a PTFE-printed glass slide were treated with 5µL of 0.01% poly-L-Lysine (Sigma Aldrich) for 10 mins and washed once by immersing the slide in a Coplin jar filled with distilled water. 5 µL of cells were then allowed to settle down on a poly-L-lysine treated dried well of the glass slide for 10 minutes. Excess liquid was removed and samples were treated with ice-cold methanol for 3 minutes immediately followed by a 10 seconds treatment with ice-cold 100% acetone. Glass slides were air-dried completely and samples incubated with 4 µL of α-Tubulin antibody at appropriate dilution for 90 minutes. Wells were washed thrice with PBS by placing a 5µL drop of PBS on the well and removing it carefully making sure the pipette tip does not touch the well. This was followed by a one-hour incubation with 4µL of FITC-labelled secondary antibody at appropriate dilution. Samples were again washed 4 times with PBS in the same manner as before. Finally, coverslips were mounted using 1µL per well of Vectashield mounting media containing DAPI (Vector Laboratories) for staining DNA. Cell cycle progression was checked by counting cells showing separated spindle poles by using tubulin stained samples. A minimum of 200 cells were counted for each time point. Compositions of all the solutions used in whole-cell immunofluorescence assay are shown in Table 2.19.

Table 2.19: Buffer compositions for whole-cell immunofluorescence

Name	***Composition***
Fixing solution	3.7% formaldehyde, 0.1M K_2HPO_4 pH6.4
Sorbitol-citrate solution	1.2M sorbitol, 0.1M K_2HPO_4, 0.04M citric acid

2.4.5 Microscopy and cytological analysis

Images of the meiotic surface spread chromosomes were acquired using 100x 1.42 NA PlanApo-N objective (Olympus) on a DeltaVision imaging system (GE Healthcare) equipped with an sCMOS camera (PCO Edge 5.5) at room temperature. In general, 10 images of serial z-stacks with 0.2 µm thickness were obtained and deconvolved using SoftWoRx software. Quantifications for Zip1, Hop1 and Gmc2 intensity on the images of surface spread chromosomes were done using Imaris software (Bitplane). To identify the DNA, the 'Surface' function was applied to the deconvolved raw images on DAPI channel. Values corresponding to the sum total fluorescence intensity of all the channels and volume within the surface selected were obtained. The 'Spots' function was used to calculate the background. Three spots were manually placed in a region that lacked DNA. The average background intensity was adjusted for volume. This value was subtracted from the chromosomal intensities corresponding to values of respective proteins in order to obtain a sum of total fluorescence intensity corrected for the background. Scatter plots were generated using Prism 8 (GraphPad). Statistical significance was determined by performing Mann-Whitney U-test. For representative images, Fiji/ImageJ software was used to obtain maximum intensity projection images.

Chapter 3
Results

During meiotic prophase, chromosomal processes like recombination and synaptonemal complex (SC) assembly ensure the necessary tight association between homologous chromosomes. Polymerization of the SC, of which Zip1 forms the central component, is a marker of progression through meiotic prophase. It leads to the synapsis of homologous chromosomes and is indispensable for the faithful segregation of chromosomes. SC is scaffolded onto the chromosome axis which is decorated with stretches of Hop1. SC polymerization is also required for the recruitment of Pch2 to the chromosomal regions (apart from the nucleolar region). Chromosomal Pch2 actively removes Hop1 from the axis sites and thus modulates the abundance of Hop1 on chromosomes. The requirement of chromosomal axis for SC establishment and the function of Pch2 in regulating axis composition raises a question as to whether Pch2 also plays a role in regulating SC assembly. Therefore, I initially aimed to explore the role of Pch2 in SC assembly by investigating the functional relationship between Pch2, Hop1 and Zip1.

3.1 Pch2 restricts higher chromosomal abundance of Zip1

With the aim to understand if SC polymerization is regulated by Pch2, I performed indirect immunofluorescence on surface spread of meiotic chromosomes in strains that are wild type or lack *PCH2*. For examining the levels of SC polymerization, a functional GFP-tagged allele of *ZIP1* (White et al. 2004) was utilized. Pch2, Hop1 and most of the components of SC, including Zip1, are meiosis-specific proteins whose expression levels peak around pachytene stage of meiotic prophase (San-Segundo and Roeder 1999; Hollingsworth, Goetsch, and Byers 1990; Sym, Engebrecht, and Roeder 1993). Once cells exit prophase, the expression level of all these proteins declines. I employed strains harboring a deletion of the transcription factor *NDT80*, absence that lead cells to arrest in meiotic prophase, with the repair of DSBs taking place up to the stage of double Holliday junction formation (Xu et al. 1995). In agreement with published literature, increased chromosomal levels of Hop1 were observed on meiotic chromosome spreads from *pch2Δ* cells, as compared to the wild type (Figure 3.1A and 3.1B). I also observed a significant increase in the chromosomal

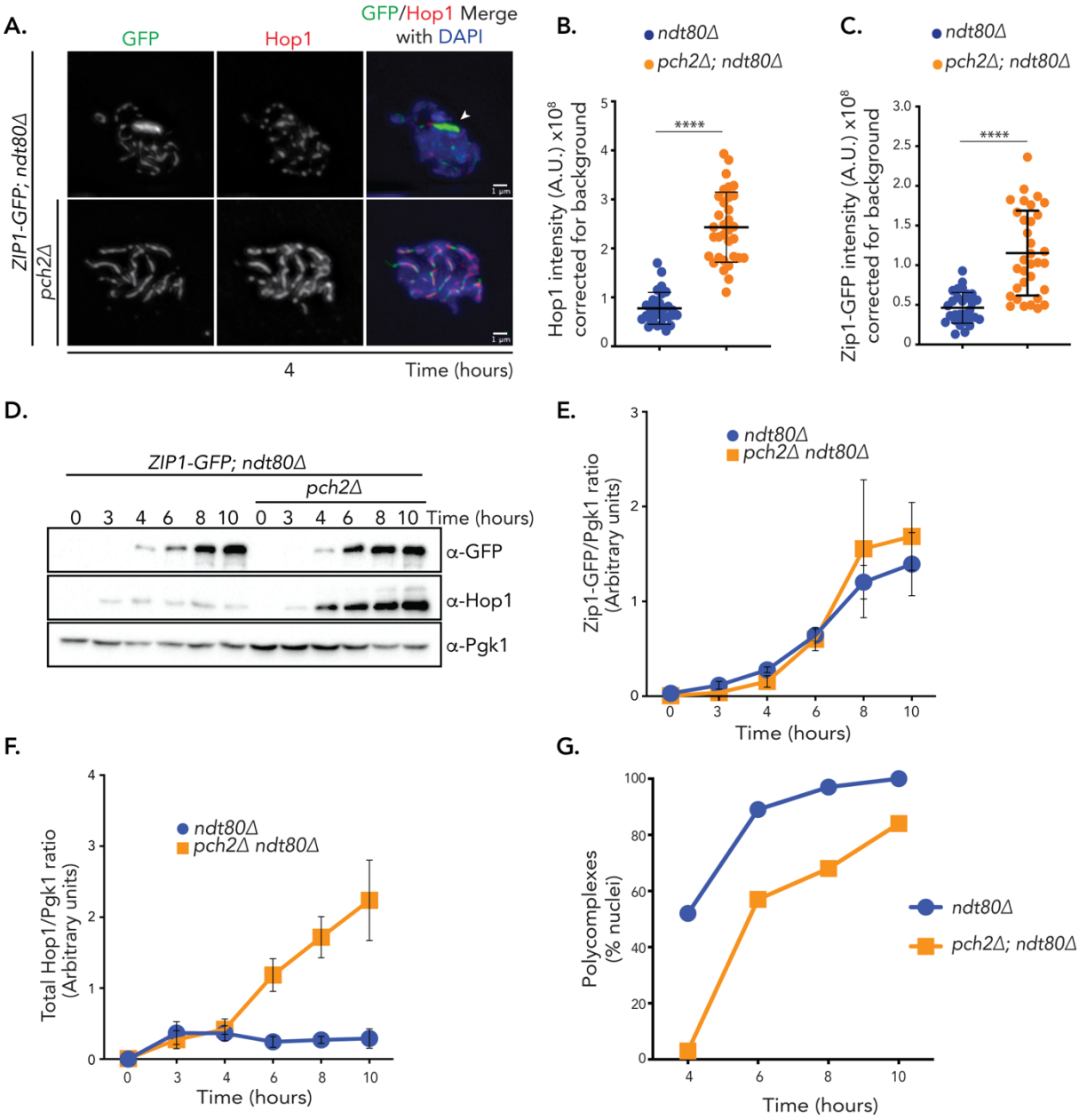

Figure 3.1: **Pch2 regulates synaptonemal complex assembly**
A. Zip1-GFP (green) and Hop1 (red) immunofluorescence images of meiotic chromosome spreads from *ndt80Δ* (yGV4463) and *pch2Δ ndt80Δ* (yGV4504) cells. Polycomplex (PC) is indicated by the arrowhead. DNA is stained with DAPI. Scale bar is 1μm. **B.** and **C.** Quantification of the total sum intensity after background correction of chromosomal Hop1 and Zip1-GFP from meiotic spreads of strains used in (A). Number of analyzed cells n=30 and n=33 for *ndt80Δ* and *pch2Δ ndt80Δ* respectively. **** indicates a significance with $p \leq 0.0001$, Mann-Whitney U test. Mean and standard deviation are indicated. **D.** Western blot analysis of strains used in (A) comparing total cellular levels of Zip1-GFP (α-GFP) and Hop1 at different time points during meiotic time course. Pgk1 is used as a loading control. **E.** and **F.** Quantification of the total cellular levels of Zip1-GFP and Hop1 from the western blots shown in (D). Mean value ± SEM from three independent experiments is indicated. **G.** Percentage of PC

Figure 3.1 continued
containing nuclei from strains used in (A) at different time points during meiotic time course. >100 nuclei were analyzed for each data point.

association of Zip1 in strains lacking Pch2 as compared with those having a wild type allele of *PCH2* (Figure 3.1A and 3.1C). This suggests that Pch2 regulates the chromosomal abundance of both Hop1 and Zip1. To investigate whether the observed increase in chromosomal levels of Hop1 and Zip1 was due to changes in total cellular levels of these proteins, I performed western blot analysis of total cellular lysates from *ndt80Δ* and *pch2Δ ndt80Δ* cells (Figure 3.1D). Although an increase in the total cellular levels of Hop1 - which correlates with the detected increase in its chromosomal levels was observed in *pch2Δ* cells - such difference was not observed in the total cellular levels of Zip1 (Figure 3.1E and 3.1F). These data indicate that Pch2 influences SC polymerization by restricting the abundance of Zip1 localization on chromosomes.

SC components are known to form extra-chromosomal aggregates, known as Polycomplexes (PCs), in response to defects in DSB formation and/or its processing (Hughes and Hawley 2020; Sym and Roeder 1995). Overexpression of Zip1 also leads to the formation of a PC (Sym and Roeder 1995; Dong and Roeder 2000). There is evidence that PCs are also observed in cells lacking *NDT80*, especially in strains of the SK1 background (as used throughout this study), which are otherwise wild type (Bhuiyan, Dahlfors, and Schmekel 2003). In line with this, I observed that PCs were present in *ndt80Δ* cells (Figure 3.1A and 3.1G). Approximately 50% of *ndt80Δ* cells showed the presence of a PC 4 hours post-induction of meiosis. The percentage of nuclei containing PC increased as cells spent more time in meiotic prophase (Figure 3.1G). Intriguingly, the number of cells containing PCs was lower in *pch2Δ* cells. The difference in PC abundance between wild type and *pch2Δ* cells was most striking when I compared cells at 4 hours post-induction of meiosis. Although *pch2Δ* cells also accumulate PCs as they spent more time in meiotic prophase, the number of cells containing PCs remained lower in *pch2Δ ndt80Δ* cells as compared to *ndt80Δ* cells (Figure 3.1G).

Although Zip1-GFP has been well characterized (White et al. 2004), it is not known if this allele leads to the untimely formation of PCs. To confirm that the presence of PCs is not an artefact of Zip1-GFP, I performed indirect immunofluorescence on

meiotic chromosome spreads from strains harboring an untagged allele of *ZIP1* in an *ndt80Δ* background using α-Zip1 antibody at 4 and 10 hours post-induction of meiosis (Figure 3.2A). Similar to strains with Zip1-GFP, I observed that approximately half of these cells contained PCs at 4 hours post-induction of meiosis. This percentage increased to ~90% at 10 hours post-induction of meiosis. Reassuringly, deletion of *PCH2* led to a decrease in the number of cells showing PC formation, as observed earlier in the *ZIP1-GFP* background. *pch2Δ ndt80Δ* cells displayed behavior similar to *ZIP1-GFP pch2Δ ndt80Δ* cells, and accumulated PCs by 10 hours post-induction of meiosis. However, the total number of cells showing PC formation was reduced as compared to *ndt80Δ* cells alone (Figure 3.2B). These data show that formation of PCs is not a consequence of the GFP-tag on Zip1, and thus likely indicative of a physiologically relevant phenomenon.

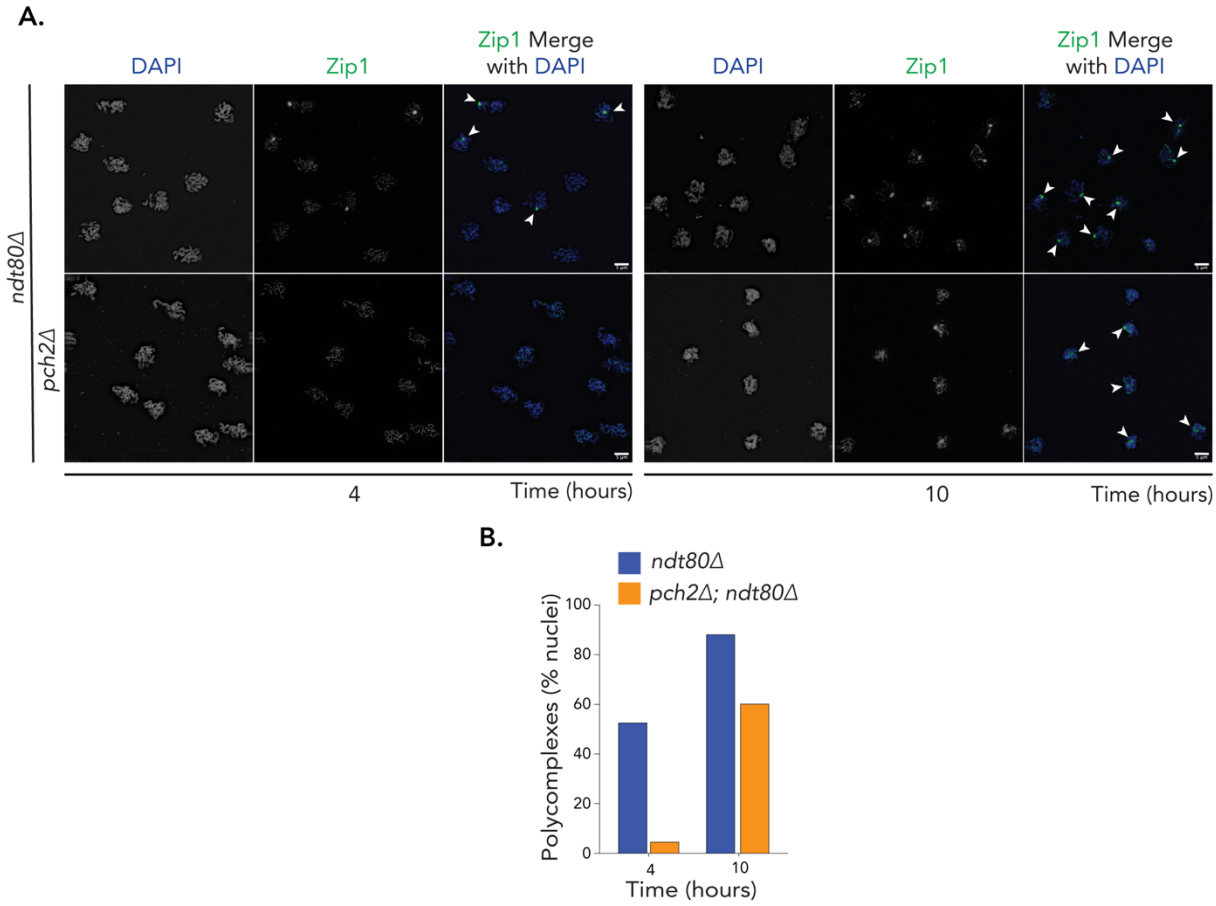

Figure 3.2: ***pch2Δ* results in a lower abundance of PC containing cells**
A. Representative images of meiotic chromosome spreads from *ndt80Δ* (yGV468) *and pch2Δ ndt80Δ* (yGV2302) stained for Zip1 (α-Zip1, green) at 4 and 10 hours post-induction of meiosis. **B.** Quantification of PC containing nuclei from strains used in (A) at indicated time points. >100 nuclei were analyzed for each data point.

The difference in the percentage of cells containing PC with and without the presence of Pch2 demonstrates that Pch2 not only regulates the assembly of Zip1 on chromosomes but also the extra-chromosomal assembly of Zip1 aggregates. Pch2 can either directly influence the formation of PCs or indirectly lead to the formation of PCs.

3.2 Pch2 does not influence PCs triggered by DSB/recombination defects

SC polymerization is a marker of normal meiotic progression. During early meiosis, SC is deposited onto chromosomes in a foci-like manner. As meiosis progresses, the appearance of SC changes to short polymerized stretches and finally culminates with extensive SC polymerization along entire chromosomes during pachytene. Aberrant SC polymerization in response to defects in DSB formation or repair results in the formation of extra-chromosomal PC formation. To investigate whether the appearance of PCs as observed here, was associated with aberrant chromosomal SC polymerization, I investigated the proportion of cells in different stages of Zip1 polymerization in *ndt80Δ* and *pch2Δ ndt80Δ* strains. SC status was classified into three classes, namely, foci-like staining (Class I), short stretches (Class II) and extensive polymerization of Zip1 (Class III), as is customary in the literature (Figure 3.3A) (Bailis and Roeder 1998). Both *ndt80Δ* and *pch2Δ ndt80Δ* strains showed similar behavior of Zip1 polymerization. After 4 hours post-induction of meiosis, both strains showed around 80% of cells with extensive Zip1 polymerization, which increased as cells spent more time in meiosis (Figure 3.3B). This suggests that the formation of PCs in these strains (see above) is not the result of aberrant synapsis and or defective DSB repair. Moreover, PCs were mostly observed in cells exhibiting Class III SC-polymerization, confirming that PC formation in these cases is not due to defective SC polymerization. Of note, all the PC quantifications as presented here were done with cells presenting a PC staining along with Class III Zip1 polymerization.

The observation that *pch2Δ ndt80Δ* cells showed a delayed appearance of PCs as compared to *ndt80Δ* cells is counterintuitive because *pch2Δ* cells are known to exhibit a delay in the repair of DNA DSBs (Borner, Barot, and Kleckner 2008; Joshi et al. 2015). Hence, if PCs observed were merely a consequence of DSB repair delays/defects, one would actually expect more PCs in *pch2Δ* cells, contrary to what I observed here. This further strengthens the idea that PC formation in these cases is not a consequence of defective DSB repair and suggests that Pch2 plays a role in

influencing the abundance of PCs in wild type conditions. To understand the role that Pch2 plays in influencing the PC abundance, I employed a catalytically dead mutant of Spo11 (*spo11-Y135F*). This mutant is unable to generate DSBs which results in the formation of PCs (Henderson and Keeney 2004; Cha et al. 2000). Indeed, most of these mutants showed a prevalence of PCs. Deletion of *PCH2* did not alleviate the formation of PCs in this strain background suggesting Pch2 does not play a direct role in the formation of PCs and does not have any effect on PC formation that is associated with defective DSB formation (Figure 3.3C and 3.3D). These data thus raise an interesting question as whether there is a crosstalk between the chromosomal and extrachromosomal pool of Zip1, which results in the formation of PCs, and if, and how, Pch2 plays a role in its regulation.

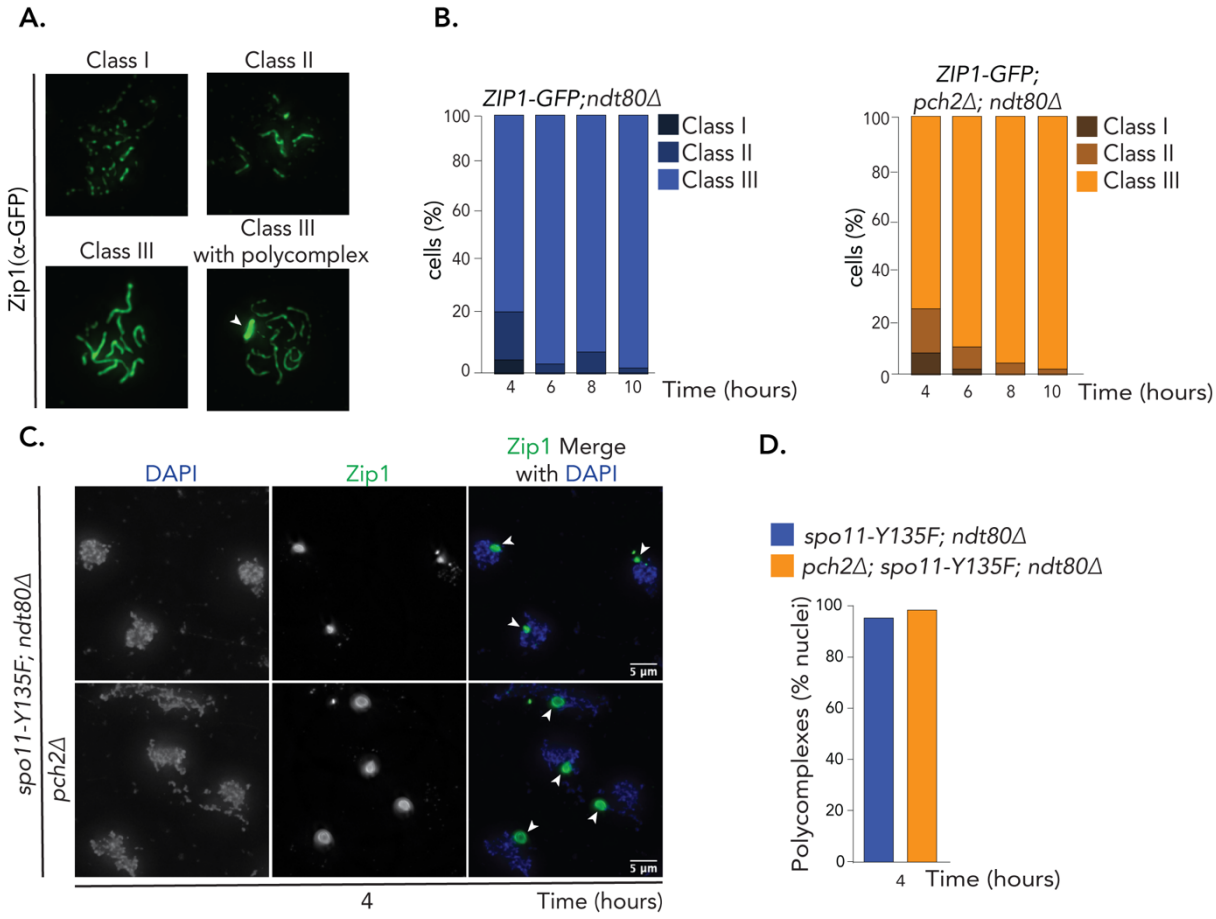

Figure 3.3: **Pch2 has no effect on PCs arising due to pathological defects.**
A. Representative images of nuclei at different stages of SC polymerization during meiotic progression. Class I shows foci-like staining, Class II shows short stretches of SC, and Class III represents extensive Zip1 polymerization along chromosomes. PC quantifications are done in cells showing PC (indicated with an arrowhead) along with Class III-like staining. Images are from *ZIP1-GFP, ndt80Δ* (yGV4463). **B.** Comparison of the percentage of cells showing different extents of Zip1 polymerization divided into

Figure 3.3 continued
Class I, II and III from *ndt80Δ* (yGV4463) and *pch2Δ ndt80Δ* (yGV4504). A minimum of 150 cells were analyzed for each data point. **C.** Representative images showing Zip1(α-Zip1, green) and DNA (DAPI, blue) staining on chromosome spreads to compare the effects of Pch2 in strains harboring the catalytically dead mutant of Spo11 (*spo11-Y135F*) at 4 hours post-induction of meiosis. Strains used are *spo11-Y135F*, *ndt80Δ* (yGV4137) and *spo11-Y135F, pch2Δ, ndt80Δ* (yGV4119) **D.** Quantification of cells containing PCs from strains used in (C) 4 hours post-induction of meiosis. More than 100 nuclei were analyzed.

3.3 Dynamic interplay of Pch2, Hop1 and Zip1 regulates SC polymerization

In *ndt80Δ* cells, total cellular levels of Zip1 increases as a function of time spent in meiotic prophase (Figure 3.1D). The increase in Zip1 levels correlates with an increase in the number of cells harboring PCs (Figure 3.1E and 3.1G). Also, *pch2Δ* cells show a reduced prevalence of PCs with an increase in the chromosomal occupancy by Zip1 (Figure 3.1C and 3.1G). This prompted me to hypothesize that PC formation can be interpreted as a proxy of the remaining excess of Zip1 available in the nucleoplasm after the successful establishment of SC along the chromosomes. To test this hypothesis, I reasoned that the number of cells showing PCs should decrease if the total levels of Zip1 is lowered. To test this premise, I decreased the total levels of Zip1 by making use of a heterozygous deletion of *ZIP1* (Figure 3.4A and 3.4B). I observed that the reduction of Zip1 led to a decrease in the number of cells showing PCs, thus confirming that the total levels of Zip1 are indeed functionally related to PC establishment (Figure 3.4C). The profile of PC abundance in cells with reduced levels of Zip1 over the meiotic time course was very similar to *pch2Δ* cells (Figure 3.4C). Deletion of *PCH2* along with lower levels of Zip1 led to a synergistic decrease in the number of cells showing PC formation (Figure 3.4C). This indicated that the decrease in total levels of Zip1 reduces the pool available for the formation of PC, which in turn affect efficiency of PC formation. Ostensibly, this pool is reduced further in *pch2Δ* cells, potentially because in cells that lack Pch2 more Zip1 can be deposited on chromosomes (Figure 3.1A and 3.1C).

Hop1 is important for the proper establishment of chromosome axis, which in turn acts as the loading platform for deposition of SC (Page and Hawley 2004). In the absence of Hop1, polymerization of SC does not take place resulting in the formation of extrachromosomal PCs (Carballo et al. 2008; Hollingsworth and Byers 1989). I

posited that the increased chromosomal association of Zip1 in cells lacking *PCH2* as seen here might be driven by the increased abundance of chromosomal Hop1 brought about by the lack of Pch2-dependent chromosomal removal, as is well-established (San-Segundo and Roeder 1999; Subramanian et al. 2016; Joshi et al. 2009). I reasoned that decreasing the total cellular levels of Hop1 might decrease the amount of Zip1 that can be deposited on chromosomes, which should thus be reflected in a higher prevalence of PCs, even in *pch2Δ* cells. To test this, I employed the same strategy as used earlier for Zip1, by using heterozygous *HOP1* strains (*i.e. HOP1/hop1Δ*) to decrease the total cellular levels of Hop1 (Figure 3.5A and 3.5B). Decreasing the total cellular levels of Hop1 in strains deleted for *PCH2*, indeed led to an increase in the number of cells containing PCs (Figure 3.5A and 3.5C). As expected, reduction of total cellular Hop1 levels correlated with the decrease in chromosomal

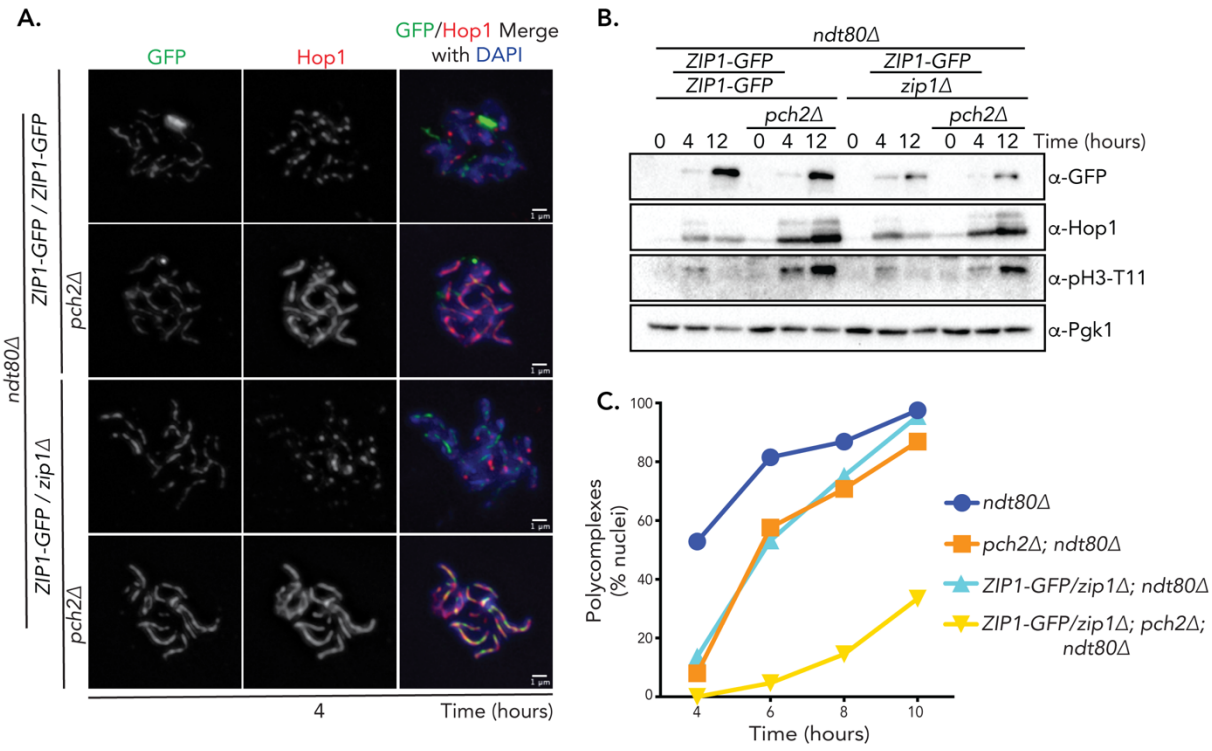

Figure 3.4: **Total Zip1 levels determine the presence of PC**
A. Representative immunofluorescence images of Zip1-GFP (green) and Hop1 (red) from the meiotic chromosome spreads belonging to *ndt80Δ* (yGV4463), *pch2Δ ndt80Δ* (yGV4504), *ZIP1-GFP/zip1Δ ndt80Δ* (yGV4609) and *ZIP1-GFP/zip1Δ pch2Δ ndt80Δ* (yGV4608) at indicated time point. **B.** Western blot analysis of the strains used in (A) comparing the total cellular levels of Zip1-GFP, Hop1 and pH3-T11 at different time points during the meiotic time course. Pgk1 is used as loading control. **C.** Comparison of the nuclei containing PCs at indicated time points in strains used in (A). >100 nuclei were analyzed for each data point.

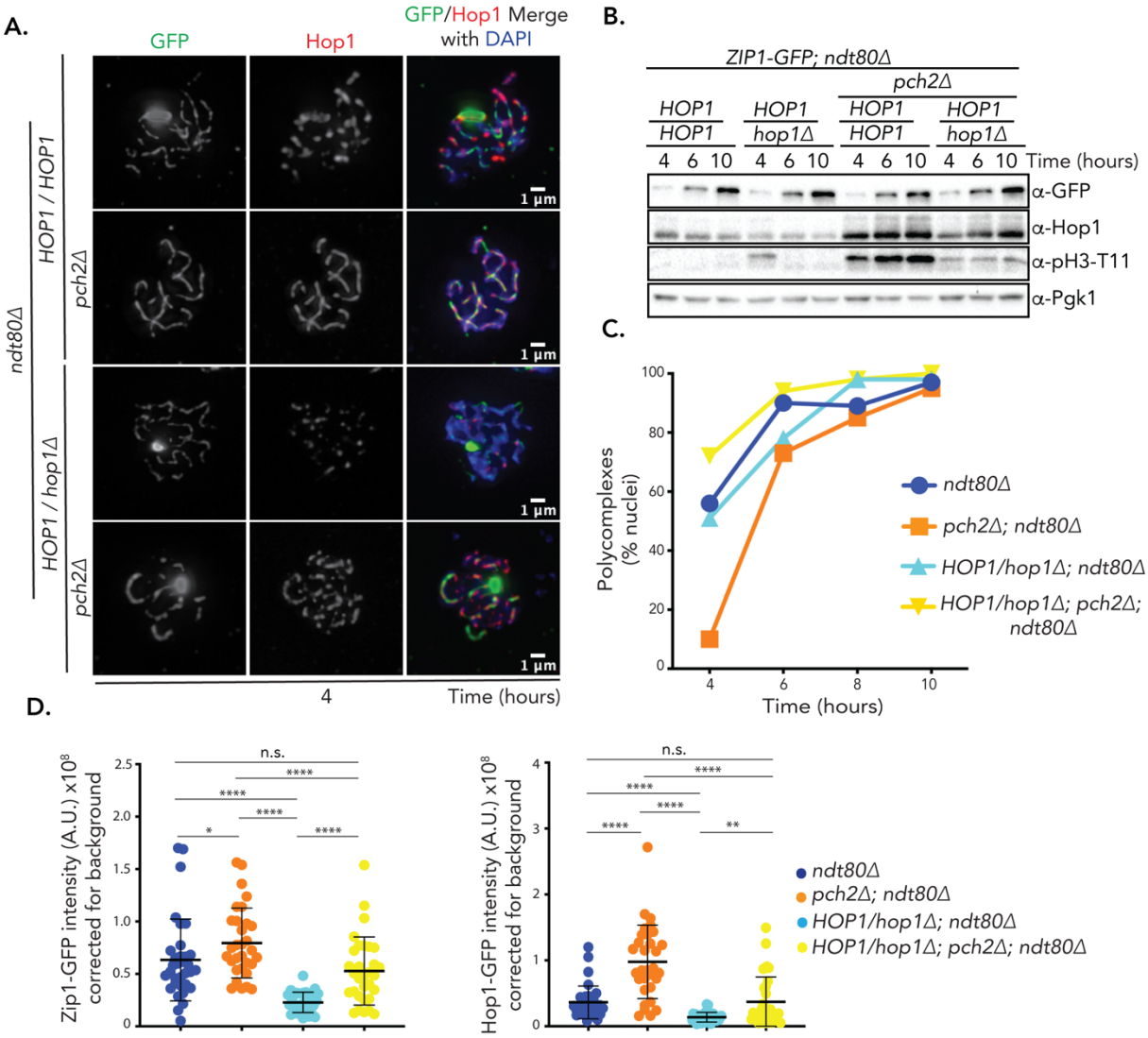

Figure 3.5: **Cellular levels of Hop1 regulate SC polymerization and formation of PCs**

A. Representative images of Zip1-GFP (green) and Hop1 (red) immunofluorescence from meiotic chromosome spreads of *ndt80Δ* (yGV4463), *pch2Δ ndt80Δ* (yGV4504), *HOP1/hop1Δ ndt80Δ* (yGV4461) and *HOP1/hop1Δ, pch2Δ, ndt80Δ* (yGV4505) cells at the indicated time points. **B.** Expression analysis of Zip1-GFP, Hop1 and pH3-T11 using western blot analysis of the strains used in (A) at different time points during the meiotic time course. Pgk1 is used as the loading control. **C.** Comparison of the PC containing nuclei at different time points during meiotic time course from strains used in (A). >100 nuclei were analyzed for each data point. **D.** Quantification of the total sum intensity after background correction of chromosomal Hop1 and Zip1-GFP from meiotic spreads of strains used in (A). Number of cells analyzed: n=33, n=31, n=31 and n=31 for *ndt80Δ, pch2Δ ndt80Δ, HOP1/hop1Δ ndt80Δ* and *HOP1/hop1Δ pch2Δ ndt80Δ*, respectively. **** indicates a significance with $p \leq 0.0001$, ** is $p \leq 0.01$ and * is $p \leq 0.05$. Mann-Whitney U test. Mean and standard deviation are indicated.

abundance of Hop1. This decrease also correlated with a decrease of Zip1 levels on chromosomes suggesting a causal relationship between chromosomal Zip1 and PC abundance (Figure 3.5D). Interestingly, western blot analysis of whole-cell extracts showed that in *pch2Δ* strains with lowered levels of Hop1, the phosphorylation of Histone H3 at Threonine 11 (pH3-T11), a substrate of active Mek1, was substantially decreased. Active Mek1 is indicative of ongoing checkpoint activity, and this observation thus indicated that checkpoint activity in *pch2Δ* strains with lowered levels of Hop1 was not as robust when compared to *pch2Δ* cells alone (Figure 3.5B). This observation provided me with a platform to understand the functional relevance of the Pch2 and Hop1 levels in meiotic prophase and in the regulation of the checkpoint cascades governing this phase of the meiotic program.

In total, the data presented in the part of the thesis suggest that the existence of a functional connection between Pch2, Hop1 and Zip1 governs Zip1-dependent SC polymerization and the formation of extrachromosomal PCs. In this system, Hop1 forms the chromosome axis, which acts as the loading platform for Zip1. Chromosomal polymerization of Zip1 subsequently recruits Pch2, which results in the removal of chromosomal Hop1. The removal of Hop1 from the chromosome axis provides a feedback to further restrict the polymerization of Zip1. Thus, Pch2 acts as the factor which dynamically coordinates SC assembly with the chromosomal localization of Hop1 (Figure 3.6).

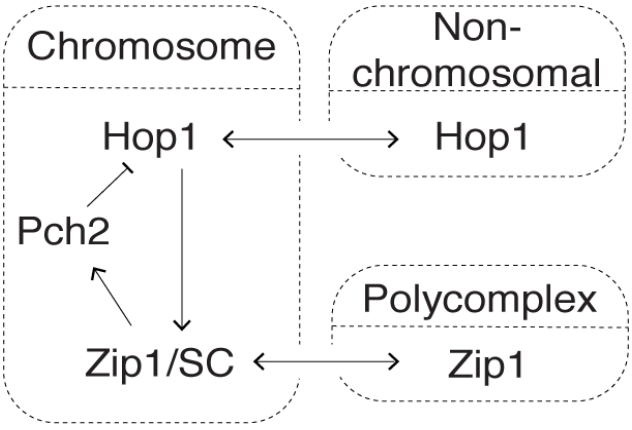

Figure 3.6: **Model of the feedback regulation of Pch2, Hop1 and Zip1 in regulating SC polymerization and PC formation**
Chromosomal Hop1 forms the chromosomal axis onto which Zip1 based SC scaffolding can take place. Polymerization of SC recruits Pch2 to the chromosomes which actively removes Hop1 from the axis, thus restricting additional Zip1

Figure 3.6 continued
polymerization. The remaining non-chromosomal Zip1 then starts to form the extrachromosomal PC aggregate. Thus, Pch2 potentially acts as the stringency factor for the SC polymerization.

3.4 Pch2 drives the activation of meiotic prophase checkpoint

Cell cycle checkpoints monitor the fidelity of critical events such as genome replication and chromosome segregation. Checkpoints operating during meiotic prophase ensure proper execution of crucial events like DSB formation, recombination and synapsis. Thus, checkpoints link cell cycle progression with essential cellular processes. Pch2 and Hop1 act as the master regulator of meiotic processes including checkpoint signaling during prophase. Pch2 plays a key role in regulating progression through meiotic prophase. First, the deletion of *PCH2* causes a delay in the meiotic prophase, potentially due to the failure to remove Hop1 from chromosomes (Hochwagen et al. 2005; Subramanian et al. 2016; San-Segundo and Roeder 1999). Second, deletion of *PCH2*, in contrast to wild type conditions, leads to an accelerated cell cycle progression in *zip1Δ* cells (Herruzo et al. 2019; San-Segundo and Roeder 1999). In absence of *ZIP1*, Pch2-driven chromosomal removal of Hop1 does not take place (Subramanian et al. 2016; San-Segundo and Roeder 1999). Finally, *pch2Δ* cells do not have any effect on the meiotic arrest caused by deletion of the meiotic recombinase *DMC1* (Hochwagen et al. 2005). As such, the effect of Pch2 on cell cycle progression seems to be conditional. It depends on the underlying genetic background: in certain instances, its activity is required for timely progress (i.e. in wild type), in others, it promotes cell cycle delays in response to defects (i.e. in *zip1Δ* cells), whereas in other conditions (i.e. *dmc1Δ*) the activity of Pch2 seems to not play a key role in cell cycle progression.

Inspired by the functional interplay between Pch2 and Hop1 in coordinating SC assembly, I aimed to investigate the role of Hop1 levels to answer these apparent differences in Pch2 functions.

3.5 Pch2 and Hop1 collaborate to robustly mediate meiotic prophase checkpoint

The phosphorylation of Histone H3 at Threonine-11 (pH3-T11) is a marker of active checkpoint signaling during meiotic prophase. The differences observed in the

pH3-T11 in *pch2Δ ndt80Δ* cells because of different levels of Hop1, prompted me to investigate the role of Pch2 and Hop1 levels in regulation of meiotic progression and meiotic prophase checkpoint. To observe meiotic progression, I queried the entry of cells into meiosis I (as a sign of exit from meiotic prophase) by monitoring the separation of spindle poles using indirect immunofluorescence of tubulin (Figure 3.7A) and by examining the activity of transcription factor Ndt80 via the expression of its target protein, Cdc5 (Sourirajan and Lichten 2008). Both separation of spindle poles and expression of Cdc5 act as markers for entry into meiosis I. Analysis of meiotic progression was complemented by investigating meiotic prophase checkpoint activity using known markers of active checkpoint signaling: phosphorylation of Hop1 and Histone H3 on Threonine-11. Phosphorylation of Hop1, a result of Mec1/Tel1 kinase activity (and thus of ongoing DSB formation/repair), is observed via a well-documented electrophoretic mobility shift during western blot analysis (Carballo et al. 2008; Subramanian et al. 2016). On the other hand, pH3-T11 was detected using an antibody which recognizes the phosphorylation of Histone H3 on Threonine 11. As mentioned earlier, H3-T11 is a substrate of active Mek1, a marker for ongoing checkpoint activity (Kniewel et al. 2017). With these tools in hand, I initially examined whether lower levels of Hop1 in combination with the absence of *PCH2* had any effect on the meiotic checkpoint and/or progression. As expected, deletion of *PCH2* alone led to a nearly two-hour delay in meiotic progression as compared to wild type cells (Figure 3.7B and 3.7C, left panel) (Hochwagen et al. 2005; Ho and Burgess 2011). Lowering the levels of Hop1, by making use of *HOP1* heterozygosity, in itself did not result in any observable changes in the cellular progression as compared to wild type cells (Figure 3.7B and 3.7C, left panel). However, reducing the levels of Hop1 in *pch2Δ* cells alleviated the meiotic delay caused due to the absence of *PCH2* (Figure 3.7B and 3.7C, right panel). In these cells, the early expression of Cdc5 was also associated with the reversal of prolonged abundance of phosphorylated Hop1 and pH3-T11, suggesting loss of meiotic checkpoint function and untimely activation of Ndt80 (Figure 3.7C). To assess whether this loss of checkpoint function resulted in chromosome segregation defects during the ensuing chromosome segregation events of Meiosis I/II, I determined the viability of spores in these strain backgrounds by tetrad analysis. Chromosome segregation defects will lead to the generation of aneuploid meiotic products (spores). When normally haploid spores lack a certain chromosome (i.e. they are nullisomic for certain chromosomes), it invariably leads to spore death (because

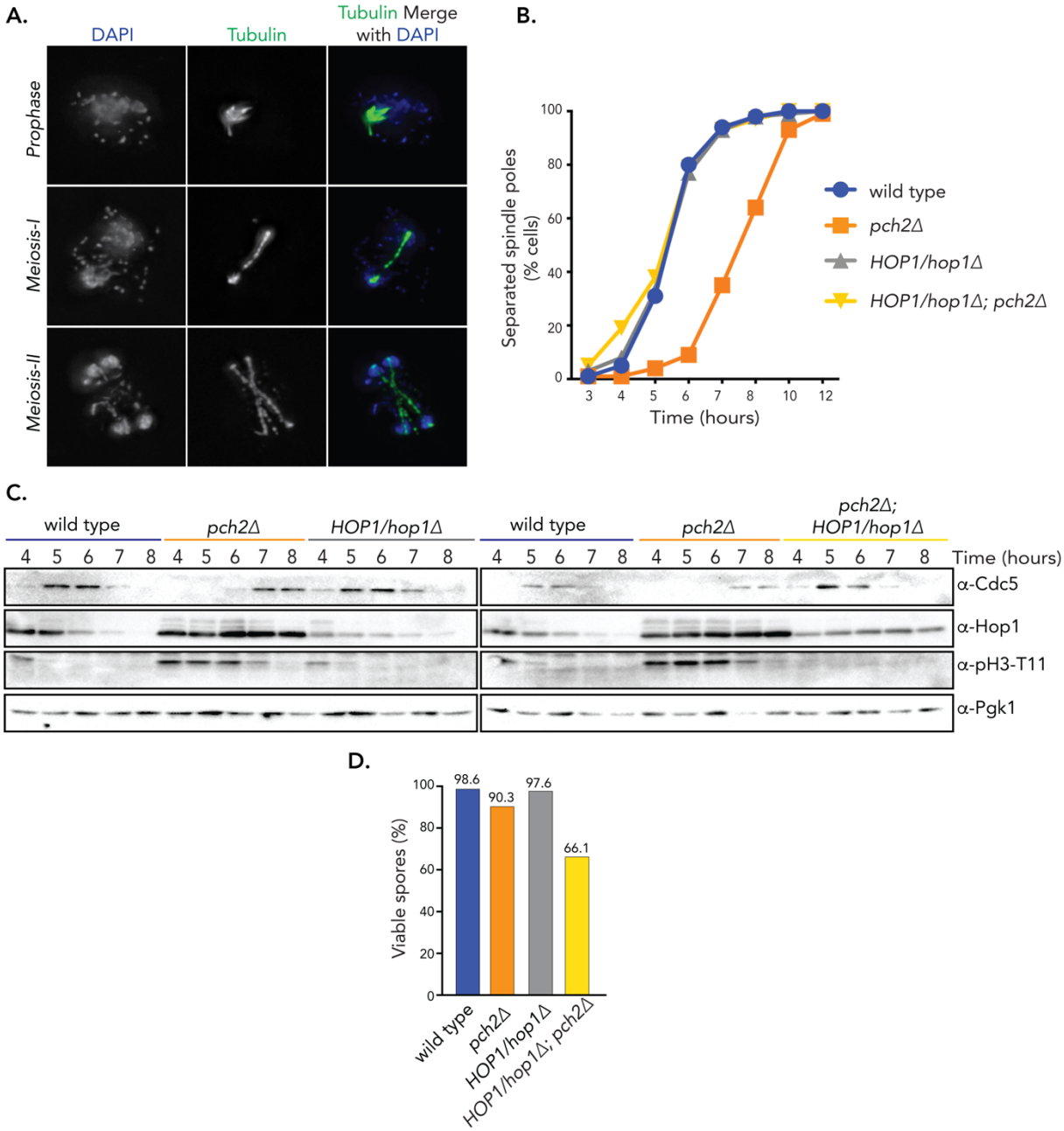

Figure 3.7: **Pch2 is indispensable for optimal meiotic checkpoint response under conditions of limiting Hop1**

A. Representative images of α-tubulin (green) whole cell immunofluorescence showing cells at different stages of meiotic progression. Separation of spindle pole represents exit from prophase and entry into meiosis I. DAPI was used to stain DNA. **B.** Comparison of cells showing separated spindle poles, analyzed by α-tubulin whole-cell immunofluorescence, to determine cell cycle progression in wild type (yGV4527), *pch2Δ* (yGV4528), *HOP1/hop1Δ* (yGV4526) and *HOP1/hop1Δ pch2Δ* (yGV4525). A minimum of 200 cells were analyzed for each data point. **C.** Western blot analysis of Cdc5, Hop1, and pH3-T11 at different time points during meiotic progression from the same strains as in (B). (B) and (C) are from the same time course experiment. **D.** Spore viability analysis of the same strains as in (B).

essential genes present on the affected chromosome(s) are absent). As such, spore viability can be used as a stringent proxy to query meiotic chromosome segregation fidelity. Wild type cells showed 98.6% viable spores, and deletion of *PCH2* showed only a slight decrease in spore viability with 90.3% of total spores being viable, as previously observed (San-Segundo and Roeder 1999). Reducing the levels of Hop1 led to spore viability scores that were similar to wild type cells, with a spore viability of 97.6%. However, combining the deletion of *PCH2* with lowered Hop1 levels resulted in a substantial drop in spore viability with only 66.1% of spores being viable (Figure 3.7D). These data show that the checkpoint defect caused due to lower levels of Hop1 and absence of *PCH2* is associated with a reduction of chromosome segregation fidelity.

Hop1 is important for the formation of the chromosomal axis, and axis formation is in turn necessary for the optimal generation of Spo11-dependent DNA DSBs (Page and Hawley 2004). Meiotic checkpoint signaling is initiated by Tel1/Mec1 kinases which are activated by DSB formation and processing, respectively. To rule out the possibility that the loss of checkpoint function in *pch2Δ HOP1* heterozygote cells is a consequence of defects in DSB formation, I aimed to perform Southern blot analysis to compare DSB levels at a known DSB hotspot, the *YCR047C* locus (Prieler et al. 2005). A background deletion of *SAE2* was employed to restrict the DNA resection around DSBs, which aids in the quantification of DSB signals on Southern blots (without *SAE2*, 5'-3' resection at DSB sites do not take place, thus impairing DSB repair) (Prinz, Amon, and Klein 1997). Analysis of Cdc5 expression revealed that lack of *SAE2* resulted in prolonged presence of cells in meiotic prophase, as expected (McKee and Kleckner 1997; Wu and Burgess 2006). This delay was rescued by the deletion of *PCH2 (Ho and Burgess 2011; Farmer et al. 2012)*, whereas decreasing Hop1 levels had no effect on the delay triggered in cells lacking *SAE2* (Figure 3.8A). However, the combination *HOP1* heterozygosity with the absence of Pch2 resulted in compromised checkpoint function, as indicated by the premature loss phosphorylation of Hop1 and H3-T11, and faster progression into meiosis I, as indicated by the expression of Cdc5 (Figure 3.8A). Southern blot analysis of these strains revealed that the DSBs were generated in all the conditions (Figure 3.8B). Quantification of these DSBs revealed that the level of DSBs at *YCR047C* in *pch2Δ HOP1/hop1Δ* cells were mildly reduced (Figure 3.8C): they were ~80% to that of wild type DSB levels (Figure

3.8C). This level of DSB activity is still able to trigger checkpoint activity (Markowitz et al. 2017), arguing that the loss of meiotic checkpoint robustness in *pch2Δ HOP1* heterozygote cells is merely not caused by an indirect effect of defective DSB formation (and upstream DSB-responsive kinase signaling).

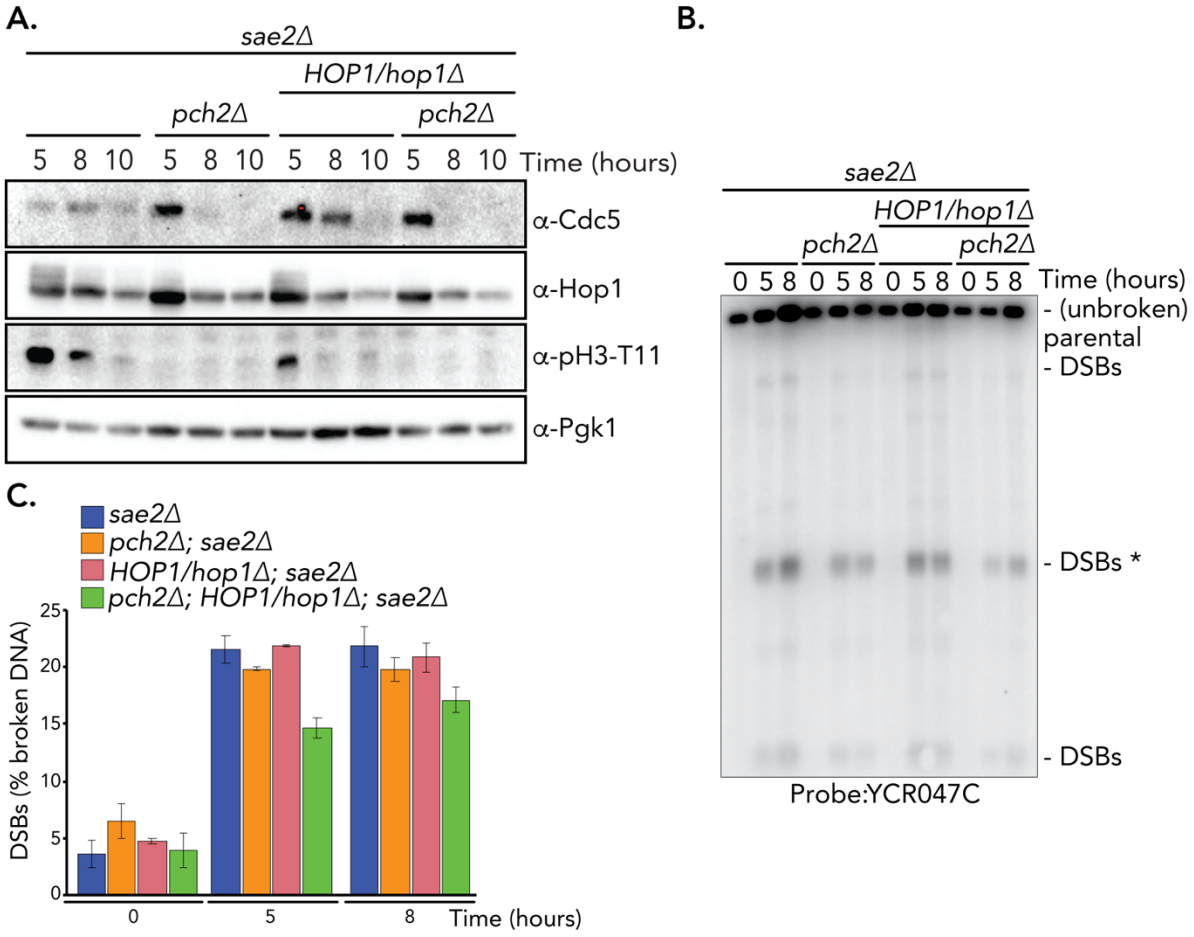

Figure 3.8: **Combination of lower levels of Hop1 with pch2Δ does not have substantial effects on DSB formation**

A. Expression analysis of Cdc5, Hop1 and pH3-T11 by western blot at different time points during meiotic time course of *sae2Δ* (yGV4744), *pch2Δ sae2Δ* (yGV4801), *HOP1/hop1Δ sae2Δ* (yGV4752) *and pch2Δ HOP1/hop1Δ sae2Δ* (yGV4800). **B.** Southern blot analysis comparing DSB levels in strains used in (A) at indicated time points during meiotic progression. DSBs were detected using a probe for *YCR047C* locus. *sae2Δ* cells are resection deficient and hence cannot repair the DSBs. **C.** Quantification of breaks from the southern blot experiment shown in (B). DSBs used for quantification are indicated by * in (B). Mean values ± SD were calculated from two independent experiments.

3.6 Pch2 has an agonistic role in checkpoint function in response to synapsis defects

Deletion of *ZIP1* leads to a delay in meiotic progression, and this delay is associated with the activation of a checkpoint cascade, dubbed the synapsis checkpoint, which operates during prophase and is believed to specifically respond to synapsis defects (Wu and Burgess 2006). I aimed to increase the understanding of this checkpoint by further investigating the roles of Pch2 and Hop1. By comparing the timing of entry of cells into meiosis I, via expression of Cdc5, as previously demonstrated, I observed that *zip1Δ* cells were delayed in meiotic prophase as compared to wild type cells (Figure 3.9A, left panel) (Xu, Weiner, and Kleckner 1997). As expected, deletion of *PCH2* was able to partially rescue this delay (Figure 3.9A, left panel) (San-Segundo and Roeder 1999; Wu and Burgess 2006). Intriguingly, I observed that *HOP1* heterozygosity alone also partially rescued this delay indicating the requirement for correct cellular levels of Hop1 for the proper functioning of this checkpoint (Figure 3.9A, right panel). These results were complemented by comparing the percentage of cells that had progressed past meiotic prophase by following spindle morphology. *zip1Δ* cells showed a meiotic delay and either deletion of *PCH2* or *HOP1* heterozygosity in these cells led to a partial rescue of this delay (Figure 3.9B). The profile of meiotic progression observed in *pch2Δ* cells and cells with lower levels of Hop1) was highly comparable. Both these conditions resulted in a faster meiotic progression as compared *zip1Δ* cells, but these cells progressed slower than wild type cells (Figure 3.9B). Strikingly, deletion of *PCH2* in combination with *HOP1* heterozygosity led to a complete rescue of the delay caused by deletion of *ZIP1* (Figure 3.9A and 3.9B). The faster progression of these cells through meiotic prophase also correlated with reduced Hop1 phosphorylation and Mek1 activity suggesting compromised checkpoint function (Figure 3.9A). These data suggest that the presence of Pch2 and levels of Hop1 synergize to play an important part in the optimal functioning of synapsis checkpoint. The rescue of the delay in *zip1Δ* cells under the described different conditions was also reflected in the number of viable spores after completion of meiosis. *zip1Δ* cells showed a spore viability of 56.8% compared to a wild type spore viability of 95.6% (Figure 3.9C). *zip1Δ* cells deleted either for *PCH2* or containing *HOP1* heterozygosity, both of which show a partial rescue of the delay, the spore viability drops comparably to 34.1% and 38.9% respectively (Figure 3.9C). The spore viability in *pch2Δ* cells expressing lower levels of Hop1 drops down drastically to

6.3% suggesting that compromising the checkpoint response under conditions that trigger synapsis defects leads to chromosomal mis-segregations and developmental aneuploidy (Figure 3.9C).

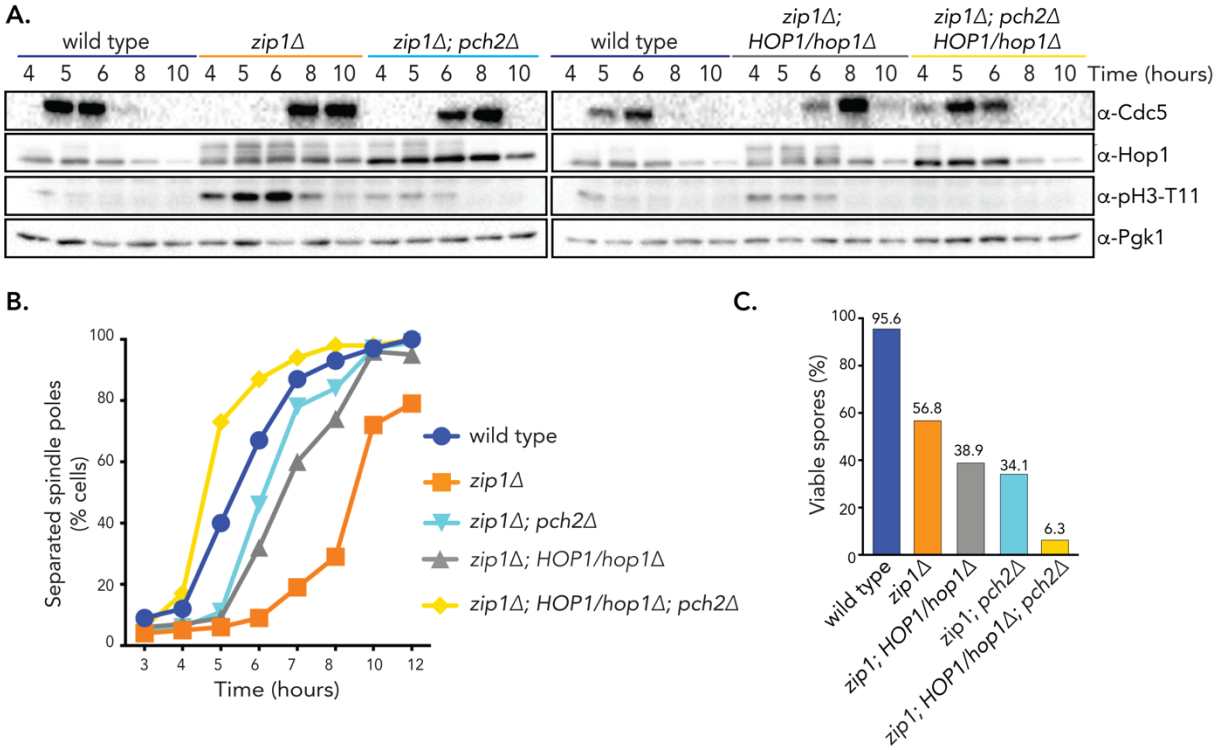

Figure 3.9: **Pch2 and Hop1 combine to regulate the synapsis checkpoint**
A. Western blot analysis to compare expression profile of Cdc5, Hop1 and pH3-T11 in wild type (yGV4577), *zip1Δ* (yGV4578), *zip1Δ pch2Δ* (yGV4581), *zip1Δ HOP1/hop1Δ* (yGV4579) and *zip1Δ pch2Δ HOP1/hop1Δ* (yGV4580). Pgk1 is used as a loading control. **B.** Comparison of the number of cells entering meiosis I by tracing the spindle morphology at indicated time points of strains used in (A). A minimum of 200 cells were analyzed for each data point. (A) and (B) are from the same time-course experiment. **C.** Spore viability analysis of strains used in (A).

During DSB repair, Pch2 aids in creating a bias towards the use of homolog as repair template instead of sister chromatid (Zanders et al. 2011; Ho and Burgess 2011; Borner, Barot, and Kleckner 2008). It has been suggested that deletion of *PCH2* results in the alleviation of *zip1Δ*-mediated delay by allowing cells to undergo (rapid) sister chromatid-based repair (Herruzo et al. 2016; Farmer et al. 2012). Deletion of *RAD51*, a recombinase required for DSB repair via this sister-chromatid based pathway, in *zip1Δ* shows a very severe delay in meiotic prophase as compared to the delay observed in *zip1Δ* cells alone (Figure 3.10A and 3.10B) (Herruzo et al. 2016). This genetic relationship lends credence to the hypothesis that DSBs in *zip1Δ pch2Δ* cells

are repaired using the sister chromatid as a template, which eventually helps in overcoming the checkpoint restrictions. However, by tracing both spindle morphology and expression of Cdc5, I found that deletion of *PCH2* in *zip1Δ rad51Δ* cells leads to the alleviation of the arrest (Figure 3.10A and 3.10B). Active checkpoint markers like phosphorylated Hop1 and pH3-T11 are also reduced under these conditions (Figure 3.10A). On lowering cellular Hop1 levels, a similar rescue and checkpoint behavior was observed suggesting that the alleviation of this arrest might be due to loss of Pch2-Hop1 mediated robustness in the meiotic checkpoint rather than via a channeling of DSB repair towards sister chromatid-based repair (Figure 3.10A and 3.10B). Further proof for this premise was provided when I observed that the combination of *pch2Δ* and *HOP1* heterozygosity led to an additive effect on meiotic progression (Figure 3.10A and 3.10B). These results suggest that the alleviation of checkpoint delay by deletion of PCH2 is directly related to checkpoint signaling rather than a decrease in the homolog bias during recombinational repair of meiotic DSBs.

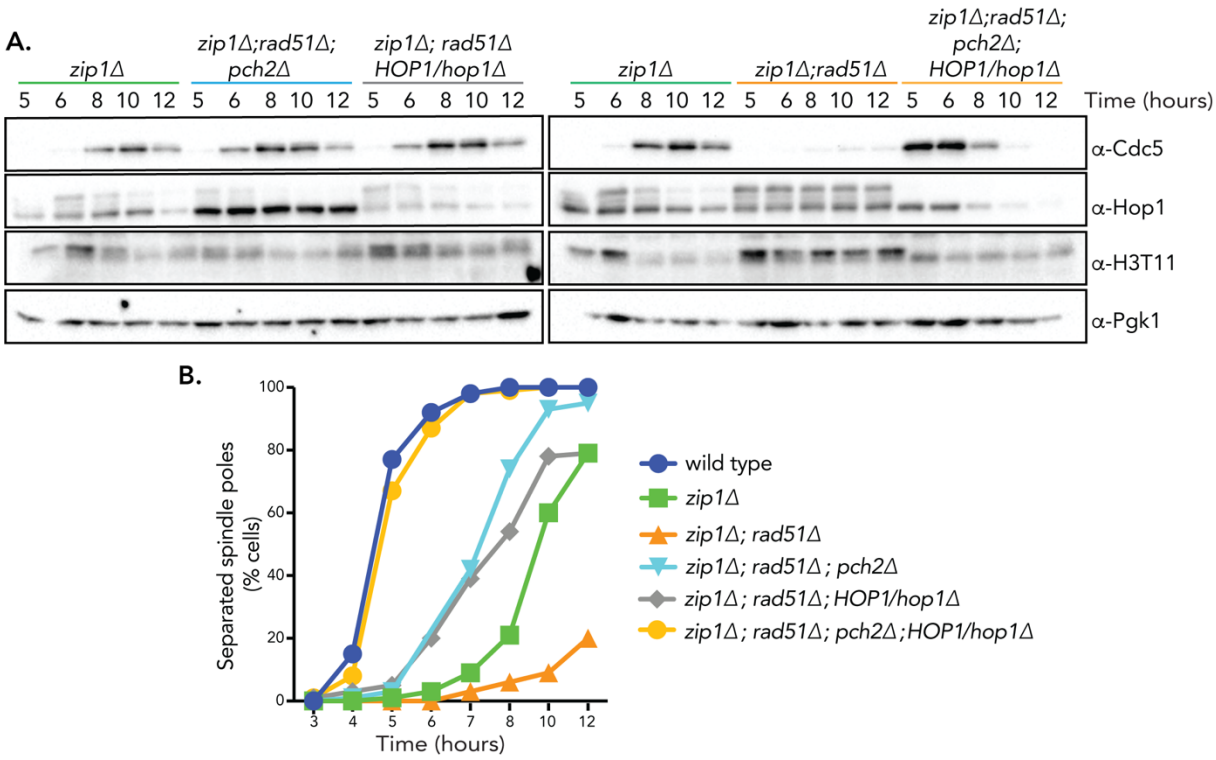

Figure 3.10: **Role of Pch2 and Hop1 in *zip1Δ rad51Δ* cells**
A. Western blot analysis of *zip1Δ* (yGV4578), *zip1Δ rad51Δ* (yGV4603), *zip1Δ rad51Δ pch2Δ* (yGV4599), *zip1Δ rad51Δ HOP1/hop1Δ* (yGV4598) and *zip1Δ rad51Δ pch2Δ HOP1/hop1Δ* (yGV4600) comparing the expression profile of Cdc5, Hop1 and pH3-T11. Pgk1 is used as a loading control. **B.** Comparison of meiotic progression of the

Figure 3.10 continued
strains used in (A) using whole-cell immunofluorescence to follow spindle pole separation. A minimum of 200 cells were analyzed for each data point. Wild type strain was used as an additional control. A minimum of 200 cells were analyzed for each data point.

3.7 Pch2 plays the role of an agonist during recombination checkpoint

Deletion of Pch2 alleviates the meiotic delay observed in *zip1Δ* cells. However, deletion of *PCH2* does not lead to alleviation of the arrest caused due to the absence of recombinase *DMC1* (Hochwagen et al. 2005). This observation has given rise to the idea that two separate checkpoints, responding uniquely to synapsis and recombination defects, operate during meiotic prophase, with Pch2 playing a role exclusively in the former (Wu and Burgess 2006). With the above described observations of Pch2 and Hop1 playing a role in modulating checkpoints during meiotic prophase, I aimed to revisit the idea of Pch2's role during recombination checkpoint. In line with the published literature, deletion of *DMC1* resulted in the near-complete arrest of cells in meiosis, and, as expected, deletion of *PCH2* did not alleviate this arrest (Figure 3.11A and 3.11B) (Hochwagen et al. 2005). Similar to *pch2Δ*, reducing the levels of Hop1 alone was also not sufficient to alleviate the *dmc1Δ* dependent arrest (Figure 3.11A and 3.11B). These cells were arrested in prophase as indicated by no detectable expression of Cdc5 protein (Figure 3.11A). However, the combination of *pch2Δ* with *HOP1* heterozygosity led to a rapid entry of cells into meiosis I associated with the elimination of checkpoint function, as confirmed by decreased abundance of phosphorylated Hop1 and pH3-T11 (Figure 3.11A and 3.11B). These observations indicate that Pch2 and Hop1 act synergistically to mediate the recombination checkpoint. Combined with the observation that Pch2 mediates the checkpoint signaling during synapsis defects, these results argue for the presence of a single general checkpoint signaling cascade instead of separate checkpoints. Both Pch2 and Hop1 act as the crucial mediators of the general meiotic checkpoint signaling cascade. Under conditions of limiting Hop1, Pch2 thus acts as an agonist in driving general meiotic checkpoint signaling.

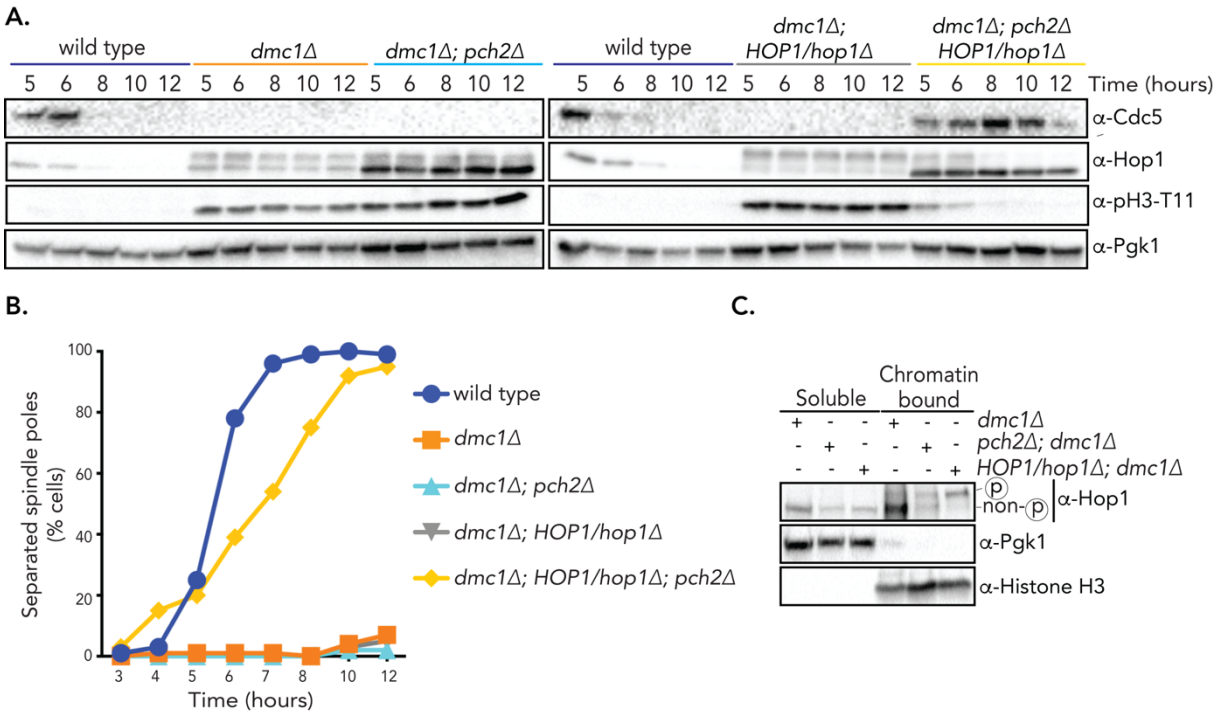

Figure 3.11: **Pch2 helps in mediating recombination checkpoint by facilitating chromosomal abundance of Hop1**

A. Expression analysis of Cdc5, Hop1 and pH3-T11 to compare the meiotic progression and checkpoint activity in wild type (yGV4577), *dmc1Δ* (yGV48), *dmc1Δ pch2Δ* (yGV1269), *dmc1Δ HOP1/hop1Δ* (yGV4546) and *dmc1Δ pch2Δ HOP1/hop1Δ* (yGV1171). **B.** Comparison of the meiotic progression by analyzing spindle morphology using whole-cell immunofluorescence in the strains used in (A). A minimum of 200 cells were analyzed for each data point. **C.** Western blot analysis of the separated soluble and chromatin fractions from *dmc1Δ* (yGV48), *pch2Δ dmc1* (yGV1269) and *HOP1/hop1Δ dmc1Δ* (yGV4546) at 7 hours post the induction of meiosis.

The role of Pch2 and Hop1 as the central components of a single signaling cascade raised the question of how these proteins might be mediating the meiotic checkpoint function. To get insights into this, I compared Hop1 status in *dmc1Δ*, *dmc1Δ pch2Δ, dmc1Δ HOP1* heterozygote conditions. The majority of Hop1 was present as slower-migrating species in *dmc1Δ HOP1* heterozygote during the time course. However, a different expression pattern of Hop1 phosphorylation was observed in *dmc1Δ pch2Δ* conditions in which Hop1 was observable both in phosphorylated and unphosphorylated forms. (Figure 3.11A). This suggests that Pch2 plays a role in facilitating the phosphorylation of Hop1, an idea that has been previously proposed (Herruzo et al. 2016). The presence of Pch2, however, is not essential for the phosphorylation of Hop1 as cells with deletion of *DMC1* and *PCH2* also show

substantial Hop1 phosphorylation accompanied with a robust arrest in meiotic prophase (Figure 3.11A and 3.11B). In *pch2Δ* cells, I observed an increase in total Hop1 levels pointing towards a role between Pch2 and Hop1 levels. Phosphorylated Hop1 is the checkpoint signaling competent form of Hop1. Since the kinases responsible for the phosphorylation of Hop1 (i.e. Mec1/Tel1) are activated locally by DSB formation and processing, it is believed that Hop1 phosphorylation takes place locally, on chromosomes in the vicinity of DSBs. To confirm that phosphorylated Hop1 is indeed chromosomal, I performed a chromatin-fractionation assay, using *dmc1Δ*, *dmc1Δ pch2Δ and dmc1Δ HOP1/hop1Δ* cells. I found that although a faster migrating version of Hop1, corresponding to non-phosphorylated Hop1, can be found in both soluble as well as on chromatin fractions, the slower migrating band, corresponding to the phosphorylated version of Hop1, is found exclusively in the chromatin fraction (Figure 3.11C). This difference becomes starker on comparing soluble and chromatin fractions in *dmc1Δ HOP1* heterozygote conditions (Figure 3.11C). These results indicate that in *dmc1Δ* and *zip1Δ* cells (where chromosomal recruitment of Pch2 does not take place because of aberrant or no SC polymerization), non-chromosomal Pch2 plays a critical role in driving the meiotic checkpoint signaling. Therefore, these data suggest that non-chromosomal Pch2 facilitates the abundance of signaling competent Hop1 to create robust checkpoint signaling.

3.8 Characterization of an inducible Pch2 expression system

To understand the role of Pch2 in facilitating the meiotic checkpoint and to explore the function of non-chromosomal Pch2, I established an estradiol-based inducible expression system (Louvion, Havaux-Copf, and Picard 1993; Benjamin et al. 2003). It is to note that under natural conditions, the product of the *GAL4* gene activates the expression from *GAL1* promoters in presence of galactose and absence of glucose (Strathern, Jones, and Broach 1982). Since budding yeast cells need to be starved of nutrients for induction of meiosis, direct use of galactose to induce expression from *GAL* promoters is unfavorable. Estradiol-based inducible expression system is used to overcome this limitation. In this system, the hormone-binding domain of the human estrogen receptor (ER) is fused to the DNA-binding domain of Gal4 transcription factor. The chimeric Gal4-ER protein results in activation of transcription from *GAL* promoters only in the presence of estradiol. Addition of estradiol to the cells results in Gal4-ER binding at the upstream activation sequence of the *GAL* promoters (*pGAL*), initiating

the transcriptional activity of genes under its influence. To make an estradiol-inducible system to conditionally express Pch2, I cloned *pGAL1* with a 3x-*FLAG* tag and a 6x-Glycine linker *(pGAL-3xFLAG-PCH2)* and integrated this construct upstream of *PCH2* (Figure 3.12A). Using this system, expression of Pch2 could be temporally controlled by the addition of estradiol to cells and induced expression observed by western blot using α-Flag antibody.

In order to better characterize this system and to establish Pch2 functionality upon inducible expression, I investigated a number of phenotypes associated with Pch2. Addition of estradiol at 3 hours post-induction of meiosis resulted in observable expression of Pch2 within one hour, demonstrating that this system functioned as envisioned. Conditionally induced Pch2 phenocopied the known effects of Pch2 on Hop1 in terms of its levels and phosphorylation status (Figure 3.12B). Additionally, it did not lead to any defects in spore viability: no difference in spore viability was observed both with and without induction of Pch2, and the percentage of viable spores were very similar to those of wild type conditions (Figure 3.12C). To ensure that the induced expression did not have any deleterious synthetic effects with *NDT80* deletion, I queried Hop1 expression in the inducible Pch2 system, harboring an *NDT80* deletion. Reassuringly, expression of Pch2 led to the expected effects on Hop1: upon expression of Pch2, overall levels of Hop1 were lower as compared to the non-induced conditions. Absence of Pch2 in *ndt80Δ* cells results in observation of phosphorylated Hop1 even at later time points (Subramanian et al. 2016). A similar phenotype was observed in conditions where Pch2 was not expressed (*i.e.* without estradiol expression this system behaved like *pch2Δ* cells, confirming stringent transcriptional shutdown in the absence of activating conditions) (Figure 3.12D). On the contrary, induction of Pch2 expression quickly resulted in a lower or absent abundance of the phosphorylated form of Hop1 at later time points, indicating functional expression of Pch2 (Figure 3.12D). Finally, inspired by my previous observations of a functional relationship between Pch2, Hop1, and Zip1, I aimed to check the effect of induction of Pch2 on PC abundance. I added estradiol 4 hours post-induction of meiosis and compared the number of cells showing the presence of PCs with and without induction of Pch2 (Figure 3.12E). Mirroring my previous observations, I found that expression of Pch2 in *ndt80Δ* cells led to a higher prevalence of cells containing PCs (Figure 3.12F). At the time of induction of Pch2, only 3% of cells contained PCs (Figure 3.12G).

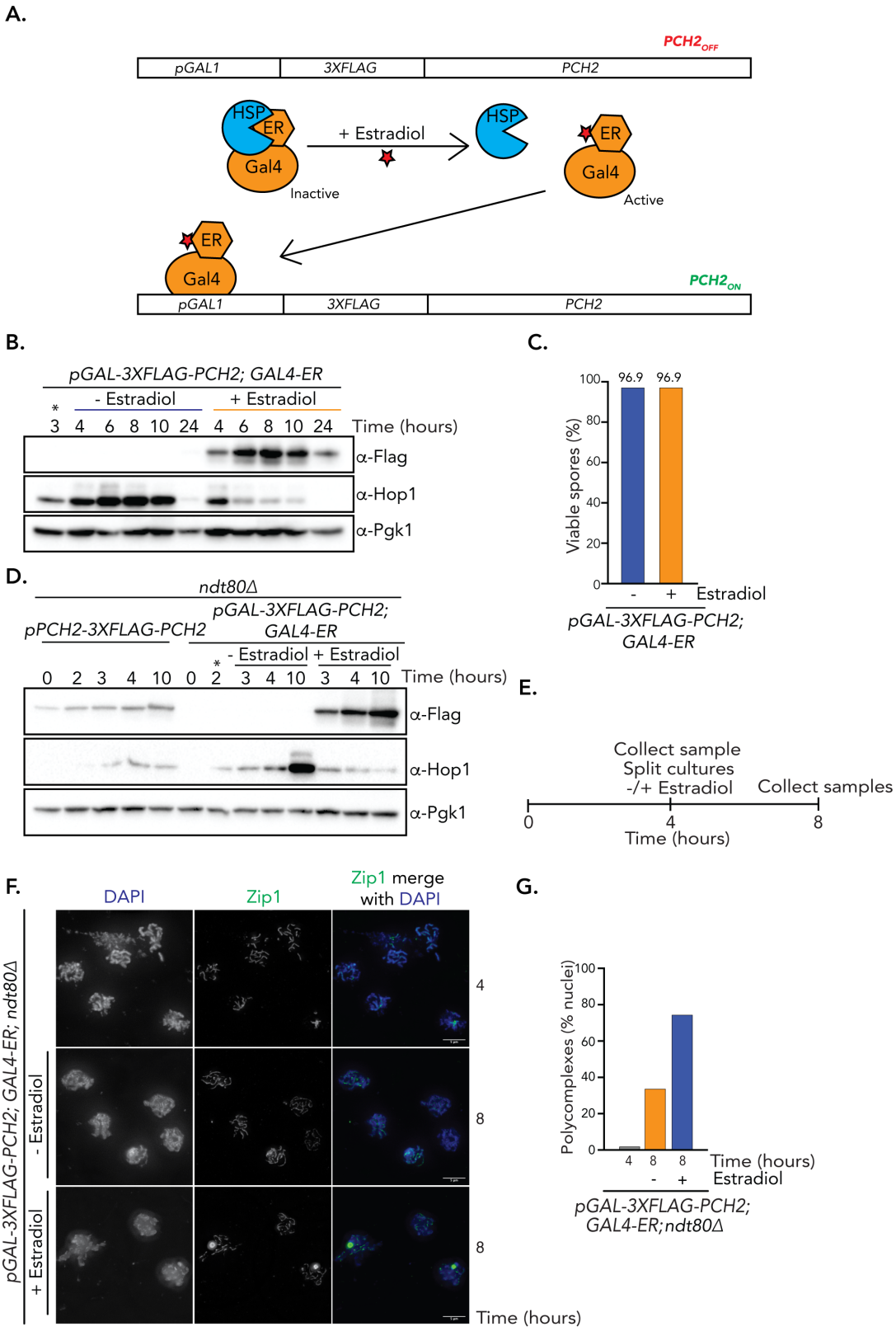

Figure 3.12: **Characterization of the inducible Pch2 system**

A. Cartoon representation of the inducible Pch2 system. A construct with p*GAL1-3xFLAG* was placed upstream of *PCH2*. Without estradiol, Gal4-ER chimeric protein remains inactive, and bound to Heat shock protein (HSP). Addition of estradiol to the cells enables Gal4 to initiate the transcriptional activity from *GAL1* promoter, resulting

Figure 3.12 continued
in the induction of the expression of Pch2. **B.** Western blot analysis to compare the expression of Hop1 at indicated time points with and without induction of Pch2 (α-Flag) in *pGAL-3XFLAG-PCH2; GAL4-ER* strain (yGV3050). The time of addition of estradiol is indicated by *. Pgk1 was used as a loading control. **C.** Spore viability analysis of the strains used in (B). **D.** Comparison of the expression levels of Pch2 and Hop1 between induced Pch2 and Pch2 expression from endogenous *PCH2* promoter. Estradiol was added at 2 hours post-induction of meiosis (indicated by *). Pgk1 was used as a loading control. Strains used are *pPCH2-3XFLAG-PCH2; ndt80Δ* (yGV2889) and p*GAL-3XFLAG-PCH2; GAL4-ER; ndt80Δ* (yGV3171) **E.** Experimental scheme for experiments depicted in (F) and (G). **F.** Representative immunofluorescence images of Zip1 (α-Zip1; green) from the strain used in (D) with and without induction of Pch2. DNA was stained with DAPI. **G.** Quantification of the number of cells showing the appearance of PC like structures from the experiment performed in (G).

However, the number of cells showing PCs increased to 76% four hours post-induction of Pch2 compared to only 30% of cells showing PC accumulation in which Pch2 expression was not induced (Figure 3.12G). This reinforces the idea that Pch2 plays a role in regulating synapsis. Altogether, these observations confirm that expression of Pch2 using the established inducible system is functional and that this system can thus be used to query Pch2 function in the control of meiotic prophase.

3.9 Pch2 drives meiotic checkpoint signaling by facilitating Hop1 phosphorylation

Phosphorylated Hop1 is present on chromosomes (Figure 3.11C) and chromosomal Pch2 enables the removal of Hop1 from chromosomes (Subramanian et al. 2016; San-Segundo and Roeder 1999). However, my earlier observations suggest an indispensable role of non-chromosomal Pch2 in checkpoint signaling, especially under Hop1 limiting conditions (Figure 3.9). To study the role of non-chromosomal Pch2 in checkpoint signaling, I employed the inducible Pch2 expression system to study checkpoint responses under SC-defective conditions, i.e. *zip1Δ* cells. Without Zip1, Pch2 cannot be recruited to the chromosomes (Herruzo et al. 2016; Herruzo et al. 2019; San-Segundo and Roeder 1999; Subramanian et al. 2016). On comparing the phenotypes associated with active checkpoint signaling with and without induction of Pch2 expression in *zip1Δ ndt80Δ* cells, I found that the abundance of phosphorylation of Hop1 and pH3-T11 were markedly higher within an hour of induction of the expression of Pch2, even though these checkpoint markers were also

present without the induction of Pch2 (Figure 3.13A). This shows the presence of an ongoing checkpoint activity, albeit at a reduced level, even without the presence of Pch2. Increase in the total levels of Hop1 because of the absence of Pch2 might explain this observation. Increased Hop1 levels ostensibly ensures sufficient availability of Hop1, ready to be incorporated into chromosome-based signaling. If this is the case, reducing the levels of Hop1 should lead to lower or completely abolished checkpoint signaling as shown above, where decreased Hop1 levels in *zip1Δ pch2Δ* cells, led to dysfunctional meiotic checkpoint function (Figure 3.9B). Indeed, without the induction of Pch2, reduced levels of Hop1 in *zip1Δ ndt80Δ* strains resulted in a lack of active checkpoint markers (Figure 3.13B). Importantly, upon induction of Pch2, a robust activation of checkpoint was observed. Hop1 and H3-T11 phosphorylation was observed after Pch2 induction but was not observed in the non-induced control (Figure 3.13B). Since under all these conditions, Pch2 cannot be recruited to chromosomes (due to lack of Zip1/SC), these results argue that non-chromosomal Pch2 drives the activation of checkpoint by facilitating the availability of signaling competent Hop1.

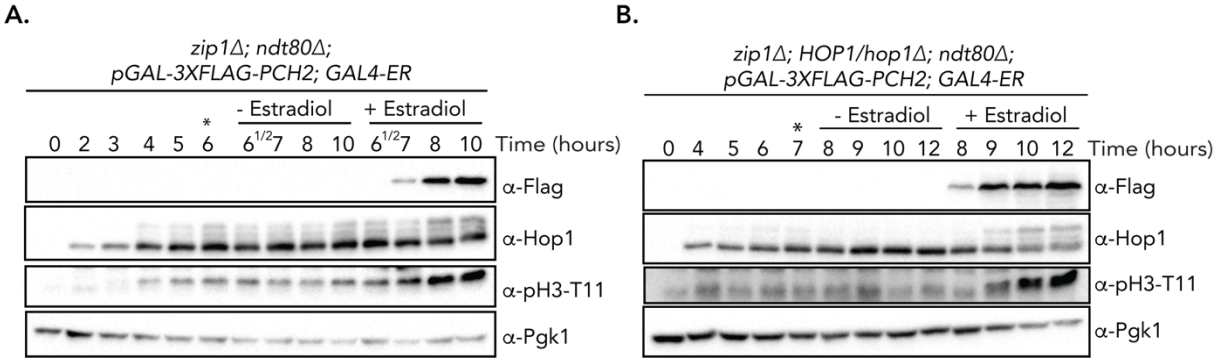

Figure 3.13: **Non-chromosomal Pch2 facilitates the phosphorylation of Hop1**
A. Western blot analysis to compare the effects on Hop1 and pH3-T11 expression profile at indicated time points during meiotic progression with and without the induction of Flag-Pch2 in zip1*Δ; ndt80Δ; pGAL-3XFLAG-PCH2; GAL4-ER* (yGV4470). Estradiol is added to induce the expression of Pch2 (indicated by *). **B.** Western blot analysis to compare the effects on Hop1 and pH3-T11 expression profile with and without the induction of Flag-Pch2 in zip1*Δ; HOP1/hop1Δ; ndt80Δ; pGAL-3XFLAG-PCH2; GAL4-ER* (yGV4637). Estradiol is added to induce the expression of Pch2 (indicated by *).

Taken together, these data suggest that Pch2 and Hop1 create a system that is indispensable for modulating the meiotic checkpoint response arising either because of defects in synapsis or in recombination. Pch2 plays a central role in this system by

facilitating the availability of signaling competent Hop1. In this model, this agonistic role is played by non-chromosomal Pch2. The presence of Pch2 is of greater importance especially when the cellular levels of Hop1 are reduced. Altogether, this behavior is reminiscent of the role of PCH-2/TRIP13 (PCH-2 and TRIP13 being *C.elegans* and mammalian homologs of Pch2 respectively) during Spindle Assembly Checkpoint (SAC) signaling. Similar to the role of Pch2 in facilitating the availability of signaling competent Hop1 during meiotic prophase checkpoint signaling, TRIP13 helps in maintaining sufficient amounts of O-Mad2 to drive SAC signaling (Ma and Poon 2018; Marks et al. 2017; Kim et al. 2018; Nelson et al. 2015; Ma and Poon 2016). Collectively, these data suggest that the contribution of Pch2 in meiotic prophase checkpoint is analogous to the contribution of PCH-2/TRIP13 in SAC.

3.10 Pch2 can drive silencing of meiotic prophase checkpoint

Pch2/TRIP13 is not only required for maintaining SAC signaling, but it also plays a role in its silencing. It does so by making use of the same biochemical activity of catalyzing the transformation of C-Mad2 to O-Mad2 (Alfieri, Chang, and Barford 2018; Kim et al. 2018; Ma and Poon 2016; Wang et al. 2019; Eytan et al. 2014). If the role of Pch2 in regulation of meiotic checkpoint is indeed analogous to the role of TRIP13 in SAC, then it should also exhibit similar checkpoint silencing functions. There is evidence pointing in this direction: Zip1 dependent chromosomal recruitment of Pch2 can help in extinguishing Mek1-dependent signaling (Subramanian et al. 2016), and deletion of *PCH2* leads to delayed progression through meiotic prophase because of sustained Hop1 phosphorylation (See above).

In order to expose a checkpoint silencing function of Pch2, I sought for a genetic condition in which despite chronic DSB repair defects cells prematurely exit meiotic prophase. I reasoned that such behavior might reflect ‘unscheduled’ checkpoint silencing, and studying this condition (and a role of Pch2 therein) might be able to inform on checkpoint silencing mechanisms. I utilized strains containing a deletion of both RecA-like recombinases i.e. *RAD51* and *DMC1*. It has been shown that under these conditions cells progress past meiotic prophase despite the presence of high levels of unrepaired DSBs (Shinohara et al. 1997; Markowitz et al. 2017; Farmer et al. 2012). However, the reasons behind this premature progression have remained completely unknown. Rad51 helps in sister chromatid-based repair and Dmc1

facilitates homolog-based repair, I initially assessed if the bypass of meiotic arrest in *dmc1Δ rad51Δ* cells was due to the absence of sister chromatid repair or if it was because of a specific function of Rad51. In this regard, I deleted an accessory factor of Rad51, called Rad54. Absence of Rad54 also hampers the sister chromatid-based DSB repair, similar to the absence of Rad51 (Clever et al. 1997; Crickard and Greene 2018). If the bypass in *dmc1Δ rad51Δ* cells is due to the absence of sister-chromatid based repair mechanisms in general, then I expect to see a similar bypass in *dmc1Δ rad54Δ* cells. I utilized the same technique of following spindle morphology and investigating Cdc5 expression by western blot analysis to investigate meiotic progression in different strains. As seen earlier, *dmc1Δ* cells showed a near-complete arrest whereas *dmc1Δ rad51Δ* cells, in accordance with existing literature (Shinohara et al. 1997; Markowitz et al. 2017), showed an entry into meiosis I with decreased prevalence of active checkpoint markers (Figure 3.14A). Compared to the *dmc1Δ rad51Δ* cells, deletion of *RAD54* did not result in the alleviation of *dmc1Δ* mediated meiotic arrest (Figure 3.14A and 3.14B). These cells also had a higher prevalence of active checkpoint markers (Figure 3.14A). These data point to a specific characteristic of Rad51 (independent of Rad54 function) which influences the *dmc1Δ* checkpoint response. To define the reasons responsible for this premature progression, I investigated the chromosomal recruitment of Gmc2, a key component of the central element of SC, which is often used as a marker of SC establishment (Humphryes et al. 2013; Voelkel-Meiman et al. 2019). Strikingly, *dmc1Δ rad51Δ* cells exhibited an increase in Gmc2-containing SC stretches on chromosomes as compared to *dmc1Δ* cells alone which contained very few stretches of SC (Figure 3.14C). (Please note that SC formation in budding yeast is normally contingent on successful DSB repair, and thus greatly impaired in cells lacking *DMC1* (Bishop 1994; Rockmill et al. 1995). Quantification of Gmc2 on chromosomes confirmed these results (Figure 3.14D) suggesting *dmc1Δ rad51Δ* cells form SC, despite failure to undergo recombinational repair of DSBs. SC-polymerization enables chromosomal recruitment of Pch2, thereby helping Pch2 actively remove Hop1 from chromosomes. In line with the thought that SC-polymerization might be recruiting Pch2 to modulate Hop1 levels, I observed that deletion of *PCH2* in *dmc1Δ rad51Δ* cells led to significantly higher amounts of Hop1 on chromosomes (Figure 3.14C and 3.14E). This shows that in *dmc1Δ rad51Δ* cells, Pch2 mediated removal of Hop1 from chromosome axis takes place. Removal of Hop1

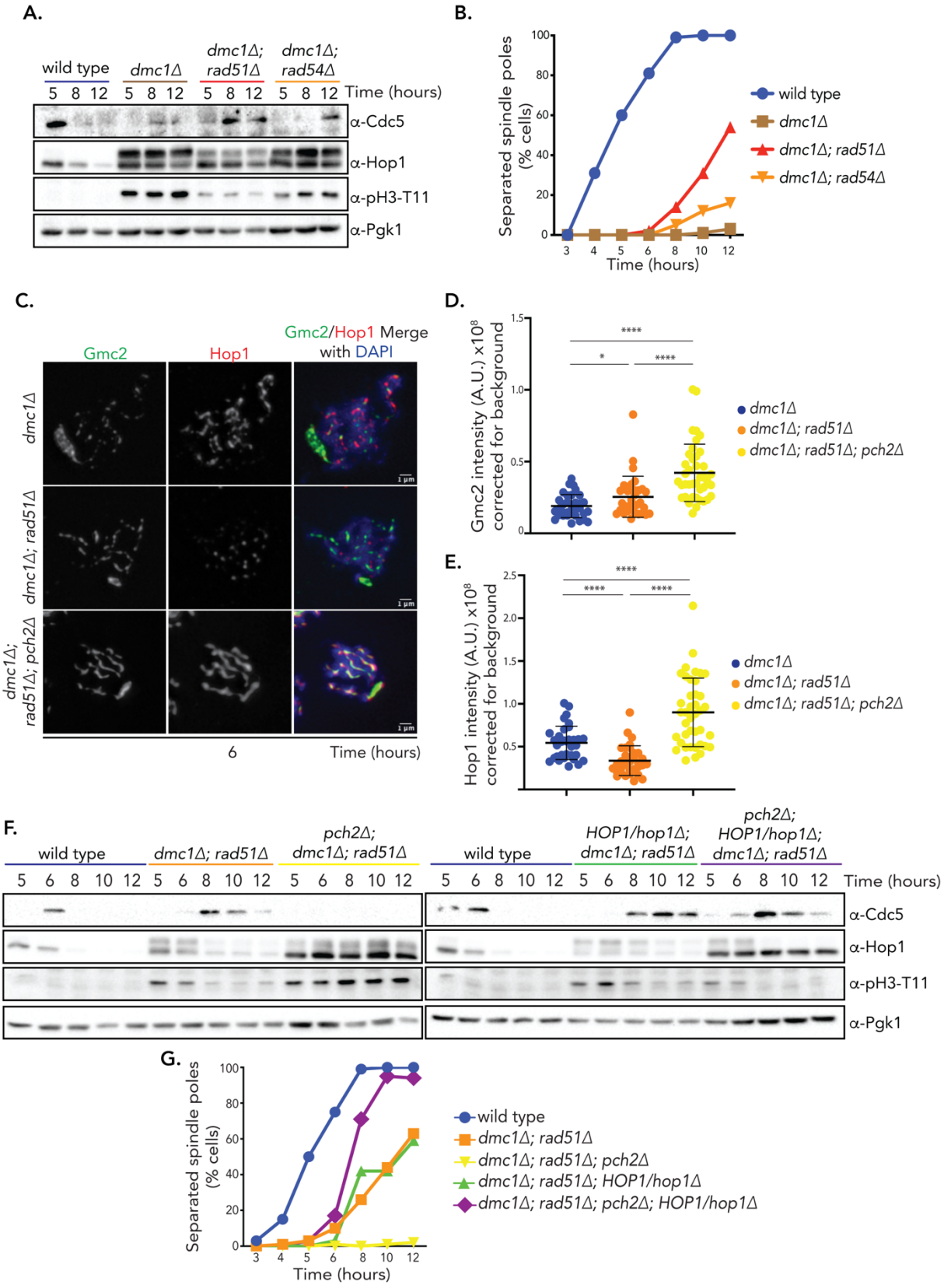

Figure 3.14: ***rad51Δ* dependent override of *dmc1Δ* meiotic arrest is mediated by Pch2**

A. Western blot analysis comparing the meiotic progression via expression of cdc5 and meiotic checkpoint markers via expression of Hop1 and pH3-T11 in wild type

Figure 3.14 continued
(yGV4577) , *dmc1Δ* (yGV48), *dmc1Δ rad51Δ* (yGV1401), and *dmc1Δ rad54Δ* (yGV4796) cells Pgk1 was employed as a loading control. **B.** Meiotic cell cycle progression of strains used in (A) using α-tubulin whole-cell immunofluorescence. A minimum of 200 cells were analyzed for each data point. **C.** Representative immunofluorescence images of meiotic spreads from *dmc1Δ* (yGV48), *dmc1Δ rad51Δ* (yGV1401) and *dmc1Δ rad51Δ pch2Δ* (yGV1409) strains stained for an SC-component Gmc2 (green) and Hop1 (red) at 6 hours post-induction of meiosis. DAPI depicts the DNA. **D.** and **E.** Quantification of the total sum intensity after background correction of chromosomal Gmc2 and Hop1 from meiotic spreads of strains used in (C). Number of cells analyzed are n=33, n=31, and n=31 for *dmc1Δ, dmc1Δ rad51Δ* and *dmc1Δ rad51Δ pch2Δ* respectively. **** indicates significance with p≤0.0001. Mann-Whitney U test. Mean and standard deviation are indicated. **F.** Expression analysis of Cdc5, Hop1 and pH3-T11 to compare meiotic progression and checkpoint activity in wild type (yGV4577), *dmc1Δ rad51Δ* (yGV1401), *dmc1Δ rad51Δ pch2Δ* (yGV1409), *dmc1Δ rad51Δ HOP1/hop1Δ* (yGV4713) and *dmc1Δ rad51Δ pch2Δ HOP1/hop1Δ* (yGV4715) strains. Pgk1 is loading control. **G.** Comparison of meiotic progression using α-tubulin immunofluorescence for analyzing spindle morphology in strains used in (F). A minimum of 200 cells were analyzed for each data point.

from chromosomes is associated with silencing of the checkpoint suggesting in *dmc1Δ rad51Δ* cells Pch2 might be involved in silencing of the meiotic prophase checkpoint. If Pch2 does play a role in silencing the checkpoint, then deletion of *PCH2* in *dmc1Δ rad51Δ* background should result in a delay or arrest in prophase. Indeed, deletion of *PCH2* in *dmc1Δ rad51Δ* resulted in a near-complete arrest of these cells in meiotic prophase (Figure 3.14F, left panel). This was confirmed by tracing the meiotic progression via spindle morphology (Figure 3.14G). Neither separation of spindles nor expression of Cdc5 was observed in *dmc1Δ rad51Δ pch2Δ* cells (Figure 3.14F and 3.14G). Additionally, active checkpoint markers of phosphorylated Hop1 and pH3-T11 were highly abundant. This data shows that without Pch2, the meiotic checkpoint function in *dmc1Δ rad51Δ* cells remains active. To show that the checkpoint mounted in *dmc1Δ rad51Δ pch2Δ* cells occur via the general meiotic checkpoint signaling cascade involving Hop1, I investigated the meiotic progression of these cells with reduced levels of Hop1. *dmc1Δ rad51Δ pch2Δ* cells with decreased Hop1 levels were unable to mount the checkpoint and could thus exit prophase and enter meiosis I (Figure 3.14F, right panel and 3.14G). This emphasized the operation of a single checkpoint signaling cascade during meiotic prophase. The appearance of long stretches of SC in *dmc1Δ rad51Δ* and dependence on Pch2 for prophase exit suggests

it is the Zip1-mediated recruitment of Pch2 to the chromosomes that is responsible for the silencing of the meiotic checkpoint. Indeed, deletion of *ZIP1* in *dmc1Δ rad51Δ* cells show a similar near-complete arrest in meiotic prophase as *dmc1Δ rad51Δ pch2Δ* (Figure 3.15A and 3.15B). Both these strains do not exit meiotic prophase and have high checkpoint activity. Taken together with previous observations, these results indicate that Pch2 plays a role in driving both the activation and silencing of meiotic prophase checkpoint function. The key determinant of whether Pch2 plays the role of an agonist or an antagonist in the meiotic prophase checkpoint is SC-polymerization and consequently the recruitment of Pch2 onto the chromosomes.

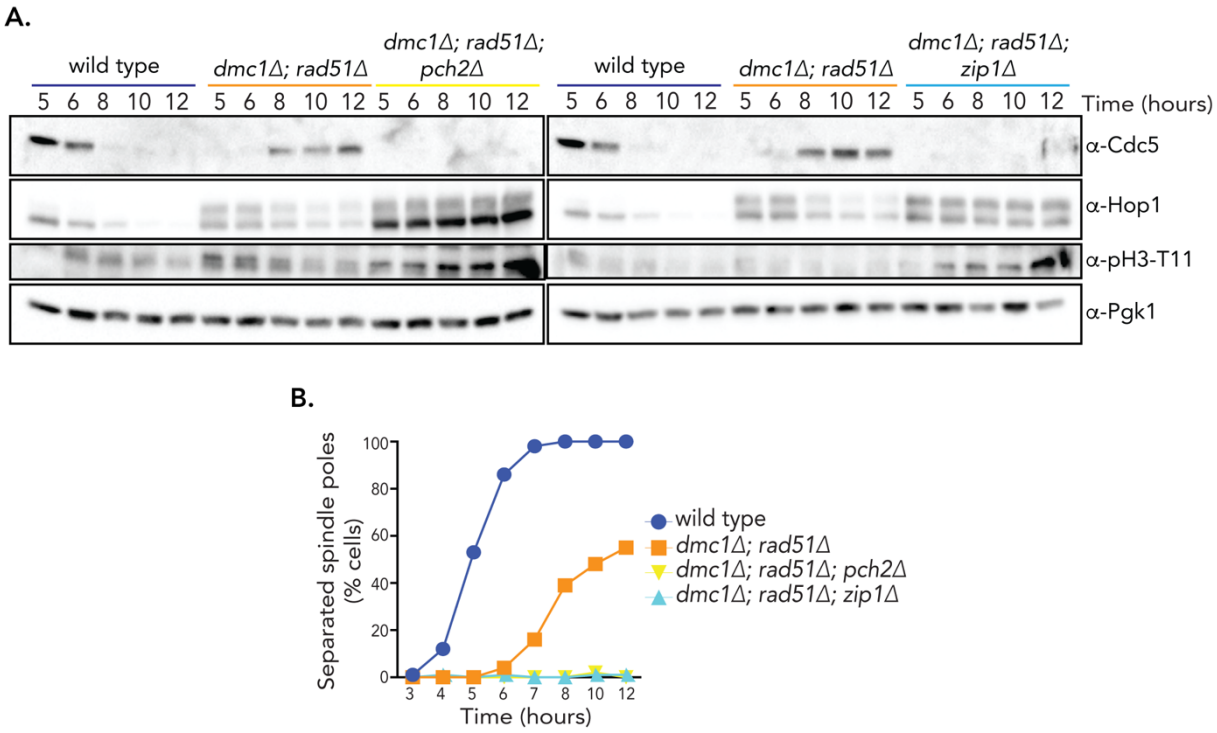

Figure 3.15: **Zip1 is important for *dmc1Δ rad51Δ* mediated meiotic progression**
A. Expression analysis of Cdc5, Hop1 and pH3-T11 to compare meiotic progression and checkpoint activity in wild type (yGV4577), *dmc1Δ rad51Δ* (yGV1401), *dmc1Δ rad51Δ pch2Δ* (yGV1409), and *dmc1Δ rad51Δ zip1Δ* (yGV4737) strains. Pgk1 is loading control. **B.** Comparison of meiotic progression using α-tubulin immunofluorescence for analyzing spindle morphology in strains used in (A). A minimum of 200 cells were analyzed for each data point.

3.11 Zip1 mediates the switch between the dual role of Pch2 in checkpoint control

To further delineate the dual role as an agonist and as an antagonist of meiotic prophase checkpoint function played by Pch2, I again utilized the inducible Pch2 system. In *ndt80Δ* cells, deletion of *PCH2* results in abundance of phosphorylated Hop1 and pH3-T11 even during later time points when the homologous chromosomes have fully synapsed. To confirm the role of Pch2 in silencing the checkpoint, and the importance of Zip1 herein, I expressed Pch2 using inducible expression system at 7 hours post-induction of meiosis. At this time, extensive SC polymerization has taken place. Expression of Pch2 led to a rapid reversal of all the markers associated with active checkpoint. Compared to the non-induced condition decreased phosphorylation of Hop1 and H3-T11 was observed on induction of Pch2 (Figure 3.16A). Non-induced conditions were comparable to *pch2Δ* and Pch2 induced phenotypes were comparable to Pch2 expressed from its endogenous promoter (Figure 3.16A). This result suggests that expression of Pch2 at later time points lead to silencing of the meiotic checkpoint ostensibly because of the rapid recruitment of Pch2 to the chromosomes.

Finally, to show that Pch2, in a Zip1-dependent manner, is able to silence the meiotic checkpoint even in the face of continuous DSB signaling, I used the above described conditions of *dmc1Δ rad51Δ* in combination with the inducible Pch2 system. Contrary to the effects of inducing Pch2 in *zip1Δ ndt80Δ* conditions, I observed that induction of Pch2 in *dmc1Δ rad51Δ* cells led to the entry of cells into meiosis I underscoring the role of Pch2 in checkpoint silencing (Figure 3.16B and 3.16C). The bypass of the meiotic arrest was possible only in the presence of Zip1, as induction of Pch2 could not alleviate the arrest in *dmc1Δ rad51Δ zip1Δ* (Figure 3.16B and 3.16C). This indicates that the untimely synapsis that occurs, and hence potential recruitment of Pch2 to the chromosomes, in *dmc1Δ rad51Δ* cells is the determining factor for the alleviation of the meiotic arrest. To show that the exit from meiotic arrest is associated with the effects of Pch2 on checkpoint silencing, I quantified the active checkpoint markers of phosphorylated Hop1 and pH3-T11. Indeed, upon induction of Pch2, the levels of both of these markers showed a substantial decrease as compared with the uninduced control (Figure 3.16D, 3.16E and 3.16F). These results highlight the importance of Zip1 in the dual role that Pch2 plays during the meiotic prophase checkpoint. Thus, the presence of Zip1 on chromosomes (in the SC) determines the

subcellular localization of Pch2, which in turn acts as a switch for Pch2 to behave either as an agonist or an antagonist of the meiotic checkpoint network.

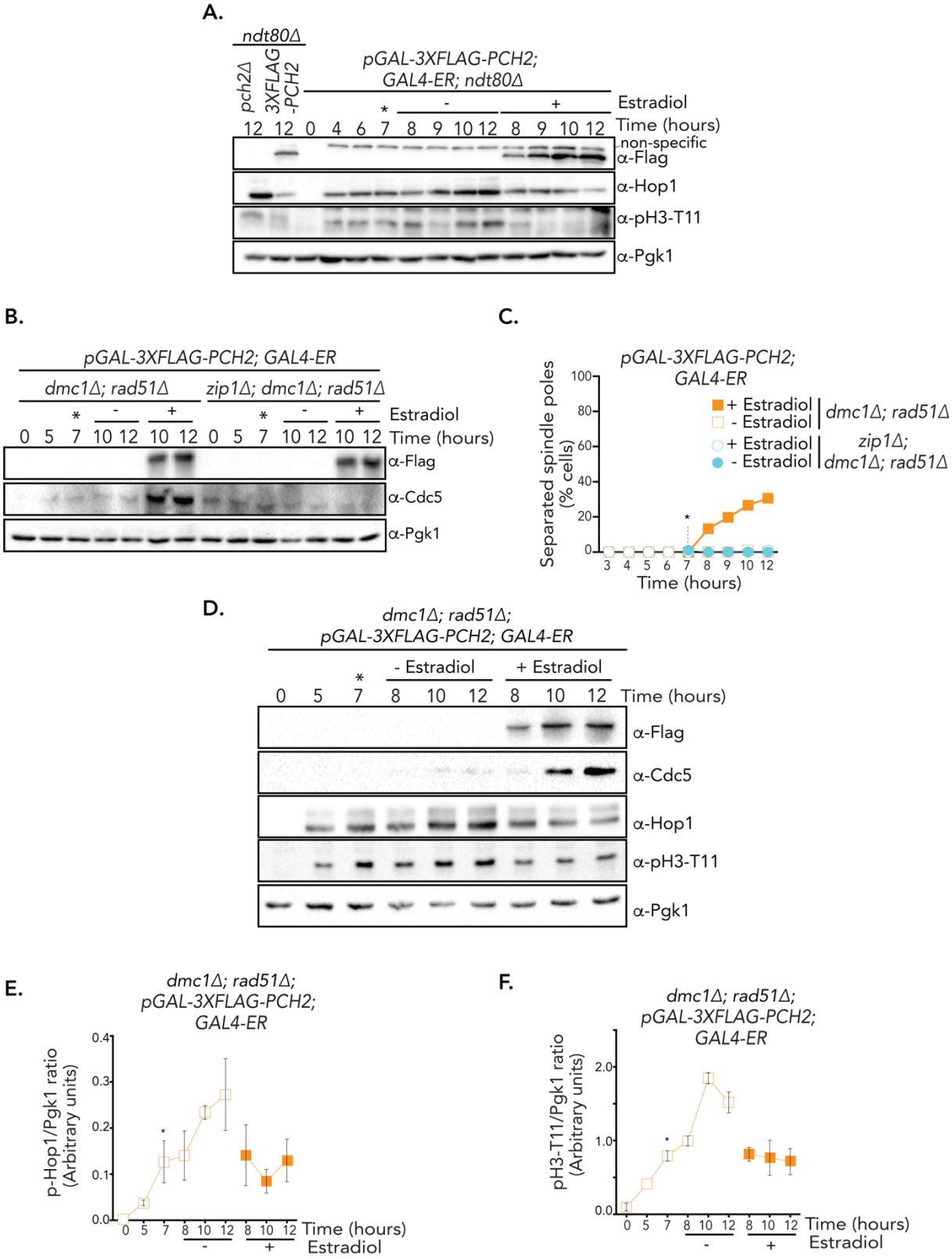

Figure 3.16: **Zip1 based SC-polymerization is important for the role of Pch2 in silencing the meiotic checkpoint**

A. Western blot analysis to compare the effects on Hop1 and pH3-T11 expression profile at indicated time points during meiotic progression with and without induction of

Figure 3.16 continued

Flag-Pch2 in *pGAL-3XFLAG-PCH2 GAL4-ER ndt80Δ* (yGV3171). Samples at 12 hours post-induction of meiosis from *pch2Δ ndt80Δ* (yGV2447) and *pPCH2-3xFLAG-PCH2; ndt80Δ* (yGV2889) are used as control. Estradiol is added at 7 hours post-induction of meiosis to induce the expression of Pch2 (indicated by *). **B.** and **C.** Comparison of meiotic progression in *dmc1Δ rad51Δ pGAL-3xFLAG-PCH2* (yGV4774) and *dmc1Δ rad51Δ zip1Δ pGAL-3xFLAG-PCH2* (yGV4835) with and without induction of Pch2 by analysis of Cdc5 expression using western blot and by counting the number of cells showing separated spindle poles using whole-cell immunofluorescence. Expression of Pch2 was induced 7 hours post-induction of meiosis (indicated by *). For whole-cell immunofluorescence, a minimum of 200 cells were analyzed for each data point. **D.** Western blot analysis to compare the meiotic checkpoint activity with and without induction of Pch2 in *dmc1Δ rad51Δ pGAL-3xFLAG-PCH2* (yGV4774). Expression of Pch2 was induced 7 hours post-induction of meiosis (indicated by *). **E.** and **F.** Quantification of the total cellular levels of phosphorylated Hop1 (slow migrating band) and pH3-T11 from the western blots shown in (D). Mean values ± SD are calculated from two different experiments.

Chapter 4
Discussion

During meiosis, one round of DNA replication is followed by two rounds of chromosome segregation events: first homologous chromosomes segregate followed by the segregation of sister chromatids. To ensure faithful segregation of homologous chromosomes, a tight association between the homologs is required. Cells depend on accurate execution of interdependent processes of homologous recombination and synaptonemal complex (SC) polymerization to establish such associations. The chromosomal localization of Hop1, a HORMA domain-containing protein, and establishment of proper chromosomal axis is pivotal for the proper assembly of the SC (Carballo et al. 2008; Hollingsworth and Byers 1989; Hollingsworth, Goetsch, and Byers 1990; Niu et al. 2005). Hop1 is also a critical component of the checkpoint signaling cascades monitoring the correct execution of both recombination and SC assembly (Subramanian et al. 2016; Ho and Burgess 2011; Carballo et al. 2008; Niu et al. 2005). Pch2, in an SC-dependent manner, is responsible for actively removing its client Hop1 from the chromosomes (Herruzo et al. 2016; San-Segundo and Roeder 1999; Chen et al. 2014; Subramanian et al. 2016). In this study, I show that, apart from regulating the levels of Hop1 on chromosomes, Pch2 is also involved in regulating the chromosomal abundance of Zip1. Pch2, Hop1 and Zip1 set up an intricate feedback system to regulate the dynamics of SC assembly. This study also sheds light on the framework for checkpoint signaling during meiotic prophase. I propose the existence of a common meiotic prophase checkpoint instead of distinct signaling cascades responding to different lesions. I show that Pch2 and Hop1 are responsible for setting the homeostatic control of this checkpoint function. Pch2 does so by playing a role in both activation and inactivation of the checkpoint. Finally, I unravel that the dual role of Pch2 is determined by the cellular context of Pch2, which in turn is determined by SC polymerization.

4.1 Pch2, Hop1 and Zip1 create a feedback system to regulate SC assembly

An initial objective of this study was to determine if Pch2 plays a role in the regulation of SC assembly. The polymerization of SC is concomitant with the

chromosomal recruitment of Pch2 (Bhalla and Dernburg 2005; San-Segundo and Roeder 1999; Subramanian et al. 2016). On the chromosomes, Pch2 helps in the active removal of Hop1 from chromosomal axis (Chen et al. 2014; Herruzo et al. 2016). In accordance with previous literature, I show that the deletion of *PCH2* leads to significantly higher levels of Hop1 on the chromosomes (Figure 3.1A and 3.1B) (Herruzo et al. 2016; Joshi et al. 2009; San-Segundo and Roeder 1999; Subramanian et al. 2016). The increase in the chromosomal occupancy by Hop1 was in agreement with an increase in the total cellular level of Hop1 (Figure 3.1D). Deletion of *PCH2* having a consequence on the total cellular levels of Hop1 suggests that Pch2 plays a role in the stability of Hop1 protein. Indeed, other AAA+ ATPases like Cdc48 are involved in substrate proteolysis by employing the Ubiquitin Fusion Degradation pathway (Ghislain et al. 1996). Whether Pch2 also regulates the stability of Hop1 using similar mechanisms is an important question that warrants investigation. Apart from the effects on Hop1, deletion of *PCH2* also led to an increase in the chromosomal abundance of Zip1 (Figure 3.1A and 3.1C). This observation strengthens previous studies that showed that deletion of *PCH2* leads to higher colocalization of Hop1 and Zip1 on the chromosomes (Borner, Barot, and Kleckner 2008; Joshi et al. 2009). Notably, the chromosomal increase of Zip1 was not associated with an increase in the total cellular levels of Zip1 (Figure 3.1D). This suggests that Pch2 regulates the SC assembly by restricting the chromosomal loading of Zip1.

The structural and mechanistic similarities between the SC and the polycomplex (PC) has resulted in the utilization of PC as a tool to study both formation and regulation of SC assembly. For example, Fpr3, a proline isomerase, was discovered as a regulator of SC assembly by examining the effects of Fpr3 on PC formation in a DSB deficient cell (Macqueen and Roeder 2009). PCs have also been observed in conditions of prolonged meiotic prophase or when SC components like Zip1 are overexpressed (Sym and Roeder 1995; Dong and Roeder 2000; Bhuiyan, Dahlfors, and Schmekel 2003). In line with this, I also observed that PCs exist in cells which experience prophase arrest because of the absence of transcription factor Ndt80 (Figure 3.1G and 3.2B). As cells spend more time in prophase, the total levels of Zip1 gradually increase, correlating with an increase in the number of cells showing PCs. In accordance with the role of Pch2 in regulating SC assembly, Pch2 was also observed to regulate the number of cells showing the presence of PC. Fewer *pch2Δ ndt80Δ* cells

contained PC structures as compared to *ndt80Δ* cells (Figure 3.1G and 3.2B). However, *pch2Δ* cells exhibited no difference in PC abundance formed due to the absence of DSBs, proving that Pch2 is not directly involved in the formation of PC (Figure 3.3C and 3.3D). This observation, along with the evidence that *pch2Δ ndt80Δ* cells accumulate PC structures at later stages of meiotic arrest, led me to speculate that PC formation can be treated as the aggregation of surplus SC components that are left after extensive polymerization of SC on chromosomes. This proposal can be extended to explain why PC formation is delayed in *pch2Δ* cells: the higher abundance of Zip1 on the chromosomes in *pch2Δ* conditions ensures less availability of non-chromosomal Zip1 for PC formation. Moreover, decrease in the number of cells showing PC formation under conditions of lower Zip1 levels provided further credence to this hypothesis (Figure 3.4C). Cells lacking *PCH2* exhibited a synergistic effect with lower levels of Zip1 on PC abundance, and strengthened the initial observation of Pch2's role in restricting levels of Zip1 deposition on chromosomes (Figure 3.4C). Lowering the levels of Hop1 and quantifying PC abundance provided insights into how Pch2 might be regulating the chromosomal abundance of Zip1, and consequently PC formation. Cells containing lower levels of Hop1 corresponded with lower amounts of chromosomal Zip1 (Figure 3.5D). The lower amount of Zip1 on chromosomes in *pch2Δ* cells with Hop1 heterozygosity reflected in a higher prevalence of cells containing PCs as compared to cells lacking Pch2 only (Figure 3.5A and 3.5C) suggesting a role of chromosomal Hop1 in facilitating the chromosomal occupancy by Zip1. Based on these observations, I conclude that PC formation is a common phenomenon, and the occurrence of PC is dependent on the extent of SC polymerization that has taken place on chromosomes. This view departs from the current opinion that PC formation is only a consequence of defective DSB formation or processing. The formation of PC is influenced by the gradual increase in the cellular levels of Zip1 during meiotic prophase and the process of SC polymerization is regulated quantitatively by the intricate interplay between Pch2, Hop1 and Zip1.

A number of SC components localize to PC structures with differential localization patterns. Zip2, Zip4 and SIC protein like Msh4 show polar localization whereas Zip3 localizes throughout the PC (Hughes and Hawley 2020). To gain further understanding of the PC, it would be interesting to investigate if the proteins showing different PC localization also behave differently in terms of total cellular levels. One

would not expect the levels of proteins that cap the PCs to increase but for the proteins that localize throughout the PC to show a trend reminiscent of Zip1 levels. Since SC is a highly dynamic structure, it is plausible that PC acts as the reservoir which provides the building blocks for the assembly of SC. However, if the PC has any physiological role relevant to the proper progression of cells during meiosis still needs an investigation.

4.2 Pch2 and Hop1 set the homeostatic control of the meiotic prophase checkpoint

Hop1 transduces signals emanating from defects in both synapsis and recombination (Wu and Burgess 2006; Wu, Ho, and Burgess 2010). However, the prevailing model indicates that Pch2 plays an exclusive role in the checkpoint signaling arising due to the synapsis defects (Wu and Burgess 2006). Absence of *PCH2* in cells containing lower levels of Hop1 causes cells to progress faster through the meiotic prophase because of a compromised checkpoint (Figure 3.7B and 3.7C). By making use of *ZIP1* and *DMC1* deletions to trigger synapsis and recombination signaling defects respectively, I showed that Pch2 is indispensable not only for synapsis checkpoint signaling but also for the recombination defect signaling (Figure 3.9B and 3.11B). Based on these observations, I propose that the checkpoint signaling initiated by the cellular defects, be it synapsis or recombination, share a common signaling cascade (Figure 4.1). The observation that both checkpoint cascades are dependent on DSB formation and employ Mek1 as the effector kinase further propagates the idea of a single signaling logic for different cellular defects (Wu, Ho, and Burgess 2010).

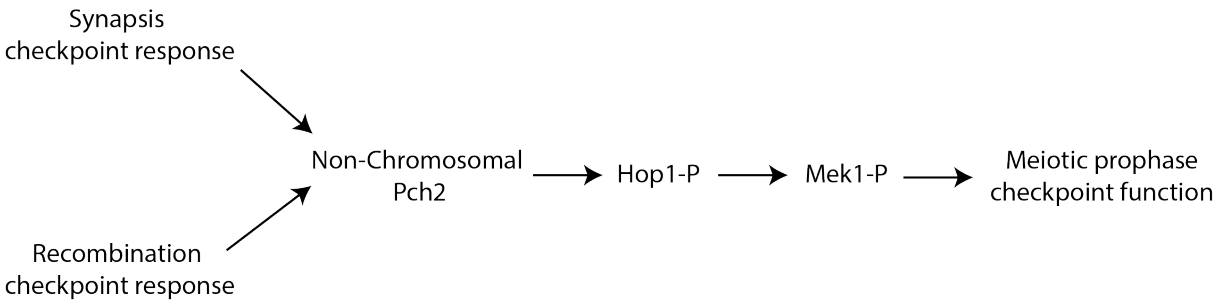

Figure 4.1: **Both synapsis and recombination defects are relayed by a general meiotic checkpoint signaling cascade**
A flowchart showing the requirement of non-chromosomal Pch2 in relaying the checkpoint response emanating from both synapsis and recombination defects. Pch2 facilitates the phosphorylation of Hop1, which in turn facilitates the activation of effector

Figure 4.1 continued
kinase Mek1 to generate a meiotic prophase checkpoint response. For simplicity, multiple other proteins involved in the signaling cascade are omitted.

To reconcile the paradoxical role of Pch2 in checkpoint signaling emanating from synapsis and recombination defects with the hypothesis of a single checkpoint operating during meiotic prophase, I posit that a crucial requirement for optimal checkpoint signaling is the presence of sufficient signaling competent Hop1. Analogous to SAC signaling, where TRIP13 helps to constantly generate the open topological conformation of Mad2 (O-Mad2), I propose a model whereby non-chromosomal Pch2 (Pch2 recruitment to chromosomes is impaired in both *zip1Δ* and *dmc1Δ* conditions) plays a role in the meiotic checkpoint signaling cascade by constantly generating the signaling competent form of Hop1, which can be readily incorporated into the chromosome axis. Hop1 is incorporated into the chromosomes by its interaction via the closure motif present in another axial element protein called Red1. Meiotic HORMA proteins like Hop1 are unique because they also contain their own closure motif. Pch2, potentially in a manner similar to how Pch2/TRIP13 works on Mad2, functions as a machine that constantly helps in freeing the Hop1 HORMA domain from its own closure motif (intra-C-Hop1) to generate a different topological conformation (most likely U-Hop1) (Ye et al. 2017). The availability of free HORMA domain facilitates the incorporation of Hop1 into the chromosomal axis, via its interaction with the closure motif present in Red1 (West, Komives, and Corbett 2018). Chromosomal incorporation results in the availability of Hop1 for phosphorylation by DSB-dependent active Mec1/Tel1 kinases resulting in the generation of the biochemical entity required for the checkpoint function, i.e. Active Mek1 (Wu, Ho, and Burgess 2010). The observation that almost all the signaling competent form of Hop1 (a slow migrating specie of Hop1) is found on the chromatin (Figure 3.11C) and that timed induction of Pch2 in synapsis-deficient cells facilitates Hop1 phosphorylation (Figure 3.13A and 3.13B) supports the idea that Pch2 helps in creating enough signaling competent U-Hop1 to be incorporated into the chromosome-based checkpoint signaling by Mec1/Tel1. In principle, this is similar to kinetochore-based MCC signaling where TRIP13 facilitates the MCC formation by providing sufficient O-Mad2 (Ma and Poon 2018; Marks et al. 2017; Kim et al. 2018; Nelson et al. 2015; Ma and Poon 2016).

The model in which the role of Pch2 in checkpoint function is to generate sufficient levels of signaling competent U-Hop1 needs to be extended to explain why under certain conditions Pch2 seems to be dispensable for the functioning of the checkpoint. *dmc1Δ* cells undergo extensive 5'-3' nucleolytic degradation (resection) of DNA after DSB formation but are deficient in enabling stable strand invasions. Deletion of *DMC1* results in the meiotic prophase arrest of cells and the presence of Pch2 seems dispensable for the meiotic arrest (Hochwagen et al. 2005; Wu and Burgess 2006). To reconcile this observation with the model proposed, I hypothesize that in *dmc1Δ* cells sufficient concentrations of signaling competent Hop1 is present, even without the presence of Pch2. However, under these conditions, sufficient signal for inducing checkpoint arrest can only be attained with very high levels of DSB-dependent Mec1/Tel kinase activity. The activity of Mec1 and Tel1 is modulated by their response to different DNA structures. Blunt DSB ends are the preferred substrate for the binding and activity of Tel1 whereas Mec1 recruitment and activity require the formation of ssDNA arising from 5'-3' resection of DNA (Shiotani and Zou 2009; Zou and Elledge 2003). Thus, in the case of *dmc1Δ* cells where extensive resection takes place, a hyperactivated Mec1 is present that potentially results in stabilizing the incorporation of sufficient Hop1 into checkpoint signaling cascade. Indeed, a similar level of phosphorylated Hop1 is observed in both *dmc1Δ* and *dmc1Δ pch2Δ* cells, and even in *dmc1Δ HOP1/hop1Δ* cells suggesting that the role of Pch2 is important only under unperturbed conditions, or under conditions of low kinase activity (Figure 3.11A and 3.11C). Strikingly, the phosphorylated form of Hop1 is readily lost in *dmc1Δ pch2Δ HOP1/hop1Δ* cells (Figure 3.11A), underscoring the importance of Pch2 in cells with lower levels of Hop1. This level of signaling competent Hop1 is maintained because of the equilibrium between the two states (U-Hop1 and C-Hop1) of Hop1, which in turn is dependent on total Hop1 levels. Thus, the role of Pch2 is indispensable either in conditions of low kinase activity or limiting levels of Hop1.

The proposal that Pch2 is important for facilitating Hop1 phosphorylation by Mec1/Tel1 kinases is further validated by the observation that another recombination deficient condition of *sae2Δ*, where DSB's occur but resection of DNA is impaired, require the presence of Pch2 for the meiotic delay (Figure 3.8A) (Prinz, Amon, and Klein 1997; Ho and Burgess 2011). Without Pch2, *sae2Δ* cells fail to generate optimal checkpoint signaling (Figure 3.8A). Because of the presence of only DSB blunt ends

and no resection, in *sae2Δ* cells, Tel1, and not Mec1, is expected to be active. Deletion of *TEL1* in *sae2Δ* cells results in similar alleviation of the checkpoint delay as caused by deletion of *PCH2* in *sae2Δ* cells, supporting the idea that Pch2 facilitates the phosphorylation of Hop1 by Mec1/Tel1 kinases (Ho and Burgess 2011; Joshi et al. 2015). On comparing observations from *dmc1Δ* and *sae2Δ* cells, it becomes evident that the presence of Pch2 is extremely critical for checkpoint signaling in cases of less extreme kinase activity, or in general, under wild type scenarios.

DSBs in *zip1Δ* cells disappear with a comparable kinetics to those of unperturbed cells (Börner, Kleckner, and Hunter 2004) resulting in less extreme Mec1/Tel1 kinase activity as compared to *dmc1Δ* cells. The less extreme kinase activity renders Pch2 important for generating optimal checkpoint signal which explains why deletion of PCH2 results in the alleviation of checkpoint delay in *zip1Δ.* In addition to this, Pch2 is also indispensable for checkpoint signaling in cells containing lower levels of Hop1 with no other perturbations (Figure 3.7C). As described above, deletion of *PCH2* results in an increase in the total cellular levels of Hop1 (Figure 3.1D). This might affect checkpoint functionality by influencing the absolute concentration of signaling competent U-Hop1, by increasing the spontaneous conformation change (see above). A recent study has also pointed out to the influence of total Hop1 levels on checkpoint functions (Herruzo et al. 2016). Overexpression of Hop1 in *zip1Δ pch2Δ* cells restores checkpoint functionality (Herruzo et al. 2016). Interestingly, decreasing the levels of Hop1 in *zip1Δ* results in the partial alleviation, comparable to the deletion of *PCH2* in *zip1Δ*, of the meiotic delay (Figure 3.9B) confirming that the total levels of Hop1 do have an influence on the competence of checkpoint function. These observations imply that Pch2 and Hop1 have an additive or combined effect on the proper functioning of the meiotic prophase checkpoint. The dependence of Pch2's checkpoint functionality on Hop1 levels is again reminiscent of the similar signaling logic operating during SAC function. Overexpression of Hop1 rendering the function of Pch2 indispensable during meiotic checkpoint function is analogous to the overexpression of Mad2 which renders the function of TRIP13 non-essential in SAC signaling (Marks et al. 2017).

4.3 SC assembly dictates the switch-like behavior of Pch2 in checkpoint function

Analogous to the role of TRIP13 in SAC function, Pch2 plays a role in the activation of meiotic prophase checkpoint. However, TRIP13 is also responsible for silencing the SAC signaling (Alfieri, Chang, and Barford 2018; Kim et al. 2018; Ma and Poon 2016; Wang et al. 2019; Eytan et al. 2014). To examine if Pch2 also plays a role in silencing of meiotic prophase checkpoint signaling, I investigated the role of Pch2 in a condition where cells exit meiotic prophase even in the presence of ongoing checkpoint signaling. Deletion of *RAD51* leads to a bypass of the checkpoint arrest caused due to a lack of *DMC1*, even in the face of unrepaired DNA DSBs (Figure 3.14B) (Shinohara et al. 1997; Markowitz et al. 2017; Farmer et al. 2012). The observation that meiotic arrest was restored in *dmc1Δ rad51Δ* on deletion of *PCH2* shows that the presence of Pch2 is also responsible for silencing of the meiotic prophase checkpoint (Figure 3.14F and 3.14G). In fact, it shows that Pch2 can lead to silencing of the checkpoint even in the face of ongoing checkpoint signaling. Thus, Pch2 can act as an agonist as well as an antagonist of the meiotic progression. However, the observation that *pch2Δ* cells eventually exit the meiotic prophase, despite exhibiting a delay in meiotic progression, argues against the idea that Pch2 is the only factor responsible for the silencing of the checkpoint. It predicts the presence of additional checkpoint silencing pathways operating redundantly with Pch2. Indeed, protein phosphatases like Glc7 and the protein phosphatase 4 (PP4) have been indicated to counteract the Mec1/Tel1 dependent phosphorylation of Hop1 and or Mek1, and hence promote checkpoint inactivation (Chuang, Cheng, and Wang 2012; Bailis and Roeder 2000) (Hochwagen et al. 2005). Presence of multiple factors for silencing of the meiotic prophase checkpoint signal is analogous to SAC signaling, where silencing of the active checkpoint is also achieved via multiple pathways. Apart from Pch2/TRIP13 mediated disassembly of MCC, multiple mechanisms involving removal of checkpoint proteins from attached kinetochore or through phosphatases that counteract the activity of mitotic kinases also contribute to the silencing of the SAC signaling (Liu et al. 2010; Meadows et al. 2011; Rosenberg, Cross, and Funabiki 2011; Howell et al. 2001).

It is well known that Pch2 is recruited to chromosomes in a Zip1 synapsis(San-Segundo and Roeder 1999) dependent manner (Subramanian et al. 2016). The

observation that *dmc1Δ rad51Δ* cells show an increase in the assembled SC structures compared to *dmc1Δ* cells alone (Figure 3.14C and 3.14D) provided an indication towards understanding the rationale behind the silencing property of Pch2 function. I speculated that synapsis in *dmc1Δ rad51Δ* cells lead to the chromosomal recruitment of Pch2 and this change in the subcellular localization i.e. Pch2 being chromosomal or non-chromosomal, determines whether it functions in the activation of the checkpoint or its inactivation. This hypothesis predicts that deletion of *ZIP1*, and hence impairing the recruitment of Pch2 to chromosomes, should lead to the impairment of the silencing effect of Pch2. Indeed, deletion of *ZIP1* in *dmc1Δ rad51Δ* cells led to the restoration of meiotic arrest, similar to the deletion of *PCH2*, indicating that is the chromosomal recruitment of Pch2 which leads to its function in silencing the checkpoint (Figure 3.15A and 3.15B).

Although polymerization of the SC is concomitant with the recruitment of Pch2 to chromosomes, a number of observations point out that SC polymerization is not the only factor responsible. Cells with *ZIP1-4LA*, a mutation in *ZIP1* where four leucine residues in the central coiled-coil region are replaced with alanine, show extensive SC polymerization without the recruitment of Pch2 to the chromosomes (Mitra and Roeder 2007; Subramanian et al. 2016) suggesting it is not SC polymerization per say which is responsible for recruitment of Pch2 to the chromosomes. Pch2 is also recruited to the chromosomes in *zip1Δ* cells also lacking *DOT1*, a histone methyltransferase (San-Segundo and Roeder 2000). Deletion of *DOT1* leads to the alleviation of the checkpoint delay caused due to *zip1Δ*, ostensibly because of the recruitment of Pch2 to chromosomes. Moreover, multiple other factors like Orc1 (a component of ORC complex), active transcription and Topoisomerase II have been shown to play a role in the recruitment of Pch2 to chromosomes (Cardoso da Silva, Villar-Fernández, and Vader 2020; Villar-Fernández et al. 2020; Heldrich et al. 2020). Whether these factors also play a role in establishing the function of Pch2 as an agonist or an antagonist of meiotic progression still needs to be examined.

4.4 Dual role of Pch2: a summary of the model

Depending on the cellular context, Pch2 can either act as an agonist or an antagonist of the meiotic prophase checkpoint. But how does the change in the cellular context of Pch2 lead to opposite functions? I propose that both activation and

inactivation functions of Pch2 are a result of the same biochemical activity of Pch2 on Hop1. During early prophase, or in cases where Pch2 cannot be recruited to chromosomes e.g. in *zip1Δ* or *dmc1Δ* cells, non-chromosomal Pch2 facilitates the activation of checkpoint by promoting the availability of U-Hop1, by inducing a conformational change from intra-C-Hop1 (Figure 4.2, depicted by A). U-Hop1 can then interact with the closure motif present in Red1, leading to the chromosomal recruitment of Hop1 and a change in conformation from U-Hop1 to C-Hop1. Interaction of Hop1 with Red1 allows Hop1 to oligomerize via its free closure motif to form an assembly resembling “beads on a string” (Figure 4.2, depicted by C). Chromosomal Hop1 acts as the substrate for Mec1/Tel1 kinase activity which are activated on the chromosomes by different DNA substrates (see above). Phosphorylation of Hop1 recruits the checkpoint effector kinase Mek1 and facilitates its activation by trans auto-phosphorylation. The active Mek1 allows the cells to maintain an arrest in the meiotic prophase until the completion of crucial events like formation of obligate crossover has taken place.

Upon successful engagement of crossover repair, SC polymerization drives the recruitment of Pch2 to the chromosomes. Chromosomal Pch2 helps in silencing the checkpoint by removing Hop1 from the chromosomes by inducing the topological conformation change in Hop1, via disruption of HORMA-closure motif interaction. Since there are two such interactions taking place: Hop1-HORMA:Red1-closure motif and Hop1-HORMA:Hop1-closure motif, there are potentially two scenarios of how Pch2 might be acting to modulate the chromosomal levels of Hop1. In Scenario 1, Pch2 is able to disrupt the Hop1-Red1 interaction, thereby removing all of the Hop1 from the chromosomes (Figure 4.2, depicted by D). Observations made by immunofluorescence experiments on meiotic chromosome spreads, where no or very less Hop1 is observed on chromosomes after recruitment of Pch2, support this scenario. However, a point mutation in the closure motif of Hop1, *HOP1-K593A*, renders the checkpoint activity of cells non-functional, irrespective of the fact that this mutant can still localize to chromosomes and can interact with Red1 (Niu et al. 2005). This observation reflects a scenario where Hop1 can interact with Red1 but the mutation in the closure motif of Hop1 renders the oligomerization of Hop1 impaired. As such, only the recruitment of Hop1 to chromosomes does not lead to checkpoint functions. This predicts another scenario where Pch2 can silence the checkpoint by

disassembly of the Hop1 oligomers via disruption of inter-Hop1 interactions (i.e. Hop1-HORMA:Hop1-closure motif) (Figure 4.2, depicted by E, Scenario 2). In both the scenarios, the activity of chromosomal Pch2 on Hop1 restricts its participation in active checkpoint signaling, thus helping in silencing of the checkpoint.

The SC polymerization provides the switch in preference of the client (from intra-C-Hop1 to C-Hop1) thereby dictating the dual role of Pch2. The SC assembly on the chromosomes initiates from two different sites: from centromeres and from crossover designated sites (also known as synapsis initiation complex (SIC) sites because of the assembly of different proteins involved in facilitating crossover and synapsis). SC assembly initiating from SIC sites may act as a local individual chromosome-based molecular signal which communicates the successful formation of an obligatory crossover to the rest of the chromosome and triggers a switch towards silencing of the checkpoint. It is a proposal put forward by multiple studies, with this doctoral work joining the list (Borner, Barot, and Kleckner 2008; Subramanian et al. 2016; Carballo et al. 2013; Thacker et al. 2014; Lao et al. 2013). In drawing parallels with SAC, the assembly of SC can be conceptually likened to chromosome biorientation, a cytological state after which MCC disassembly needs to be promoted.

The switch-like characteristic in Pch2 function is potentially also favored because of the inherent capability of Hop1 to adopt intra-C-Hop1 conformation immediately after it is removed from the chromosomes. The intra-C-Hop1 cannot be incorporated into the checkpoint signaling cascade without the active conformation change induced by Pch2. With Pch2 localized to the chromosomes, no active intra-C-Hop1 to U-Hop1 conformation change can take place, leading to the gradual suppression of checkpoint and entry into meiosis I. Recent studies in *Arabidopsis thaliana* have made observations that support this prediction and suggest conserved behavior (Yang et al. 2020). The interplay between Pch2 and Hop1 is highly dynamic. Removal of Pch2 from chromosomes, by making use of a Zip1 anchor away method, leads to fast recovery of Hop1 onto the chromosomes (Subramanian et al. 2016). The dynamicity of the Pch2-Hop1 module accounts for the fact there is a basal level of spontaneous U-Hop1 being formed from intra-C-Hop1, without active conformational change by Pch2 (Figure 4.2, depicted by B). Even if basal levels of U-Hop1 is converted into C-Hop1 at chromosomes and is incorporated into the checkpoint

signaling, the rate of conversion of C-Hop1 to U-Hop1 will remain high because of high local concentration of Pch2 at the chromosomes. Thus, this difference in the rate of conformation conversion of Hop1 at chromosomal and non-chromosomal sites by Pch2 ensures silencing of the checkpoint signaling upon chromosomal recruitment of Pch2.

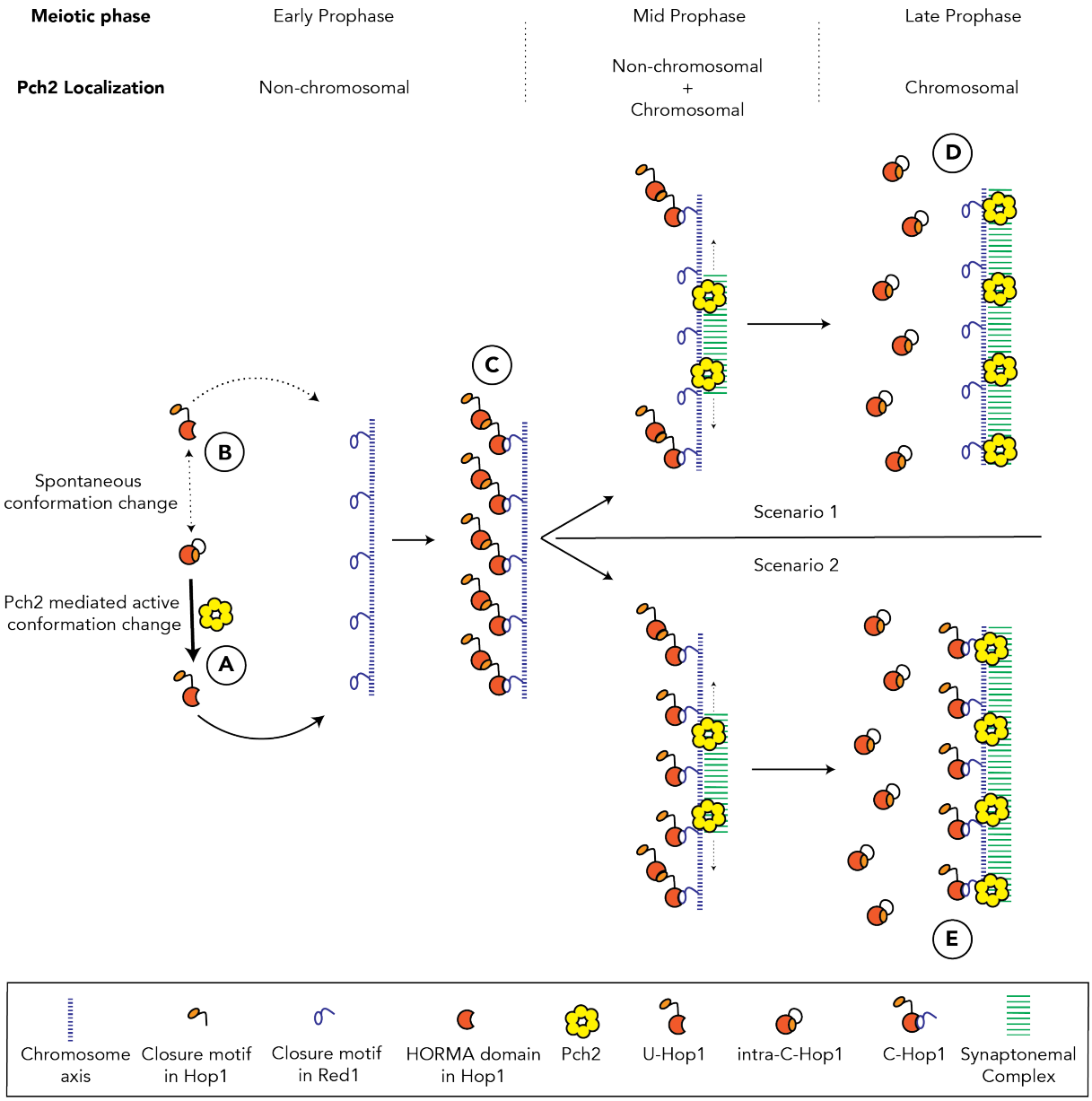

Figure 4.2: **Model explaining the dual role of Pch2 in meiotic prophase checkpoint function**

A change in conformation of Hop1 (intra-C-Hop1 to U-Hop1) is required for it to associate with the closure motif of chromosomal Red1. Hop1 can undergo this conformational change by non-chromosomal Pch2 mediated active transformation (depicted by A) or by a spontaneous transformation (depicted by B). U-Hop1 associates with Red1, and Hop1 then oligomerizes by interaction via closure motif on interacting Hop1 forming assemblies which resemble “beads on a string” (depicted by

Figure 4.2 continued
C). SC polymerization then drives the change in localization of Pch2. On chromosomes, Pch2 removes the assemblies of Hop1 either by disrupting the Hop1 HORMA:Red1 closure motif interaction (depicted by D) or by disrupting Hop1 HORMA:Hop1 closure motif interaction (depicted by E). Disruption of Hop1 assemblies leads to removal of Hop1 from the checkpoint siganlling cascade, thus silencing the checkpoint function.

To summarize, it is the same biochemical activity of disrupting HORMA-closure motif interaction by AAA+ ATPase Pch2 that can lead to differential outcomes depending on the subcellular localization and context of Pch2, which in turn is dictated by the polymerization of SC.

In light of these observations and the proposed model, it is attractive to revisit the checkpoint role of Fpr3, a proline isomerase protein. Fpr3 plays a role in maintaining the continued checkpoint arrest caused due to the deletion of *dmc1Δ* (Hochwagen et al. 2005). In the same study, in contrast to Pch2 function, deletion of *FPR3* was shown to bypass the checkpoint arrest in *dmc1Δ* cells but did not lead to the alleviation of the meiotic delay in *zip1Δ* cells. These observations prompted authors to propose that Pch2 and Fpr3 function in genetically distinct pathways. Fpr3 also regulates the assembly of SC, especially SC polymerization initiating from the centromeres (Macqueen and Roeder 2009). Considering the observations made in this doctoral work regarding recombination and synapsis defects being relayed via the same signaling cascade, and with the available literature about the role of Fpr3 in regulating SC assembly, I propose that *dmc1Δ fpr3Δ* cells bypass the meiotic arrest in a manner similar to how deletion of *RAD51* allows *dmc1Δ* cells to exit meiotic prophase: that is by allowing untimely synapsis. Evidently, this proposition would imply that the bypass of meiotic arrest in *dmc1Δ fpr3Δ* would depend on the checkpoint silencing functions of Pch2. Indeed, deletion of *PCH2* restores the meiotic arrest in *dmc1Δ fpr3Δ* cells *(personal communication, Andreas Hochwagen, New York University).* In fact, restricting the chromosomal recruitment of Pch2 to the chromosomes by deleting *ZIP1* in *dmc1Δ fpr3Δ* cells, also leads to the restoration of checkpoint arrest in *dmc1Δ fpr3Δ* cells *(personal communication, Andreas Hochwagen, New York University)*. These observations suggest that Fpr3 functions in the same genetic pathway as Rad51, and in both cases Pch2 enables the exit from

meiotic prophase. This, however, raises important questions about how Rad51 and Fpr3 regulate the SC assembly.

4.5 AAA+ HORMA: a conserved module across cellular processes, organisms and evolution

HORMA domain proteins are involved in regulation of a multitude of cellular processes. There is a rapid increase in literature suggesting that HORMA domain proteins are almost always accompanied with a AAA+ ATPase to modulate their function. The observation of the co-occurrence of HORMA domain protein and the presence of TRIP13-like ATPase in a single operon in bacterial genomes show that this module of AAA+ HORMA is evolutionarily ancient (van Hooff et al. 2017). A recent bioinformatic study does provide some answers to the question of the evolutionary history of this module. It shows that both eukaryotic HORMA domain proteins and Pch2/TRIP13 ATPases form a monophyletic group within bacterial HORMA proteins and bacterial Trip13 proteins respectively (Tromer et al. 2019). Further, a recent study showed that the mode of action of Trip13-like ATPase and HORMA proteins in imparting immunity to bacteria against bacteriophage is very similar to eukaryotic AAA+ HORMA module suggesting the conservation of this module and its modus operandi from bacteria to mammals(Ye et al. 2020) .

The presence of AAA+ HORMA module across organisms and the conservation of mode of action raises a fundamental question of the reasons for adaptation of this module to signaling cascades responding to different stimuli. One reason could be to impart a higher level of dynamicity and responsiveness to the system. AAA+ HORMA module typically relies on the same biochemical activity but mostly responds to the external changes via a switch in the preference of substrate or a change in localization. However, AAA+ HORMA module is generally dependent on the initial burst of signaling via a post-translational modification, in most cases the activity of a kinase. For example, in meiotic prophase checkpoint, Mec1/Tel plays the role of initiating the signaling cascade. Similarly, SAC signaling initiates with the activity of Mps1 and other kinases on kinetochore proteins. The interdependency of this module on typical signaling cascade pathways potentially helps in bringing a higher order of dynamicity to the system while still maintaining the robustness of a kinase-phosphatase signaling module.

Chapter 5
Perspectives

Cell cycle checkpoints ensure that critical events such as genome replication and chromosome segregation are completed with high fidelity. Checkpoints that operate during meiotic prophase control meiotic progression to ensure proper execution of crucial events like DSB formation, recombination and synapsis. Pch2 and Hop1 are critical components of the meiotic prophase checkpoint signaling. This doctoral work further advances the understanding of Pch2 and Hop1 during meiotic processes and establishes a unified model explaining what previously seemed paradoxical roles played by Pch2 during meiotic checkpoint function. Along with these advances, this doctoral work also lays a platform for future investigations. The immediate questions which need further examinations are *i*) understanding the mechanistic details of chromosomal recruitment of Pch2, *ii*) the molecular explanation of the role of Rad51 in maintaining the arrest in *dmc1Δ* cells, and *iii*) the evolutionary conservation of these processes in other organisms.

Pch2 and Hop1 synergistically modulate the meiotic checkpoint function. The cellular context of Pch2 is a major determinant for its role in the checkpoint function: non-chromosomal Pch2 functions as an agonist whereas chromosomal Pch2 functions as an antagonist of the meiotic checkpoint function. As such, chromosomal recruitment of Pch2 provides the switch in the function of Pch2. The recruitment of Pch2 to chromosomes is dependent on factors like synapsis, chromatin modifications, active transcription, and Orc1 (Cardoso da Silva, Villar-Fernández, and Vader 2020; Villar-Fernández et al. 2020; Heldrich et al. 2020; San-Segundo and Roeder 2000). However, the mechanistic details of recruitment of Pch2 to the chromosomes remain poorly understood. A subset of chromosomal Pch2 localizes at the synapsis initiation complex (SIC) sites (Joshi et al. 2009). My initial investigations towards understanding the mechanistic details of chromosomal recruitment of Pch2 suggested that Pch2 associates with a SIC factor, Msh4. The association of Msh4 with Pch2 was first observed by performing a label-free mass spectrometric analysis of an NH_2-terminally Flag-Pch2 and later confirmed by co-immunoprecipitation analysis (Figure 8.1,

Appendices). AAA+ ATPases with a mutation in the Walker B domain, which can bind to ATP but cannot hydrolyze it, are known to bind stably to their substrates. *Pch2-E399Q*, a Walker B domain mutant version of Pch2, also associates with Msh4 but does not show a stronger association as compared to wild type Pch2 suggesting Msh4 might not be a substrate of Pch2. Interaction of Pch2 with a SIC component is particularly interesting in light of Pch2's role in processes like crossover interference. Apart from providing answers to chromosomal recruitment of Pch2, investigation of functional consequences of Pch2 and Msh4 association might uncover the role of Pch2 in other meiotic processes.

One of the exciting discoveries of this doctoral work is the long unanswered question of how *dmc1Δ rad51Δ* cells bypass the checkpoint signaling. Deletion of *RAD51* in *dmc1Δ* cells leads to the untimely polymerization of SC, which eventually leads to silencing of the checkpoint, ostensibly via recruitment of Pch2 to the chromosomes. However, the molecular details of how Rad51 regulates SC assembly and protects cells from untimely SC polymerization still remain elusive. The inability of cells lacking *RAD54* (an accessory factor of Rad51 facilitating recombination function of Rad51) to bypass meiotic arrest in *dmc1Δ* cells, suggests a recombination independent mechanism of SC regulation by Rad51. These observations point for the first time to a recombination independent function of Rad51. Future investigations should be directed towards understanding the molecular mechanisms behind this specific characteristic of Rad51 in regulating the SC assembly.

In budding yeast, initiation of SC assembly takes place at two different sites: at SIC sites, which designate future crossover sites, and at centromeres. Preliminary experiments performed as part of this thesis showed that the alleviation of the meiotic arrest in *dmc1Δ rad51Δ* is dependent on the kinetochore component Ctf19. The deletion of *CTF19* in *dmc1Δ rad51Δ* restores the high abundance of active meiotic checkpoint markers and consequently the meiotic arrest (Figure 8.2, Appendices). The fact that Ctf19 is a component of kinetochore and is known to localize and perform functions on or near centromeres suggests that Rad51 might be regulating synapsis initiating from centromeres. Based on these results, I hypothesize that Ctf19 and Rad51 have antagonizing effects on the initiation of SC polymerization from centromeres. Ctf19 facilitates Zip1 polymerization which helps in the initial pairing of

the chromosomes. On the other hand, Rad51 negatively regulates the SC polymerization thereby ensuring cells do not prematurely silence the checkpoint. Silencing should only take place when SC polymerization initiates from SIC after the successful engagement of a crossover. Future studies testing this hypothesis would help provide molecular details of the role of Ctf19 and Rad51 in the regulation of SC assembly. Fpr3 is another protein that regulates the SC assembly initiating from centromeres and evidences suggest that Fpr3 and Rad51 participate in the same genetic pathway. Whether these proteins co-ordinate to regulate SC assembly is also an interesting question that warrants an investigation. Moreover, the differential regulation of SC assembly at two different sites raises an important question about the evolutionary importance and conservation of this dual SC initiation system.

Finally, the conservation of AAA+-HORMA module across organisms and different cellular processes raises a key question: is the combined function of Pch2 and Hop1 in modulating the checkpoint also conserved in higher eukaryotes? TRIP13, the mammalian homolog of Pch2, modulates the chromosomal abundance of Hop1 homologs in mammals, HORMAD proteins, in a similar manner to how Pch2 modulates the chromosomal abundance of Hop1 in budding yeast (Wojtasz et al. 2009). Additionally, phosphorylation of HORMAD proteins in mice is restricted to the unsynapsed chromosome axes (Fukuda et al. 2012). These observations are highly suggestive of a higher order conservation of the function of Pch2 and Hop1 proteins. Apart from AAA+ HORMA proteins, an observation from studies on *Oryza sativa* suggests a conserved role for Rad51 in restricting the non-homologous interactions (Zhang et al. 2020). Whether the mechanisms of dual sites for synapsis initiation exist in higher organisms and if the role of Rad51 in the regulation of SC is also conserved are fascinating questions to be answered in subsequent studies.

Chapter 6
Summary

Meiosis is a specialized cell division program utilized by sexually reproducing organisms to produce gametes (e.g. egg and sperm). As cell progress through meiotic prophase, the formation of physical linkages between the initially unpaired homologous chromosomes is established. Without the linkage between homologs, the probability of chromosome missegregation, and the associated rate of aneuploidy, increases manifold during chromosomal segregation events. Recombination, where programmed DNA double-strand breaks (DSBs) are repaired via homologous chromosomes, generates physical linkages between homologous chromosomes. This process is facilitated by synapsis, where two homologs come in close proximity to each other by virtue of the polymerization of synaptonemal complex (SC) at the interface of two homologs. Checkpoints operate during meiotic prophase to ensure the timely execution of both recombination and synapsis. Hop1, a HORMA domain-containing protein plays a central role in checkpoint signaling cascade emanating because of defects in either recombination or synapsis. On the other hand, Pch2, an AAA+ ATPase, is believed to play a role exclusively in relaying checkpoint function in response to defects in synapsis. Although Pch2 is known to execute almost all of its functions via its action on a single client protein, Hop1, it is not fully understood why Pch2 plays a role specifically in only one checkpoint signaling operating during the meiotic prophase. In addition, how does Pch2 function in checkpoint regulation during meiotic prophase has remained elusive.

Chromosomal Hop1 is essential for proper assembly of SC, and Pch2 regulates the chromosomal abundance of Hop1. Deletion of *PCH2* leads to increased colocalization of Hop1 and Zip1, the central component of SC on the chromosomes. In this doctoral work, by exploiting budding yeast genetics, I provide a framework of the feedback mechanism between Pch2, Hop1, and Zip1 responsible for regulating the SC assembly. I show that Pch2 restricts the chromosomal recruitment of Zip1 by modulating the chromosomal abundance of Hop1. I also revisited the idea of multiple checkpoints operating during meiotic prophase and the role of Pch2 in the signaling of

these checkpoints. I show that, in contrast to the current understanding, Pch2 plays a role in both recombination and synapsis checkpoint signaling. I propose that both these checkpoints follow the same signaling logic in which Pch2 and Hop1 play a combined role in optimal checkpoint signaling. I also define and explain the dual role of Pch2 in checkpoint signaling whereby Pch2, depending on the cellular context, can play the role of an agonist as well as an antagonist in checkpoint signaling. I show that, under conditions where Pch2 cannot be recruited to the chromosomes, Pch2 helps in facilitating the incorporation of Hop1 in chromosome-based checkpoint signaling. On the other hand, under conditions where Pch2 can be recruited to the chromosomes, Pch2 fuels checkpoint silencing by removing Hop1 from chromosomes. Pch2 is able to perform this checkpoint silencing activity even in the face of unrepaired DSBs. Although multiple factors control chromosomal recruitment of Pch2, I show that, under unperturbed conditions, by determining the cellular localization of Pch2, polymerization of SC dictates switch-like checkpoint behavior of Pch2. Collectively, this study shows that Pch2 and Hop1 establishes a dynamic AAA+ HORMA module that regulates the meiotic checkpoint function in a manner analogous to the way the AAA+ HORMA module of Pch2/TRIP13 and Mad2 acts during checkpoint that monitors chromosome segregation during mitosis and meiosis.

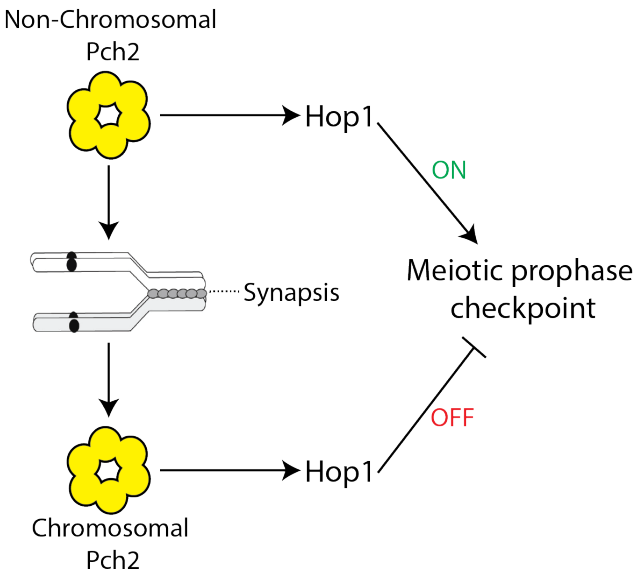

Figure 6.1: **Graphical summary**
This doctoral work uncovers and explains the dual role of Pch2 in meiotic checkpoint function. Non-chromosomal Pch2 acts as an agonist by facilitating the incorporation of Hop1 in meiotic checkpoint signaling. Upon synapsis, Pch2 is recruited to chromosomes where it acts as an antagonist of the meiotic checkpoint signaling by

Figure 6.1 continued
removing chromosomal Hop1 from the signaling cascade. Thus, depending on the cellular context, the activity of Pch2 on Hop1 can result in opposing outcomes. Image modified from Raina and Vader, 2020.

Chapter 7
Zusammenfassung

Sexuell fortpflanzende Organismen bilden Gameten (Eizellen und Spermien) mittels einer speziellen Art von Zellteilung, die Meiose. In der meiotischen Prophase werden ursprünglich ungepaarte homologe Chromosomen in der Zelle physisch miteinander verbunden. Ohne die Verbindung bzw. Paarung der homologen Chromosomen, ist die Wahrscheinlichkeit der Fehlverteilung der Chromosomen und die damit assoziierte Aneuploidie während der chromosomalen Teilungen um ein vielfaches erhöht. Die Paarung der homologen Chromosomen erfolgt durch Rekombination, ein Vorgang bei dem programmierte DNA Doppelstrang-Brüche (DSBs) via homologe Chromosomen repariert werden. Dies wird durch einen Prozess unterstützt, der als Synapse bezeichnet wird. Durch die Polymerisation des synaptonemalen Komplexes (SC) werden bei der Synapse zwei homologe Chromosomen in unmittelbarer Nähe zu einander gebracht. Der zeitliche Ablauf der Rekombination und der Synapse wird durch Kontrollpunkte während der meiotischen Prophase reguliert. Fehler bei der Rekombination oder Synapse lösen eine Kontrollpunkt-Signalkaskade aus, bei der das HORMA-Domän beinhaltende Protein Hop1 eine zentrale Rolle spielt. Der AAA+ ATPase Pch2 hingegen, wird eine Rolle bei der Übermittlung der Kontrollpunkt-Funktion zugesprochen, wenn Fehler bei der Synapse auftreten. Obwohl Pch2 dafür bekannt ist, dass es fast all seine Funktionen über das Protein Hop1 ausübt, ist nicht vollständig verstanden, warum Pch2 eine spezielle Rolle in nur einer Kontrollpunkt Signalübertragung, während der meiotischen Prophase spielt. Des Weiteren ist es nur schwer nachvollziehbar wie Pch2 in der Kontrollpunkt Regulation, während der meiotischen Prophase funktioniert.

Chromosomales Hop1 ist für die korrekte Zusammensetzung des SC erforderlich, und Pch2 reguliert die chromosomale Häufigkeit von Hop1. Deletion von PCH2 führt zu einer erhöhten Kolokalisierung von Hop1 und Zip1, die zentrale Komponente des SC auf den Chromosomen. Mithilfe der Hefe Genetik, stelle ich in dieser Doktorarbeit ein Gerüst für den Feedback Mechanismus zwischen Pch2, Hop1 und Zip1, der für die Regulierung der SC Zusammensetzung verantwortlich ist dar. Ich

zeige, dass Pch2 die chromosomale Rekrutierung von Zip1 durch das Modulieren der chromosomalen Häufigkeit von Hop1 begrenzt. Dabei komme ich auf die Idee zu sprechen, dass mehrere Kontrollpunkte während der meiotischen Prophase operieren und die Rolle von Pch2 in der Signalisierung dieser Kontrollpunkte. Ich veranschauliche, dass, im Gegensatz zu dem heutigen Verständnis, Pch2 eine Funktion in der Kontrollpunkt Signalisierung der Rekombination und Synapse hat. Des Weiteren schlage ich vor, dass beide Kontrollpunkte der gleichen Signalisierungslogik folgen, bei der Pch2 und Hop1 eine gemeinsame Funktion für die optimale Kontrollpunkte Signalisierung ausüben. Außerdem definiere und erkläre ich die duale Funktion von Pch2 in der Kontrollpunkt Signalisierung. Dabei kann Pch2, abhängig von den zellulären Umständen, als Agonist, wie auch als Antagonist in der Checkpoint Signalisierung fungieren. Unter Bedingungen, wo Pch2 nicht zu den Chromosomen rekrutiert werden kann, zeige ich, dass Pch2 die Einbindung von Hop1 in die Chromosomen-basierende Kontrollpunkt Signalisierung unterstützt. Andererseits, unter Bedingungen wo Pch2 zu den Chromosomen rekrutiert werden kann, verstärkt es die Kontrollpunkt Stillegung durch das Entfernen von Hop1 von den Chromosomen. Pch2 kann trotz unreparierter DSBs die Kontrollpunkt Inaktivierung ausführen. Obwohl mehrere Faktoren die chromosomale Rekrutierung von Pch2 kontrollieren, erläutere ich, dass unter unbeeinflussten, bzw. regulären Bedingungen die Polymerisation des SC, das wechselnde Verhalten von Pch2 bei dem Checkpoint befiehlt. (Auslöst) Insgesamt wird in dieser Studie gezeigt, dass Pch2 und Hop1 ein dynamisches AAA+ HORMA Modul bilden, dass die meiotische Kontrollpunkt Funktion auf eine Art reguliert, die mit der Überwachung der Chromosomen Teilung während der Mitose und Meiose durch das AAA+ HORMA Modul, bestehend aus Pch2/ TRIP13 und Mad2 ist, vergleichbar ist.

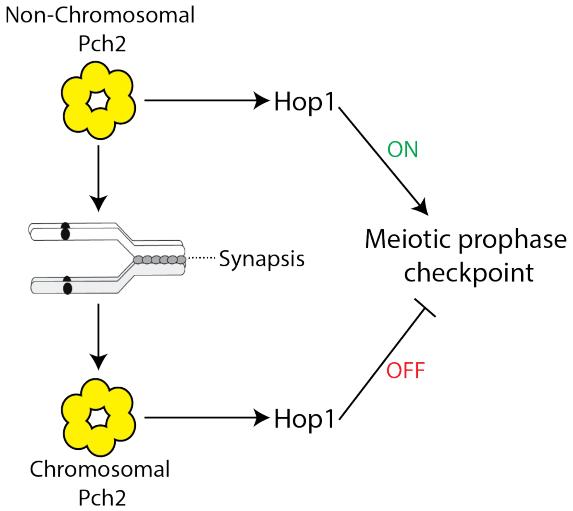

Abbildung 7.1: **Grafische Zusammenfassung**

Diese Doktorarbeit enthüllt und erklärt die duale Rolle von Pch2 in der meiotischen Kontrollpunkt-Funktion. Nicht-chromosomales Pch2 fungiert als Agonist, indem es die Inkorporation von Hop1 in die meiotische Kontrollpunkt Signalisierung vermittelt. Bei der Synapse wird Pch2 zu den Chromosomen rekrutiert, wo es als Antagonist der meiotischen Kontrollpunkt Signalisierung wirkt da es chromosomales Hop1 von der Signalisierungskaskade entfernt. In Abhängigkeit von den zellulären Umständen, kann die Aktivität von Pch2 auf Hop1 dementsprechend gegensätzliche Auswirkungen haben. Abbildung modifiziert nach Raina und Vader, 2020.

Chapter 8
Appendices

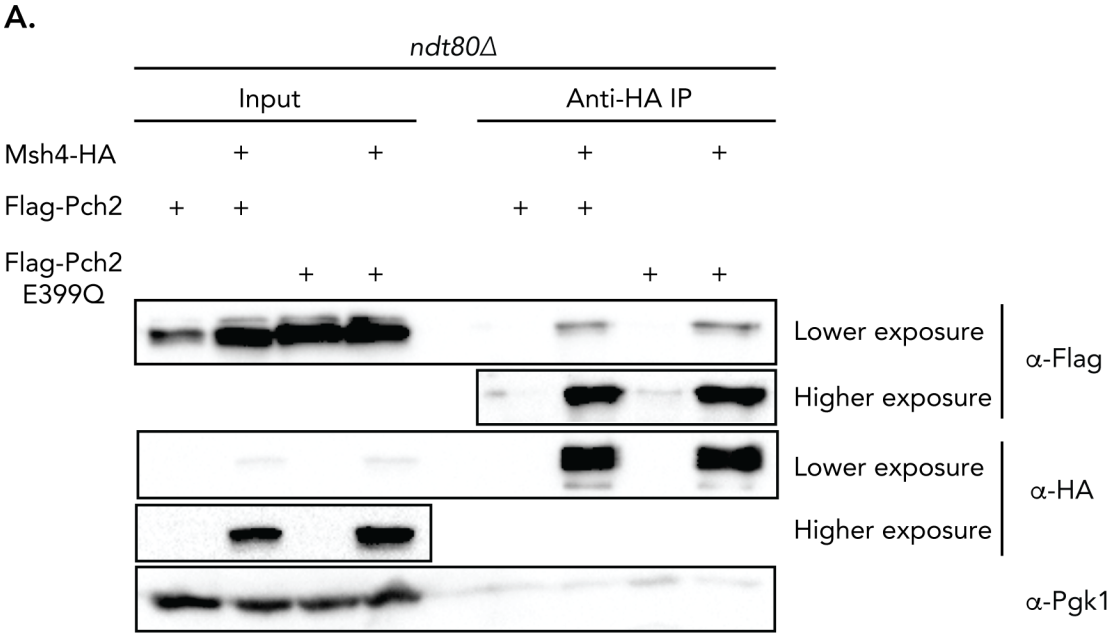

Figure 8.1: **Msh4 interacts with both wild type Pch2 and substrate trapping mutant of Pch2 (Pch2-E399Q).**
A. Co-immunoprecipitation (co-IP) of wild type Flag-Pch2 and Flag-Pch2-E399Q with Msh4-HA (via α-HA-IP) during the meiotic prophase (4 h into meiotic program) in strains deleted for *NDT80*. Strains used are yGV2889, yGV2919, yGV2991 and yGV3192.

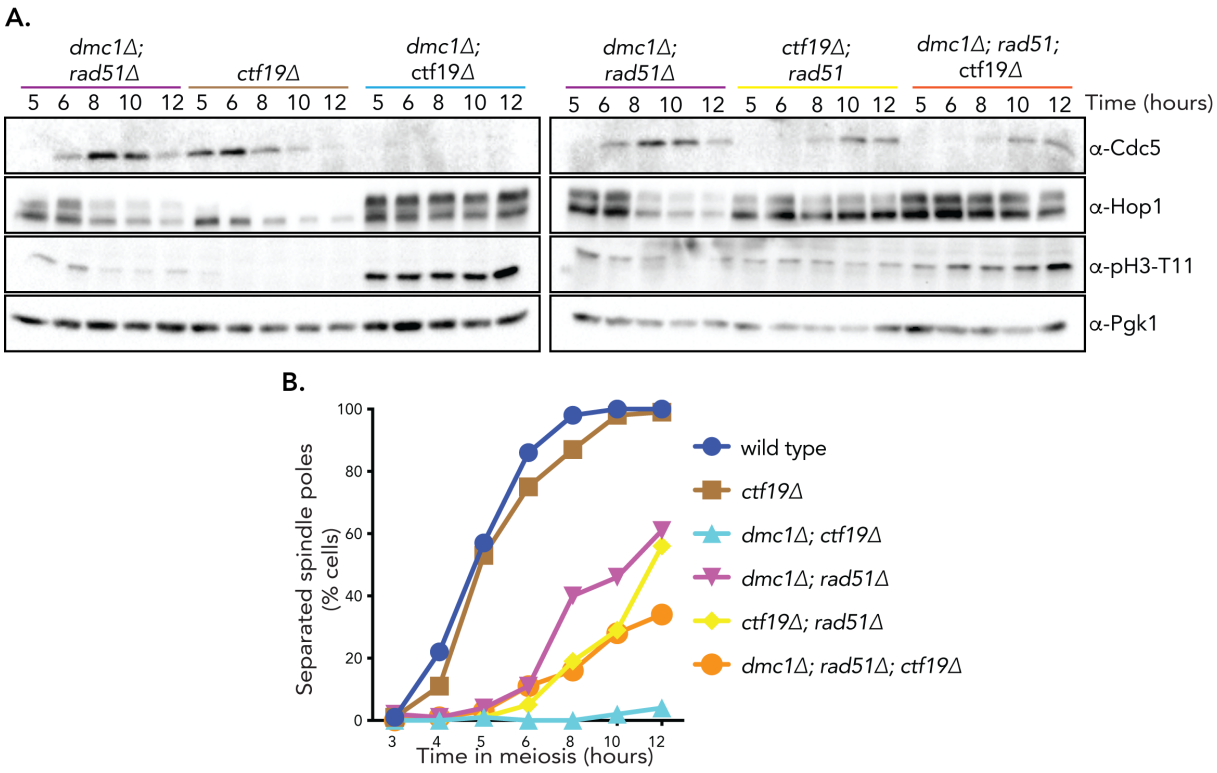

Figure 8.2: **The premature silencing of checkpoint in *dmc1Δ rad51Δ* is dependent on Ctf19**

A. Western blot analysis to compare expression profile of Cdc5, Hop1 and pH3-T11 in *dmc1Δ rad51Δ* (yGV1401), *ctf19Δ* (yGV3049), *dmc1Δ ctf19Δ* (yGV1912), *ctf19Δ rad51Δ* (yGV4798) and *dmc1Δ rad51Δ ctf19Δ* (yGV4791). Pgk1 is used as a loading control. **B.** Comparison of the number of cells entering meiosis I by tracing the spindle morphology at indicated time points of strains used in (A). A minimum of 200 cells were analyzed for each data point. (A) and (B) are from the same time-course experiment.

Table 8.1: **Yeast strains used in this study.**
All strains are of the SK1 background.

Name	***Genotype***
yGV48	*MATa/MATα, ho::LYS2, lys2, leu2::hisG, arg4, his4X::LEU2-URA3/ his4B::LEU2, ura3, dmc1Δ::ARG4*
yGV468	*MATa/MATα,, ho::LYS2, lys2, leu2::hisG, ura3(Δsma-pst::hisG), TRP1, HIS4::LEU2-(NBam)/ his4X::LEU2-(NBam)-URA3, ndt80Δ::LEU2*
yGV1171	*MATa/MATα, ho::LYS2, lys2, leu2::hisG, his4X::LEU2-URA3, his3::hisG, ura3, arg4-nsp/ARG4, dmc1Δ::ARG4, pch2Δ::KanMX, HOP1/ hop1::LEU2*
yGV1269	*MATa/MATα, ho::LYS2, lys2, ura3, leu2::hisG, TRP, his4B::LEU2, arg4-Bgl II, dmc1Δ::ARG4, pch2Δ::KanMX4*
yGV1401	*MATa/MATα, ho::LYS2, lys2, ura3, leu2::hisG, TRP1, his4B::LEU2, arg4-Bgl II(?), dmc1Δ::ARG4, rad51::HIS3*
yGV1409	*MATa/MATα, ho::LYS2, lys2, ura3, leu2::hisG, TRP1/ trp1::hisG, arg4-Bgl II(?), his3::hisG(?), his4B::LEU2, pch2Δ::KanMX4, dmc1Δ::ARG4, rad51::HIS3*
yGV1912	*MATa/MATα, ho::LYS2, lys2, leu2::hisG, his4X::LEU2-URA3, ura3, dmc1Δ::ARG4, ctf19Δ::KanMX4*
yGV2302	*MATa/MATα, ho::LYS2, lys2, leu2::hisG, ura3(Δsma-pst::hisG), ARG4, TRP1, his4X::LEU2-(NBam)-URA3, pch2Δ::KanMX4, ndt80Δ::LEU2*
yGV2447	*MATa/MATα, ho::LYS2, lys2, ura3, leu2::hisG, his3::hisG, trp1::hisG, ARG4, his4X::LEU2-URA3, DMC1/ dmc1Δ::ARG4, trp1::pPch2::TRP1, pch2Δ::KanMX, ndt80Δ::LEU2*

yGV2889 *MATa/MATα, ho::LYS2, lys2, leu2::hisG, his4X::LEU2-URA3, his3::hisG, ura3, trp1:pPCH2-3XFLAG-PCH2::TRP1, pch2Δ::KanMX, ARG4, ndt80Δ::TRP1*

yGV2919 *MATa/MATα, ho::LYS2, lys2, ura3, leu2::hisG, ARG4, his4X::LEU2-URA3, pch2Δ::KanMX, trp1::pPCH2-FLAG-PCH2E399Q::TRP1, ndt80Δ::TRP1*

yGV2991 *MATa/MATα, ho::LYS2, lys2, ura3, leu2::hisG, ARG4, his4X::LEU2-URA3, pch2Δ::KanMX, trp1::pPCH2-FLAG-PCH2E399Q::TRP1, msh4::MSH4-HA::HIS3, ndt80Δ::TRP1*

yGV3049 *MATa/MATα, ho::LYS2, lys2, leu2::hisG, TRP1, his4X::LEU2-URA3, ura3, arg4, ctf19Δ::KanMX4*

yGV3050 *MATa/MATα, ho::LYS2, lys2, ura3, leu2::hisG, his3::hisG, ARG4, ura3::pGPD1-GAL4(848).ER::URA3, HIS3MX::pGAL1-3XFLAG-6xGLYPCH2*

yGV3171 *MATa/MATα, ho::LYS2, lys2, ura3, leu2::hisG, his3::hisG, ARG4, his4x, ura3::pGPD1-GAL4(848).ER::URA3, pch2::HIS3MX::pGAL1-3XFLAG6xGLY-PCH2, ndt80Δ::TRP1*

yGV3192 *MATa/MATα, ho::LYS2, lys2, ura3, leu2::hisG, ARG4, his4X::LEU2-URA3, pch2Δ::KanMX, trp1::pPCH2-FLAG-PCH2::TRP1, msh4::MSH4-HA::HIS3, ndt80Δ::TRP1*

yGV4119 *MATa/MATα, ho::LYS2/ho::hisG, lys2, leu2::hisG, URA3/ura3(Δsmapst::hisG), his3::hisG, ARG4, TRP1, pch2Δ::KanMX4, spo11- Y135F::KanMX4, ndt80Δ::LEU2*

yGV4137 *MATa/MATα, ho::hisG/ho::LYS2, lys2, leu2::hisG, ura3(Δsmapst::hisG)/URA3, ARG4, his3::hisG, TRP1, spo11-Y135F::KanMX4, ndt80Δ::LEU2*

yGV4461 *MATa/MATα, ho::LYS2, leu2::hisG, ura3, ARG4, TRP1, his4X, HIS3, zip1::URA3::ZIP1-GFP, HOP1/hop1::URA3, ndt80Δ::LEU2*

yGV4463 *MATa/MATα, ho::LYS2, leu2::hisG, ura3, ARG4, TRP1/trp1, his4X, HIS3, zip1::URA3::ZIP1-GFP, ndt80Δ::LEU2*

yGV4470 *MATa/MATα, ho::LYS2, lys2, leu2::hisG, ura3(Δsma-pst::hisG), his3::hisG, trp1::hisG, ARG4, zip1Δ::NatMX4, ura3::pGPD1-GAL4(848).ER::URA3, pch2::HIS3MX::pGAL1-3XFLAG-6xGLY-PCH2, ndt80Δ::LEU2*

yGV4504 *MATa/MATα, ho::LYS2, leu2::hisG, ura3, ARG4, TRP1/trp1, his4X, HIS3, zip1::URA3::ZIP1-GFP, pch2Δ::KanMX4, ndt80Δ::LEU2*

yGV4505 *MATa/MATα, ho::LYS2, leu2::hisG, ura3, ARG4, TRP1/ trp1, his4X, HIS3, zip1::URA3::ZIP1-GFP, pch2Δ::KanMX4, hop1::URA3/HOP1, ndt80Δ::LEU2*

yGV4525 *MATa/MATα, ho::LYS2, leu2::hisG, ura3, ARG4, TRP1/trp1, his4X(?), HIS3(?), ndt80Δ::LEU2/NDT80, zip1::URA3::ZIP1-GFP, pch2Δ::KanMX4, HOP1/hop1::URA3*

yGV4526 *MATa/MATα, ho::LYS2, leu2::hisG, ura3, ARG4, TRP1/trp1, his4X(?), HIS3(?), ndt80Δ::LEU2/NDT80, zip1::URA3::ZIP1-GFP, HOP1/hop1::URA3*

yGV4527 *MATa/MATα, ho::LYS2, leu2::hisG, ura3, ARG4, TRP1/trp1, his4X(?), HIS3(?), NDT80/ndt80Δ::LEU2, zip1::URA3::ZIP1-GFP*

yGV4528 *MATa/MATα, ho::LYS2, leu2::hisG, ura3, ARG4, TRP1/trp1, his4X(?), HIS3(?), NDT80/ndt80Δ::LEU2, zip1::URA3::ZIP1-GFP, pch2Δ::KanMX4*

yGV4545 *MATa/MATα,, ho::LYS2, lys2, ura3, leu2::hisG, his3::hisG, ARG4, ura3::pGPD1-GAL4(848).ER::URA3, HIS3MX::pGAL1-3xFLAG-6xGLYPCH2, ZIP1::URA3::ZIP1::GFP, ndt80Δ::TRP1*

yGV4546 *MATa/MATα, ho::LYS2, lys2, leu2::hisG, TRP1, HIS4/his4B::LEU2, ura3, ARG4/arg4-Bgl,hop1::LEU2/HOP1,dmc1Δ::ARG4*

yGV4577 *MATa/MATα, ho::LYS2, lys2, leu2::hisG, ura3(Δsma-pst::hisG), TRP1, his4X::LEU2-(NBam)-URA3 yGV4578 MATa/MATa, ho::LYS2, lys2, leu2::hisG, ura3(Δsma-pst::hisG), TRP1, his4X::LEU2-(NBam)-URA3, zip1Δ::NatMX4*

yGV4579 *MATa/MATα, ho::LYS2, lys2, leu2::hisG, ura3(Δsma-pst::hisG), TRP1, his4X::LEU2-(NBam)-URA3, zip1Δ::NatMX4, hop1::URA3/HOP1*

yGV4580 *MATa/MATα, ho::LYS2, lys2, leu2::hisG, ura3(Δsma-pst::hisG), TRP1, his4X::LEU2-(NBam)-URA3, zip1Δ::NatMX4, pch2Δ::KanMX4, hop1::URA3/HOP1*

yGV4581 *MATa/MATα, ho::LYS2, lys2, leu2::hisG, ura3(Δsma-pst::hisG), trp1::hisG /TRP1, his4X::LEU2-(NBam)-URA3, zip1Δ::NatMX4, pch2Δ::KanMX4*

yGV4598 *MATa/MATα, ho::LYS2, lys2, ura3, leu2::hisG, TRP1, ARG4, his4B::LEU2- (NBam)-URA3, rad51::HIS3, zip1Δ::NatMX4, hop1::URA3/HOP1*

yGV4599 *MATa/MATα, ho::LYS2, lys2, ura3, leu2::hisG, TRP1, ARG4, his4B::LEU2(NBam)-URA3/his4B::LEU2, rad51::HIS3, zip1Δ::NatMX4, pch2Δ::KanMX4*

yGV4600 *MATa/MATα, ho::LYS2, lys2, ura3, leu2::hisG, TRP1, ARG4, his4B::LEU2(NBam)-URA3/his4B::LEU2, rad51::HIS3, zip1Δ::NatMX4, pch2Δ::KanMX4, HOP1/hop1::URA3*

yGV4603 *MATa/MATα, ho::LYS2, lys2, ura3, leu2::hisG, TRP1, ARG4, his4B::LEU2/his4B::LEU2-(NBam)-URA3, rad51::HIS3, zip1Δ::NatMX4*

yGV4608 *MATa/MATα, ho::LYS2, leu2::hisG, ura3, ARG4, TRP1, his4X, HIS3, zip1::URA3::ZIP1-GFP/zip1Δ::NatMX4, pch2Δ::KanMX4, ndt80Δ::LEU2*

yGV4609 *MATa/MATα, ho::LYS2, leu2::hisG, ura3, ARG4, TRP1, his4X, HIS3, zip1::URA3::ZIP1-GFP /zip1Δ::NatMX4, ndt80Δ::LEU2*

yGV4637 *MATa/MATα, ho::LYS2, lys2, leu2::hisG, ura3(Δsma-pst::hisG), his3::hisG, trp1::hisG, ARG4, zip1Δ::NatMX4, ura3::pGPD1-GAL4(848).ER::URA3, pch2::HIS3MX::pGAL1-3XFLAG-6xGLY-PCH2, hop1::LEU2/HOP1, ndt80Δ::LEU2*

yGV4713 *MATa/MATα, ho::LYS2, lys2, TRP1/trp1::hisG, his3::hisG, leu2::hisG, ura3, his4B::LEU2, ARG4, dmc1Δ::ARG4, rad51::HIS3, HOP1/hop1::LEU2*

yGV4715 *MATa/MATα, ho::LYS2, lys2, trp1::hisG, his3::hisG, leu2::hisG, ura3, his4B::LEU2, ARG4, pch2Δ::KanMX4, dmc1Δ::ARG4, rad51::HIS3, hop1::LEU2/HOP1*

yGV4737 *MATa/MATα, ho::LYS2, lys2, ura3, leu2::hisG, TRP1, ARG4, his4B::LEU2- (NBam)-URA3, rad51::HIS3, zip1Δ::NatMX4, dmc1Δ::ARG4 yGV4744 MATa/MATa, ho::LYS2, lys2, ura3, leu2::hisG, his3::hisG, trp1::hisG sae2Δ::LEU2*

yGV4752 *MATa/MATα, ho::LYS2, lys2, ura3, leu2::hisG, his3::hisG, trp1::hisG sae2: Δ:LEU2, hop1 Δ::LEU2/HOP1*

yGV4774 *MATa/MATα, ho::LYS2, lys2, ura3, leu2::hisG, trp1, his4B::LEU2/HIS4, ARG4, his3::hisG(?), dmc1Δ::ARG4, rad51::HIS3, ura3::pGPD1-GAL4(848).ER::URA3, pch2::HIS3MX::pGAL1-3XFLAG-6xGLY-PCH2*

yGV4776 *MATa/MATα, ho::LYS2, lys2, ura3, leu2::hisG, trp1, ARG4, his3::hisG(?), his4B::LEU2, dmc1Δ::ARG4, rad51::HIS3/RAD51, ura3::pGPD1- GAL4(848).ER::URA3, pch2::HIS3MX::pGAL1-3XFLAG-6xGLY-PCH2*

yGV4791 *MATa/MATα, ho::LYS2, lys2, leu2::hisG, ura3, TRP1, his3::hisG, dmc1Δ::ARG4, ctf19Δ::KanMX4, rad51Δ::HIS3*

yGV4796 *MATa/MATα, ho::LYS2, lys2, ura3, leu2::hisG, TRP1, ARG4, his4B::LEU2/his4B::LEU2-(NBam)-URA3, rad54::URA3, dmc1Δ::ARG4, ZIP1/ zip1Δ::NatMX4*

yGV4798 *MATa/MATα, ho::LYS2, lys2, leu2::hisG, ura3, TRP1, ARG4, his3::hisG, ctf19Δ::KanMX4, rad51Δ::HIS3*

yGV4800 *MATa/MATα, ho::LYS2, lys2, ura3, leu2::hisG, his3::hisG, trp1::hisG sae2 Δ::LEU2, pch2Δ::KanMX4, hop1Δ::LEU2/HOP1*

yGV4801 *MATa/MATα, ho::LYS2, lys2, ura3, leu2::hisG, his3::hisG, trp1::hisG sae2Δ::LEU2, pch2Δ::KanMX4*

yGV4811 *MATa/MATα, ho::LYS2, lys2, ura3, leu2::hisG, his3::hisG, ARG4, ura3::pGPD1-GAL4(848).ER::URA3, HIS3MX::pGAL1-3xFLAG-6xGLYPCH2, ZIP1::URA3::ZIP1::GFP, ndt80Δ::TRP1, hop1Δ::URA3/HOP1*

yGV4835 *MATa/MATα, ho::LYS2, lys2, leu2::hisG, ura3(Δsma-pst::hisG), his3::hisG, trp1::hisG, ARG4, zip1Δ::NatMX4, dmc1Δ::ARG4, rad51::HIS3, ura3::pGPD1-GAL4(848).ER::URA3, pch2::HIS3MX::pGAL1-3xFLAG6xGLY-PCH2*

Bibliography

Acosta, I., D. Ontoso, and P. A. San-Segundo. 2011. 'The budding yeast polo-like kinase Cdc5 regulates the Ndt80 branch of the meiotic recombination checkpoint pathway', *Mol. Biol. Cell*, 22: 3478-90.

Agarwal, S., and G. S. Roeder. 2000. 'Zip3 provides a link between recombination enzymes and synaptonemal complex proteins', *Cell*, 102: 245-55.

Alberts, Bruce, Alexander Johnson, Julian Lewis, David Morgan, Martin C. Raff, Keith Roberts, Peter Walter, John Wilson, and Tim Hunt. 2015. *Molecular biology of the cell*.

Alfieri, C., L. Chang, and D. Barford. 2018. 'Mechanism for remodelling of the cell cycle checkpoint protein MAD2 by the ATPase TRIP13', *Nature*, 559: 274-78.

Allers, T., and M. Lichten. 2001. 'Differential timing and control of noncrossover and crossover recombination during meiosis', *Cell*, 106: 47-57.

Aravind, L., and E. V. Koonin. 1998. 'The HORMA domain: a common structural denominator in mitotic checkpoints, chromosome synapsis and DNA repair', *Trends Biochem. Sci.*, 23: 284-6.

Bailis, J. M., and G. S. Roeder. 1998. 'Synaptonemal complex morphogenesis and sister-chromatid cohesion require Mek1-dependent phosphorylation of a meiotic chromosomal protein', *Genes Dev.*, 12: 3551-63.

Bailis, J. M., and G. S. Roeder.. 2000. 'Pachytene exit controlled by reversal of Mek1-dependent phosphorylation', *Cell*, 101: 211-21.

Baudat, F., K. Manova, J. P. Yuen, M. Jasin, and S. Keeney. 2000. 'Chromosome synapsis defects and sexually dimorphic meiotic progression in mice lacking Spo11', *Mol. Cell*, 6: 989-98.

Benjamin, K. R., C. Zhang, K. M. Shokat, and I. Herskowitz. 2003. 'Control of landmark events in meiosis by the CDK Cdc28 and the meiosis-specific kinase Ime2', *Genes Dev*, 17: 1524-39.

Bhalla, N., and A. F. Dernburg. 2005. 'A conserved checkpoint monitors meiotic chromosome synapsis in Caenorhabditis elegans', *Science*, 310: 1683-6.

Bhuiyan, H., G. Dahlfors, and K. Schmekel. 2003. 'Lateral elements inside synaptonemal complex-like polycomplexes in Ndt80 mutants of yeast bind DNA', *Genetics*, 163: 539-44.

Bishop, D. K. 1994. 'RecA homologs Dmc1 and Rad51 interact to form multiple nuclear complexes prior to meiotic chromosome synapsis', *Cell*, 79: 1081-92.

Bishop, D. K., D. Park, L. Xu, and N. Kleckner. 1992. '*DMC1*: a meiosis-specific yeast homolog of *E. coli* recA required for recombination, synaptonemal complex formation, and cell cycle progression', *Cell*, 69: 439-56.

Blat, Y., R. U. Protacio, N. Hunter, and N. Kleckner. 2002. 'Physical and functional interactions among basic chromosome organizational features govern early steps of meiotic chiasma formation', *Cell*, 111: 791-802.

Borgogno, M. V., M. R. Monti, W. Zhao, P. Sung, C. E. Argaraña, and R. J. Pezza. 2016. 'Tolerance of DNA Mismatches in Dmc1 Recombinase-mediated DNA Strand Exchange', *J Biol .Chem.*, 291: 4928-38.

Borner, G. V., A. Barot, and N. Kleckner. 2008. 'Yeast Pch2 promotes domainal axis organization, timely recombination progression, and arrest of defective recombinosomes during meiosis', *Proc. Natl. Acad. Sci. U S A*, 105: 3327-32.

Börner, G. V., N. Kleckner, and N. Hunter. 2004. 'Crossover/noncrossover differentiation, synaptonemal complex formation, and regulatory surveillance at the leptotene/zygotene transition of meiosis', *Cell*, 117: 29-45.

Braun, S., K. Matuschewski, M. Rape, S. Thoms, and S. Jentsch. 2002. 'Role of the ubiquitin-selective CDC48(UFD1/NPL4)chaperone (segregase) in ERAD of OLE1 and other substrates', *EMBO J*, 21: 615-21.

Brown, M. S., and D. K. Bishop. 2014. 'DNA strand exchange and RecA homologs in meiosis', *Cold Spring Harb. Perspect Biol.*, 7: a016659.

Busygina, V., M. G. Sehorn, I. Y. Shi, H. Tsubouchi, G. S. Roeder, and P. Sung. 2008. 'Hed1 regulates Rad51-mediated recombination via a novel mechanism', *Genes Dev*, 22: 786-95.

Callender, T. L., R. Laureau, L. Wan, X. Chen, R. Sandhu, S. Laljee, S. Zhou, R. T. Suhandynata, E. Prugar, W. A. Gaines, Y. Kwon, G. V. Börner, A. Nicolas, A. M. Neiman, and N. M. Hollingsworth. 2016. 'Mek1 Down Regulates Rad51 Activity during Yeast Meiosis by Phosphorylation of Hed1', *PLoS Genet.*, 12: e1006226.

Cao, L., E. Alani, and N. Kleckner. 1990. 'A pathway for generation and processing of double-strand breaks during meiotic recombination in *S. cerevisiae*', *Cell*, 61: 1089-101.

Carballo, J. A., and R. S. Cha. 2007. 'Meiotic roles of Mec1, a budding yeast homolog of mammalian ATR/ATM', *Chromosome Res.*, 15: 539-50.

Carballo, J. A., A. L. Johnson, S. G. Sedgwick, and R. S. Cha. 2008. 'Phosphorylation of the axial element protein Hop1 by Mec1/Tel1 ensures meiotic interhomolog recombination', *Cell*, 132: 758-70.

Carballo, J. A., S. Panizza, M. E. Serrentino, A. L. Johnson, M. Geymonat, V. Borde, F. Klein, and R. S. Cha. 2013. 'Budding yeast ATM/ATR control meiotic double-strand break (DSB) levels by down-regulating Rec114, an essential component of the DSB-machinery', *PLoS Genet.*, 9: e1003545.

Cardoso da Silva, R., M. A. Villar-Fernández, and G. Vader. 2020. 'Active transcription and Orc1 drive chromatin association of the AAA+ ATPase Pch2 during meiotic G2/prophase', *PLoS Genet.*, 16: e1008905.

Cha, R. S., B. M. Weiner, S. Keeney, J. Dekker, and N. Kleckner. 2000. 'Progression of meiotic DNA replication is modulated by interchromosomal interaction proteins, negatively by Spo11p and positively by Rec8p', *Genes Dev.*, 14: 493-503.

Chen, C., A. Jomaa, J. Ortega, and E. E. Alani. 2014. 'Pch2 is a hexameric ring ATPase that remodels the chromosome axis protein Hop1', *Proc. Natl. Acad. Sci U S A*, 111: E44-53.

Chen, Z., H. Yang, and N. P. Pavletich. 2008. 'Mechanism of homologous recombination from the RecA-ssDNA/dsDNA structures', *Nature*, 453: 489-4.

Cheng, Y. H., C. N. Chuang, H. J. Shen, F. M. Lin, and T. F. Wang. 2013. 'Three distinct modes of Mec1/ATR and Tel1/ATM activation illustrate differential checkpoint targeting during budding yeast early meiosis', *Mol. Cell Biol.*, 33: 3365-76.

Chua, P. R., and G. S. Roeder. 1998. 'Zip2, a meiosis-specific protein required for the initiation of chromosome synapsis', *Cell*, 93: 349-59.

Chuang, C. N., Y. H. Cheng, and T. F. Wang. 2012. 'Mek1 stabilizes Hop1-Thr318 phosphorylation to promote interhomolog recombination and checkpoint responses during yeast meiosis', *Nucleic Acids Res.*, 40: 11416-27.

Clever, B., H. Interthal, J. Schmuckli-Maurer, J. King, M. Sigrist, and W. D. Heyer. 1997. 'Recombinational repair in yeast: functional interactions between Rad51 and Rad54 proteins', *EMBO J*, 16: 2535-44.

Coudreuse, D., and P. Nurse. 2010. 'Driving the cell cycle with a minimal CDK control network', *Nature*, 468: 1074-9.

Crickard, J. B., and E. C. Greene. 2018. 'The biochemistry of early meiotic recombination intermediates', *Cell Cycle*, 17: 2520-30.

Dernburg, A. F., K. McDonald, G. Moulder, R. Barstead, M. Dresser, and A. M. Villeneuve. 1998. 'Meiotic recombination in C. elegans initiates by a conserved mechanism and is dispensable for homologous chromosome synapsis', *Cell*, 94: 387-98.

Dick, A. E., and D. W. Gerlich. 2013. 'Kinetic framework of spindle assembly checkpoint signalling', *Nat. Cell Biol.*, 15: 1370-7.

Dong, H., and G. S. Roeder. 2000. 'Organization of the yeast Zip1 protein within the central region of the synaptonemal complex', *J Cell Biol*, 148: 417-26.

Eytan, E., K. Wang, S. Miniowitz-Shemtov, D. Sitry-Shevah, S. Kaisari, T. J. Yen, S. T. Liu, and A. Hershko. 2014. 'Disassembly of mitotic checkpoint complexes by the joint action of the AAA-ATPase TRIP13 and p31(comet)', *Proc Natl Acad Sci U S A*, 111: 12019-24.

Farah, J. A., G. A. Cromie, and G. R. Smith. 2009. 'Ctp1 and Exonuclease 1, alternative nucleases regulated by the MRN complex, are required for efficient meiotic recombination', *Proc. Natl. Acad. Sci. U S A*, 106: 9356-61.

Farmer, S., E. J. Hong, W. K. Leung, B. Argunhan, Y. Terentyev, N. Humphryes, H. Toyoizumi, and H. Tsubouchi. 2012. 'Budding yeast Pch2, a widely conserved meiotic protein, is involved in the initiation of meiotic recombination', *PLoS One*, 7: e39724.

Fukuda, T., F. Pratto, J. C. Schimenti, J. M. Turner, R. D. Camerini-Otero, and C. Höög. 2012. 'Phosphorylation of chromosome core components may serve as axis marks for the status of chromosomal events during mammalian meiosis', *PLoS Genet.*, 8: e1002485.

Funabiki, H., H. Yamano, K. Kumada, K. Nagao, T. Hunt, and M. Yanagida. 1996. 'Cut2 proteolysis required for sister-chromatid seperation in fission yeast', *Nature*, 381: 438-41.

Ghislain, M., R. J. Dohmen, F. Levy, and A. Varshavsky. 1996. 'Cdc48p interacts with Ufd3p, a WD repeat protein required for ubiquitin-mediated proteolysis in Saccharomyces cerevisiae', *EMBO J.*, 15: 4884-99.

Giroux, C. N., M. E. Dresser, and H. F. Tiano. 1989. 'Genetic control of chromosome synapsis in yeast meiosis', *Genome*, 31: 88-94.

Gladstone, M. N., D. Obeso, H. Chuong, and D. S. Dawson. 2009. 'The synaptonemal complex protein Zip1 promotes bi-orientation of centromeres at meiosis I', *PLoS Genet.*, 5: e1000771.

Glotzer, M., A. W. Murray, and M. W. Kirschner. 1991. 'Cyclin is degraded by the ubiquitin pathway', *Nature*, 349: 132-8.

Goldfarb, T., and M. Lichten. 2010. 'Frequent and efficient use of the sister chromatid for DNA double-strand break repair during budding yeast meiosis', *PLoS Biol.*, 8: e1000520.

Haering, C. H., A. M. Farcas, P. Arumugam, J. Metson, and K. Nasmyth. 2008. 'The cohesin ring concatenates sister DNA molecules', *Nature*, 454: 297-301.

Hanson, P. I., and S. W. Whiteheart. 2005. 'AAA+ proteins: have engine, will work', *Nat. Rev. Mol. Cell Biol.*, 6: 519-29.

Hartwell, L. H. 1974. 'Saccharomyces cerevisiae cell cycle', *Bacteriol Rev*, 38: 164-98.

Hartwell, L. H., and T. A. Weinert. 1989. 'Checkpoints: controls that ensure the order of cell cycle events', *Science*, 246: 629-34.

Hassold, T., and P. Hunt. 2001. 'To err (meiotically) is human: the genesis of human aneuploidy', *Nat. Rev. Genet.*, 2: 280-91.

Heldrich, J., X. Sun, L. A. Vale-Silva, T. E. Markowitz, and A. Hochwagen. 2020. 'Topoisomerases Modulate the Timing of Meiotic DNA Breakage and Chromosome Morphogenesis in Saccharomyces cerevisiae', *Genetics*, 215: 59-73.

Henderson, K. A., and S. Keeney. 2004. 'Tying synaptonemal complex initiation to the formation and programmed repair of DNA double-strand breaks', *Proc. Natl. Acad. Sci. U S A*, 101: 4519-24.

Herruzo, E., D. Ontoso, S. González-Arranz, S. Cavero, A. Lechuga, and P. A. San-Segundo. 2016. 'The Pch2 AAA+ ATPase promotes phosphorylation of the Hop1 meiotic checkpoint adaptor in response to synaptonemal complex defects', *Nucleic Acids Res.*, 44: 7722-41.

Herruzo, E., B. Santos, R. Freire, J. A. Carballo, and P. A. San-Segundo. 2019. 'Characterization of Pch2 localization determinants reveals a nucleolar-independent role in the meiotic recombination checkpoint', *Chromosoma*, 128: 297-316.

Ho, H. C., and S. M. Burgess. 2011. 'Pch2 acts through Xrs2 and Tel1/ATM to modulate interhomolog bias and checkpoint function during meiosis', *PLoS Genet*, 7: e1002351.

Hochwagen, A., W. H. Tham, G. A. Brar, and A. Amon. 2005. 'The FK506 binding protein Fpr3 counteracts protein phosphatase 1 to maintain meiotic recombination checkpoint activity', *Cell*, 122: 861-73.

Hollingsworth, N. M., and B. Byers. 1989. *'HOP1*: a yeast meiotic pairing gene', *Genetics*, 121: 445-62.

Hollingsworth, N. M., L. Goetsch, and B. Byers. 1990. 'The *HOP1* gene encodes a meiosis-specific component of yeast chromosomes', *Cell*, 61: 73-84.

Holloway, S. L., M. Glotzer, R. W. King, and A. W. Murray. 1993. 'Anaphase is initiated by proteolysis rather than by the inactivation of maturation-promoting factor', *Cell*, 73: 1393-402.

Horesh, O., G. Simchen, and A. Friedmann. 1979. 'Morphogenesis of the synapton during yeast meiosis', *Chromosoma*, 75: 101-15.

Howell, B. J., B. F. McEwen, J. C. Canman, D. B. Hoffman, E. M. Farrar, C. L. Rieder, and E. D. Salmon. 2001. 'Cytoplasmic dynein/dynactin drives kinetochore protein transport to the spindle poles and has a role in mitotic spindle checkpoint inactivation', *J. Cell Biol.*, 155: 1159-72.

Hughes, S. E., and R. S. Hawley. 2020. 'Alternative Synaptonemal Complex Structures: Too Much of a Good Thing?', *Trends Genet*.

Humphryes, N., W. K. Leung, B. Argunhan, Y. Terentyev, M. Dvorackova, and H. Tsubouchi. 2013. 'The Ecm11-Gmc2 complex promotes synaptonemal complex formation through assembly of transverse filaments in budding yeast', *PLoS Genet.*, 9: e1003194.

Hunter, N., and N. Kleckner. 2001. 'The single-end invasion: an asymmetric intermediate at the double-strand break to double-holliday junction transition of meiotic recombination', *Cell*, 106: 59-70.

Iyer, L. M., D. D. Leipe, E. V. Koonin, and L. Aravind. 2004. 'Evolutionary history and higher order classification of AAA+ ATPases', *J Struct Biol*, 146: 11-31.

Jarosch, E., C. Taxis, C. Volkwein, J. Bordallo, D. Finley, D. H. Wolf, and T. Sommer. 2002. 'Protein dislocation from the ER requires polyubiquitination and the AAA-ATPase Cdc48', *Nat Cell Biol*, 4: 134-9.

Jeggo, P. A., and M. Löbrich. 2007. 'DNA double-strand breaks: their cellular and clinical impact?', *Oncogene*, 26: 7717-9.

Jordan, P., A. Copsey, L. Newnham, E. Kolar, M. Lichten, and E. Hoffmann. 2009. 'Ipl1/Aurora B kinase coordinates synaptonemal complex disassembly with cell cycle progression and crossover formation in budding yeast meiosis', *Genes Dev.*, 23: 2237-51.

Joshi, N., A. Barot, C. Jamison, and G. V. Börner. 2009. 'Pch2 links chromosome axis remodeling at future crossover sites and crossover distribution during yeast meiosis', *PLoS Genet.*, 5: e1000557.

Joshi, N., M. S. Brown, D. K. Bishop, and G. V. Börner. 2015. 'Gradual implementation of the meiotic recombination program via checkpoint pathways controlled by global DSB levels', *Mol. Cell*, 57: 797-811.

Joyce, E. F., and K. S. McKim. 2009. *'Drosophila* PCH2 is required for a pachytene checkpoint that monitors double-strand-break-independent events leading to meiotic crossover formation', *Genetics*, 181: 39-51.

Judis, L., E. R. Chan, S. Schwartz, A. Seftel, and T. Hassold. 2004. 'Meiosis I arrest and azoospermia in an infertile male explained by failure of formation of a component of the synaptonemal complex', *Fertil Steril*, 81: 205-9.

Keeney, S. 2001. 'Mechanism and control of meiotic recombination initiation', *Curr Top Dev Biol*, 52: 1-53.

Keeney, S., C. N. Giroux, and N. Kleckner. 1997. 'Meiosis-specific DNA double-strand breaks are catalyzed by Spo11, a member of a widely conserved protein family', *Cell*, 88: 375-84.

Keeney, S., and N. Kleckner. 1995. 'Covalent protein-DNA complexes at the 5' strand termini of meiosis-specific double-strand breaks in yeast', *Proc. Natl. Acad. Sci. U S A*, 92: 11274-8.

Kim, D. H., J. S. Han, P. Ly, Q. Ye, M. A. McMahon, K. Myung, K. D. Corbett, and D. W. Cleveland. 2018. 'TRIP13 and APC15 drive mitotic exit by turnover of interphase- and unattached kinetochore-produced MCC', *Nat Commun*, 9: 4354.

Kleckner, N. 1996. 'Meiosis: how could it work?', *Proc. Natl. Acad. Sci. U S A*, 93: 8167-74.

Klein, F., P. Mahr, M. Galova, S. B. Buonomo, C. Michaelis, K. Nairz, and K. Nasmyth. 1999. 'A central role for cohesins in sister chromatid cohesion, formation of axial elements, and recombination during yeast meiosis', *Cell*, 98: 91-103.

Kniewel, R., H. Murakami, Y. Liu, M. Ito, K. Ohta, N. M. Hollingsworth, and S. Keeney. 2017. 'Histone H3 Threonine 11 Phosphorylation Is Catalyzed Directly by the Meiosis-Specific Kinase Mek1 and Provides a Molecular Readout of Mek1 Activity in Vivo', *Genetics*, 207: 1313-33.

Knop, M., K. Siegers, G. Pereira, W. Zachariae, B. Winsor, K. Nasmyth, and E. Schiebel. 1999. 'Epitope tagging of yeast genes using a PCR-based strategy: more tags and improved practical routines', *Yeast*, 15: 963-72.

Kundu, S. C., and P. B. Moens. 1982. 'The ultrastructural meiotic phenotype of the radiation sensitive mutant rad 6-1 in yeast', *Chromosoma*, 87: 125-32.

Lao, J. P., V. Cloud, C. C. Huang, J. Grubb, D. Thacker, C. Y. Lee, M. E. Dresser, N. Hunter, and D. K. Bishop. 2013. 'Meiotic crossover control by concerted action of Rad51-Dmc1 in homolog template bias and robust homeostatic regulation', *PLoS Genet.*, 9: e1003978.

Lao, J. P., and N. Hunter. 2010. 'Trying to avoid your sister', *PLoS Biol*, 8: e1000519.

Lara-Gonzalez, P., F. G. Westhorpe, and S. S. Taylor. 2012. 'The spindle assembly checkpoint', *Curr. Biol.*, 22: R966-80.

Lee, J. Y., J. B. Steinfeld, Z. Qi, Y. Kwon, P. Sung, and E. C. Greene. 2017. 'Sequence imperfections and base triplet recognition by the Rad51/RecA family of recombinases', *J Biol. Chem.*, 292: 11125-35.

Lee, J. Y., T. Terakawa, Z. Qi, J. B. Steinfeld, S. Redding, Y. Kwon, W. A. Gaines, W. Zhao, P. Sung, and E. C. Greene. 2015. 'DNA RECOMBINATION. Base triplet stepping by the Rad51/RecA family of recombinases', *Science*, 349: 977-81.

Leung, W. K., N. Humphryes, N. Afshar, B. Argunhan, Y. Terentyev, T. Tsubouchi, and H. Tsubouchi. 2015. 'The synaptonemal complex is assembled by a polySUMOylation-driven feedback mechanism in yeast', *J. Cell Biol.*, 211: 785-93.

Li, X. C., and J. C. Schimenti. 2007. 'Mouse pachytene checkpoint 2 (*trip13*) is required for completing meiotic recombination but not synapsis', *PLoS Genet*, 3: e130.

Liu, D., M. Vleugel, C. B. Backer, T. Hori, T. Fukagawa, I. M. Cheeseman, and M. A. Lampson. 2010. 'Regulated targeting of protein phosphatase 1 to the outer kinetochore by KNL1 opposes Aurora B kinase', *J Cell Biol*, 188: 809-20.

Longtine, M. S., A. McKenzie, 3rd, D. J. Demarini, N. G. Shah, A. Wach, A. Brachat, P. Philippsen, and J. R. Pringle. 1998. 'Additional modules for versatile and economical PCR-based gene deletion and modification in Saccharomyces cerevisiae', *Yeast*, 14: 953-61.

Loog, M., and D. O. Morgan. 2005. 'Cyclin specificity in the phosphorylation of cyclin-dependent kinase substrates', *Nature*, 434: 104-8.

Louvion, J. F., B. Havaux-Copf, and D. Picard. 1993. 'Fusion of GAL4-VP16 to a steroid-binding domain provides a tool for gratuitous induction of galactose-responsive genes in yeast', *Gene*, 131: 129-34.

Luo, X., Z. Tang, G. Xia, K. Wassmann, T. Matsumoto, J. Rizo, and H. Yu. 2004. 'The Mad2 spindle checkpoint protein has two distinct natively folded states', *Nat. Struct. Mol. Biol.*, 11: 338-45.

Ma, H. T., and R. Y. C. Poon. 2016. 'TRIP13 Regulates Both the Activation and Inactivation of the Spindle-Assembly Checkpoint', *Cell Rep.*, 14: 1086-99.

Ma, H. T., and R. Y. C. Poon. 2018. 'TRIP13 Functions in the Establishment of the Spindle Assembly Checkpoint by Replenishing O-MAD2', *Cell Rep.*, 22: 1439-50.

MacQueen, A. J., M. P. Colaiácovo, K. McDonald, and A. M. Villeneuve. 2002. 'Synapsis-dependent and -independent mechanisms stabilize homolog pairing during meiotic prophase in *C. elegans'*, *Genes Dev.*, 16: 2428-42.

Macqueen, A. J., and G. S. Roeder. 2009. 'Fpr3 and Zip3 ensure that initiation of meiotic recombination precedes chromosome synapsis in budding yeast', *Curr. Biol.*, 19: 1519-26.

Mapelli, M., and A. Musacchio. 2007. 'MAD contortions: conformational dimerization boosts spindle checkpoint signaling', *Curr Opin Struct Biol*, 17: 716-25.

Markowitz, T. E., D. Suarez, H. G. Blitzblau, N. J. Patel, A. L. Markhard, A. J. MacQueen, and A. Hochwagen. 2017. 'Reduced dosage of the chromosome axis factor Red1 selectively disrupts the meiotic recombination checkpoint in Saccharomyces cerevisiae', *PLoS Genet.*, 13: e1006928.

Marks, D. H., R. Thomas, Y. Chin, R. Shah, C. Khoo, and R. Benezra. 2017. 'Mad2 Overexpression Uncovers a Critical Role for TRIP13 in Mitotic Exit', *Cell Rep*, 19: 1832-45.

McKee, A. H., and N. Kleckner. 1997. 'A general method for identifying recessive diploid-specific mutations in Saccharomyces cerevisiae, its application to the

isolation of mutants blocked at intermediate stages of meiotic prophase and characterization of a new gene SAE2', *Genetics*, 146: 797-816.

McKim, K. S., B. L. Green-Marroquin, J. J. Sekelsky, G. Chin, C. Steinberg, R. Khodosh, and R. S. Hawley. 1998. 'Meiotic synapsis in the absence of recombination', *Science*, 279: 876-8.

Meadows, J. C., L. A. Shepperd, V. Vanoosthuyse, T. C. Lancaster, A. M. Sochaj, G. J. Buttrick, K. G. Hardwick, and J. B. Millar. 2011. 'Spindle checkpoint silencing requires association of PP1 to both Spc7 and kinesin-8 motors', *Dev. Cell*, 20: 739-50.

Meyer, H., and C. C. Weihl. 2014. 'The VCP/p97 system at a glance: connecting cellular function to disease pathogenesis', *J Cell Sci*, 127: 3877-83.

Mitra, N., and G. S. Roeder. 2007. 'A novel nonnull *ZIP1* allele triggers meiotic arrest with synapsed chromosomes in Saccharomyces cerevisiae', *Genetics*, 176: 773-87.

Miyamoto, T., S. Hasuike, L. Yogev, M. R. Maduro, M. Ishikawa, H. Westphal, and D. J. Lamb. 2003. 'Azoospermia in patients heterozygous for a mutation in SYCP3', *Lancet*, 362: 1714-9.

Morgan, David. 2012. *The cell cycle principles of control* (Oxford University Press: Oxford).

Moses, M. J. 1969. 'Structure and function of the synaptonemal complex', *Genetics*, 61: Suppl:41-51.

Mullally, J. E., T. Chernova, and K. D. Wilkinson. 2006. 'Doa1 is a Cdc48 adapter that possesses a novel ubiquitin binding domain', *Mol. Cell Biol.*, 26: 822-30.

Musacchio, A. 2015. 'The Molecular Biology of Spindle Assembly Checkpoint Signaling Dynamics', *Curr. Biol.*, 25: R1002-18.

Musacchio, A., and A. Ciliberto. 2012. 'The spindle-assembly checkpoint and the beauty of self-destruction', *Nat. Struct. Mol. Biol.*, 19: 1059-61.

Musacchio, A., and E. D. Salmon. 2007. 'The spindle-assembly checkpoint in space and time', *Nat. Rev. Mol. Cell Biol.*, 8: 379-93.

Neale, M. J., and S. Keeney. 2006. 'Clarifying the mechanics of DNA strand exchange in meiotic recombination', *Nature*, 442: 153-8.

Nelson, C. R., T. Hwang, P. H. Chen, and N. Bhalla. 2015. 'TRIP13PCH-2 promotes Mad2 localization to unattached kinetochores in the spindle checkpoint response', *J Cell Biol*, 211: 503-16.

Nishikori, S., M. Esaki, K. Yamanaka, S. Sugimoto, and T. Ogura. 2011. 'Positive cooperativity of the p97 AAA ATPase is critical for essential functions', *J Biol Chem*, 286: 15815-20.

Niu, H., X. Li, E. Job, C. Park, D. Moazed, S. P. Gygi, and N. M. Hollingsworth. 2007. 'Mek1 kinase is regulated to suppress double-strand break repair between sister chromatids during budding yeast meiosis', *Mol Cell Biol*, 27: 5456-67.

Niu, H., L. Wan, B. Baumgartner, D. Schaefer, J. Loidl, and N. M. Hollingsworth. 2005. 'Partner choice during meiosis is regulated by Hop1-promoted dimerization of Mek1', *Mol Biol Cell*, 16: 5804-18.

Niu, H., L. Wan, V. Busygina, Y. Kwon, J. A. Allen, X. Li, R. C. Kunz, K. Kubota, B. Wang, P. Sung, K. M. Shokat, S. P. Gygi, and N. M. Hollingsworth. 2009. 'Regulation of meiotic recombination via Mek1-mediated Rad54 phosphorylation', *Mol Cell*, 36: 393-404.

Norbury, C., and P. Nurse. 1992. 'Animal cell cycles and their control', *Annu Rev Biochem*, 61: 441-70.

Ogura, T., S. W. Whiteheart, and A. J. Wilkinson. 2004. 'Conserved arginine residues implicated in ATP hydrolysis, nucleotide-sensing, and inter-subunit interactions in AAA and AAA+ ATPases', *J Struct Biol*, 146: 106-12.

Page, S. L., and R. S. Hawley. 2004. 'The genetics and molecular biology of the synaptonemal complex', *Annu Rev Cell Dev Biol*, 20: 525-58.

Page, Scott L., and R. Scott Hawley. 2003. 'Chromosome Choreography: The Meiotic Ballet', *Science*, 301: 785-89.

Panizza, S., M. A. Mendoza, M. Berlinger, L. Huang, A. Nicolas, K. Shirahige, and F. Klein. 2011. 'Spo11-accessory proteins link double-strand break sites to the chromosome axis in early meiotic recombination', *Cell*, 146: 372-83.

Penedos, A., A. L. Johnson, E. Strong, A. S. Goldman, J. A. Carballo, and R. S. Cha. 2015. 'Essential and Checkpoint Functions of Budding Yeast *ATM* and *ATR* during Meiotic Prophase Are Facilitated by Differential Phosphorylation of a Meiotic Adaptor Protein, Hop1', *PLoS One*, 10: e0134297.

Prieler, S., A. Penkner, V. Borde, and F. Klein. 2005. 'The control of Spo11's interaction with meiotic recombination hotspots', *Genes Dev*, 19: 255-69.

Prinz, S., A. Amon, and F. Klein. 1997. 'Isolation of *COM1*, a new gene required to complete meiotic double-strand break-induced recombination in Saccharomyces cerevisiae', *Genetics*, 146: 781-95.

Rieder, C. L., R. W. Cole, A. Khodjakov, and G. Sluder. 1995. 'The checkpoint delaying anaphase in response to chromosome monoorientation is mediated by an inhibitory signal produced by unattached kinetochores', *J Cell Biol*, 130: 941-8.

Rockmill, B., and G. S. Roeder. 1990. 'Meiosis in asynaptic yeast', *Genetics*, 126: 563-74.

Rockmill, B., M. Sym, H. Scherthan, and G. S. Roeder. 1995. 'Roles for two RecA homologs in promoting meiotic chromosome synapsis', *Genes Dev*, 9: 2684-95.

Roig, I., J. A. Dowdle, A. Toth, D. G. de Rooij, M. Jasin, and S. Keeney. 2010. 'Mouse TRIP13/PCH2 is required for recombination and normal higher-order chromosome structure during meiosis', *PLoS Genet*, 6.

Romanienko, P. J., and R. D. Camerini-Otero. 2000. 'The mouse Spo11 gene is required for meiotic chromosome synapsis', *Mol Cell*, 6: 975-87.

Rosenberg, J. S., F. R. Cross, and H. Funabiki. 2011. 'KNL1/Spc105 recruits PP1 to silence the spindle assembly checkpoint', *Curr Biol*, 21: 942-7.

Rosenberg, S. C., and K. D. Corbett. 2015. 'The multifaceted roles of the HORMA domain in cellular signaling', *J Cell Biol*, 211: 745-55.

Sale, J. E. 2013. 'Translesion DNA synthesis and mutagenesis in eukaryotes', *Cold Spring Harb Perspect Biol*, 5: a012708.

San Filippo, J., P. Sung, and H. Klein. 2008. 'Mechanism of eukaryotic homologous recombination', *Annu Rev Biochem*, 77: 229-57.

San-Segundo, P. A., and G. S. Roeder. 1999. 'Pch2 links chromatin silencing to meiotic checkpoint control', *Cell*, 97: 313-24.

San-Segundo, P. A., and G. S. Roeder. 2000. 'Role for the silencing protein Dot1 in meiotic checkpoint control', *Mol Biol Cell*, 11: 3601-15.

Schwacha, A., and N. Kleckner. 1995. 'Identification of double Holliday junctions as intermediates in meiotic recombination', *Cell*, 83: 783-91.

Shinohara, A., S. Gasior, T. Ogawa, N. Kleckner, and D. K. Bishop. 1997. 'Saccharomyces cerevisiae recA homologues RAD51 and DMC1 have both distinct and overlapping roles in meiotic recombination', *Genes Cells*, 2: 615-29.

Shinohara, M., K. Hayashihara, J. T. Grubb, D. K. Bishop, and A. Shinohara. 2015. 'DNA damage response clamp 9-1-1 promotes assembly of ZMM proteins for formation of crossovers and synaptonemal complex', *J Cell Sci*, 128: 1494-506.

Shiotani, B., and L. Zou. 2009. 'Single-stranded DNA orchestrates an ATM-to-ATR switch at DNA breaks', *Mol Cell*, 33: 547-58.

Simchen, G., Y. Kassir, O. Horesh-Cabilly, and A. Friedmann. 1981. 'Elevated recombination and pairing structures during meiotic arrest in yeast of the nuclear division mutant cdc5', *Mol Gen Genet*, 184: 46-51.

Sironi, L., M. Mapelli, S. Knapp, A. De Antoni, K. T. Jeang, and A. Musacchio. 2002. 'Crystal structure of the tetrameric Mad1-Mad2 core complex: implications of a 'safety belt' binding mechanism for the spindle checkpoint', *EMBO J*, 21: 2496-506.

Sironi, L., M. Melixetian, M. Faretta, E. Prosperini, K. Helin, and A. Musacchio. 2001. 'Mad2 binding to Mad1 and Cdc20, rather than oligomerization, is required for the spindle checkpoint', *EMBO J*, 20: 6371-82.

Smith, A. V., and G. S. Roeder. 1997. 'The yeast Red1 protein localizes to the cores of meiotic chromosomes', *J Cell Biol*, 136: 957-67.

Sourirajan, A., and M. Lichten. 2008. 'Polo-like kinase Cdc5 drives exit from pachytene during budding yeast meiosis', *Genes Dev*, 22: 2627-32.

Storlazzi, A., L. Xu, L. Cao, and N. Kleckner. 1995. 'Crossover and noncrossover recombination during meiosis: timing and pathway relationships', *Proc Natl Acad Sci U S A*, 92: 8512-6.

Strathern, Jeffrey N., Elizabeth W. Jones, and James R. Broach. 1982. *The molecular biology of the yeast Saccharomyces* (Cold Spring Harbor Laboratory: Cold Spring Harbor, N.Y.).

Subramanian, V. V., and A. Hochwagen. 2014. 'The meiotic checkpoint network: step-by-step through meiotic prophase', *Cold Spring Harb Perspect Biol*, 6: a016675.

Subramanian, V. V., A. J. MacQueen, G. Vader, M. Shinohara, A. Sanchez, V. Borde, A. Shinohara, and A. Hochwagen. 2016. 'Chromosome Synapsis Alleviates Mek1-Dependent Suppression of Meiotic DNA Repair', *PLoS Biol*, 14: e1002369.

Sun, H., D. Treco, N. P. Schultes, and J. W. Szostak. 1989. 'Double-strand breaks at an initiation site for meiotic gene conversion', *Nature*, 338: 87-90.

Sym, M., J. A. Engebrecht, and G. S. Roeder. 1993. 'ZIP1 is a synaptonemal complex protein required for meiotic chromosome synapsis', *Cell*, 72: 365-78.

Sym, M., and G. S. Roeder. 1995. 'Zip1-induced changes in synaptonemal complex structure and polycomplex assembly', *J Cell Biol*, 128: 455-66.

Szostak, J. W., T. L. Orr-Weaver, R. J. Rothstein, and F. W. Stahl. 1983. 'The double-strand-break repair model for recombination', *Cell*, 33: 25-35.

Thacker, D., N. Mohibullah, X. Zhu, and S. Keeney. 2014. 'Homologue engagement controls meiotic DNA break number and distribution', *Nature*, 510: 241-6.

Tipton, A. R., K. Wang, P. Oladimeji, S. Sufi, Z. Gu, and S. T. Liu. 2012. 'Identification of novel mitosis regulators through data mining with human centromere/kinetochore proteins as group queries', *BMC Cell Biol*, 13: 15.

Tromer, E. C., J. J. E. van Hooff, Gjpl Kops, and B. Snel. 2019. 'Mosaic origin of the eukaryotic kinetochore', *Proc Natl Acad Sci U S A*, 116: 12873-82.

Tsubouchi, H., and G. S. Roeder. 2002. 'The Mnd1 protein forms a complex with hop2 to promote homologous chromosome pairing and meiotic double-strand break repair', *Mol Cell Biol*, 22: 3078-88.

Tsubouchi, H., and G. S. Roeder. 2006. 'Budding yeast Hed1 down-regulates the mitotic recombination machinery when meiotic recombination is impaired', *Genes Dev*, 20: 1766-75.

Tsubouchi, T., and G. S. Roeder. 2005. 'A synaptonemal complex protein promotes homology-independent centromere coupling', *Science*, 308: 870-3.

Tucker, P. A., and L. Sallai. 2007. 'The AAA+ superfamily--a myriad of motions', *Curr Opin Struct Biol*, 17: 641-52.

Tung, K. S., E. J. Hong, and G. S. Roeder. 2000. 'The pachytene checkpoint prevents accumulation and phosphorylation of the meiosis-specific transcription factor Ndt80', *Proc Natl Acad Sci U S A*, 97: 12187-92.

Uhlmann, F., F. Lottspeich, and K. Nasmyth. 1999. 'Sister-chromatid separation at anaphase onset is promoted by cleavage of the cohesin subunit Scc1', *Nature*, 400: 37-42.

Uhlmann, F., and K. Nasmyth. 1998. 'Cohesion between sister chromatids must be established during DNA replication', *Curr Biol*, 8: 1095-101.

Uhlmann, F., D. Wernic, M. A. Poupart, E. V. Koonin, and K. Nasmyth. 2000. 'Cleavage of cohesin by the CD clan protease separin triggers anaphase in yeast', *Cell*, 103: 375-86.

Vader, G. 2015. 'Pch2(TRIP13): controlling cell division through regulation of HORMA domains', *Chromosoma*, 124: 333-9.

Vader, G., H. G. Blitzblau, M. A. Tame, J. E. Falk, L. Curtin, and A. Hochwagen. 2011. 'Protection of repetitive DNA borders from self-induced meiotic instability', *Nature*, 477: 115-9.

van Hooff, J. J., E. Tromer, L. M. van Wijk, B. Snel, and G. J. Kops. 2017. 'Evolutionary dynamics of the kinetochore network in eukaryotes as revealed by comparative genomics', *EMBO Rep*, 18: 1559-71.

Varetti, G., C. Guida, S. Santaguida, E. Chiroli, and A. Musacchio. 2011. 'Homeostatic control of mitotic arrest', *Mol Cell*, 44: 710-20.

Vazquez, J., A. S. Belmont, and J. W. Sedat. 2002. 'The dynamics of homologous chromosome pairing during male Drosophila meiosis', *Curr Biol*, 12: 1473-83.

Villar-Fernández, M. A., R. Cardoso da Silva, M. Firlej, D. Pan, E. Weir, A. Sarembe, V. B. Raina, T. Bange, J. R. Weir, and G. Vader. 2020. 'Biochemical and functional characterization of a meiosis-specific Pch2/ORC AAA+ assembly', *Life Sci Alliance*, 3.

Voelkel-Meiman, K., S. Y. Cheng, M. Parziale, S. J. Morehouse, A. Feil, O. R. Davies, A. de Muyt, V. Borde, and A. J. MacQueen. 2019. 'Crossover recombination and synapsis are linked by adjacent regions within the N terminus of the Zip1 synaptonemal complex protein', *PLoS Genet*, 15: e1008201.

Voelkel-Meiman, K., S. S. Moustafa, P. Lefrançois, A. M. Villeneuve, and A. J. MacQueen. 2012. 'Full-length synaptonemal complex grows continuously during meiotic prophase in budding yeast', *PLoS Genet*, 8: e1002993.

Wang, J., J. J. Song, M. C. Franklin, S. Kamtekar, Y. J. Im, S. H. Rho, I. S. Seong, C. S. Lee, C. H. Chung, and S. H. Eom. 2001. 'Crystal structures of the HslVU peptidase-ATPase complex reveal an ATP-dependent proteolysis mechanism', *Structure*, 9: 177-84.

Wang, K., B. Sturt-Gillespie, J. C. Hittle, D. Macdonald, G. K. Chan, T. J. Yen, and S. T. Liu. 2019. 'Correction: Thyroid hormone receptor interacting protein 13 (TRIP13) AAA-ATPase is a novel mitotic checkpoint-silencing protein', *J Biol Chem*, 294: 10019.

Weibezahn, J., C. Schlieker, B. Bukau, and A. Mogk. 2003. 'Characterization of a trap mutant of the AAA+ chaperone ClpB', *J Biol Chem*, 278: 32608-17.

West, A. M. V., E. A. Komives, and K. D. Corbett. 2018. 'Conformational dynamics of the Hop1 HORMA domain reveal a common mechanism with the spindle checkpoint protein Mad2', *Nucleic Acids Res*, 46: 279-92.

Westhorpe, F. G., A. Tighe, P. Lara-Gonzalez, and S. S. Taylor. 2011. 'p31comet-mediated extraction of Mad2 from the MCC promotes efficient mitotic exit', *J Cell Sci*, 124: 3905-16.

White, E. J., C. Cowan, W. Z. Cande, and D. B. Kaback. 2004. 'In vivo analysis of synaptonemal complex formation during yeast meiosis', *Genetics*, 167: 51-63.

Wojtasz, L., K. Daniel, I. Roig, E. Bolcun-Filas, H. Xu, V. Boonsanay, C. R. Eckmann, H. J. Cooke, M. Jasin, S. Keeney, M. J. McKay, and A. Toth. 2009. 'Mouse HORMAD1 and HORMAD2, two conserved meiotic chromosomal proteins, are depleted from synapsed chromosome axes with the help of TRIP13 AAA-ATPase', *PLoS Genet*, 5: e1000702.

Wu, H. Y., and S. M. Burgess. 2006. 'Two distinct surveillance mechanisms monitor meiotic chromosome metabolism in budding yeast', *Curr. Biol.*, 16: 2473-9.

Wu, H. Y., H. C. Ho, and S. M. Burgess. 2010. 'Mek1 kinase governs outcomes of meiotic recombination and the checkpoint response', *Curr. Biol.*, 20: 1707-16.

Xu, L., M. Ajimura, R. Padmore, C. Klein, and N. Kleckner. 1995. *'NDT80*, a meiosis-specific gene required for exit from pachytene in Saccharomyces cerevisiae', *Mol. Cell Biol.*, 15: 6572-81.

Xu, L., B. M. Weiner, and N. Kleckner. 1997. 'Meiotic cells monitor the status of the interhomolog recombination complex', *Genes Dev.*, 11: 106-18.

Yamamoto, A., V. Guacci, and D. Koshland. 1996. 'Pds1p, an inhibitor of anaphase in budding yeast, plays a critical role in the APC and checkpoint pathway(s)', *J Cell. Biol.*, 133: 99-110.

Yang, C., B. Hu, S. M. Portheine, P. Chuenban, and A. Schnittger. 2020. 'State changes of the HORMA protein ASY1 are mediated by an interplay between its closure motif and PCH2', *Nucleic Acids. Res*.

Ye, Q., D. H. Kim, I. Dereli, S. C. Rosenberg, G. Hagemann, F. Herzog, A. Tóth, D. W. Cleveland, and K. D. Corbett. 2017. 'The AAA+ ATPase TRIP13 remodels HORMA domains through N-terminal engagement and unfolding', *EMBO J*, 36: 2419-34.

Ye, Q., R. K. Lau, I. T. Mathews, E. A. Birkholz, J. D. Watrous, C. S. Azimi, J. Pogliano, M. Jain, and K. D. Corbett. 2020. 'HORMA Domain Proteins and a Trip13-like ATPase Regulate Bacterial cGAS-like Enzymes to Mediate Bacteriophage Immunity', *Mol. Cell*, 77: 709-22.e7.

Ye, Q., S. C. Rosenberg, A. Moeller, J. A. Speir, T. Y. Su, and K. D. Corbett. 2015. 'TRIP13 is a protein-remodeling AAA+ ATPase that catalyzes MAD2 conformation switching', *Elife*, 4.

Ye, Y., H. H. Meyer, and T. A. Rapoport. 2001. 'The AAA ATPase Cdc48/p97 and its partners transport proteins from the ER into the cytosol', *Nature*, 414: 652-6.

Yost, S., B. de Wolf, S. Hanks, A. Zachariou, C. Marcozzi, M. Clarke, R. de Voer, B. Etemad, E. Uijttewaal, E. Ramsay, H. Wylie, A. Elliott, S. Picton, A. Smith, S. Smithson, S. Seal, E. Ruark, G. Houge, J. Pines, Gjpl Kops, and N. Rahman. 2017. 'Biallelic TRIP13 mutations predispose to Wilms tumor and chromosome missegregation', *Nat Genet*, 49: 1148-51.

Zakharyevich, K., Y. Ma, S. Tang, P. Y. Hwang, S. Boiteux, and N. Hunter. 2010. 'Temporally and biochemically distinct activities of Exo1 during meiosis: double-strand break resection and resolution of double Holliday junctions', *Mol. Cell*, 40: 1001-15.

Zanders, S., M. Sonntag Brown, C. Chen, and E. Alani. 2011. 'Pch2 modulates chromatid partner choice during meiotic double-strand break repair in Saccharomyces cerevisiae', *Genetics*, 188: 511-21.

Zhang, F., Y. Shen, C. Miao, Y. Cao, W. Shi, G. Du, D. Tang, Y. Li, Q. Luo, and Z. Cheng. 2020. '*OsRAD51D* promotes homologous pairing and recombination by preventing nonhomologous interactions in rice meiosis', *New. Phytol.*, 227: 824-39.

Zickler, D., and N. Kleckner. 2015. 'Recombination, Pairing, and Synapsis of Homologs during Meiosis', *Cold Spring Harb. Perspect. Biol.*, 7.

Zou, L., and S. J. Elledge. 2003. 'Sensing DNA damage through ATRIP recognition of RPA-ssDNA complexes', *Science*, 300: 1542-8.

Acknowledgements

Anyone who has met me even once knows of my (unhealthy) love for Rafael Nadal and I truly believe that Nadal would not have been what he is today without his coach Toni there to guide him. In this case, I am a little luckier than Nadal as I have had the support and guidance of so many people without whom I could not have completed this journey.

First and foremost, I would like to thank Dr. Gerben Vader for countless scientific discussions which have helped me further develop my scientific rationale. That's not to say we only discussed science. We had many conservations revolving around football, which helped me take my mind off of work whenever an experiment bombed (which happened way more times than I like to admit). Thanks for the open door to your office and for taking such an active interest in my future. I am also thankful to you for your help with Southern blot experiments. I extend my heartfelt thanks to Prof. Andrea Musacchio and Prof. Roger Goody for their support during the course of my PhD. Their support helped me turn the tide and overcome the difficulties in my project. During my PhD, I had the opportunity to mentor two fantastic Masters students: Inga Herfort and Richard Kosinski. I am thankful to both of them for their help with the experiments. I am immensely grateful to Christa Hornemann for her support during my stay at MPI and for helping me overcome bureaucratic difficulties.

I am indebted to all the past and present members of the Bird-Vader labs who made it an incredibly friendly and welcoming place. It is because of the atmosphere created by people of both the labs that I always enjoyed being in lab. I met some incredible people in these labs. Thank you, Divya for numerous lengthy discussions on experimental design and for being a rock-solid support. I know that somewhere deep within your heart you too believe that Nadal is a better player than Djokovic (don't deny it, we both saw it during the French Open). I want to thank Richie for always being open to discussing my weird hypotheses; Arnaud for always wanting to see the glass as half full; Hendrik for always trying to improve my music choices. Richie, Arnaud and Henrik- my PhD would have been the same if there were no Schocken sessions with you three. I will always cherish our drinking sessions at GänseMarkt, followed by intense political and moral discussions at Richie's place. Next, I would like to thank

Lisa and María for always cheering me up whenever my dissected plate got contaminated or when the cells decided not to sporulate, and for letting me steal your buffers. I hope one day we can start a company with a *spo*-perfume.

I am also thankful to all the present and past members of our department especially Giuseppe, Marion, Valentina, Nadine, Pim, Harish, Stefano, Lisa Mazul, Satya, Caro, Franzi, and Isabelle for creating a helpful and jovial atmosphere. It has been a fantastic time.

I am thankful to all my wonderful friends who provided me with gentle and not-so-gentle reminders that there is life outside my PhD. A huge shout out to all my people: Sumer and Kalyani for being the closest thing that I had to a family here; Amit for taking care of me like an elder brother; Amal for never saying no to a round of beer (unless his girlfriend was in town); Suruchi for being there for all the milestones and for always celebrating small achievements; Devika and Sara for much needed coffee breaks and lunch trips to Mensa; Pragya for being the only one who could understand my joy when I made *roganjosh*; Shweta for her sound advice when I needed it; Prachi for sending me small things every now and then, your insane laughter never failed to brighten up my day.

I would also like to take an opportunity to extend my gratitude to all my mentors Sonu Handoo, Shri Ratan Lal Bhat, Late Aman Thakur and Dr. Mahak Sharma. Thank you for laying the foundation for my love for science.

Finally, I would like to thank my family for their continuing support and love. Thank you, Jija and Daddy for believing in me even when I didn't. Also, thank you for always reminding me that success in career can come and go, but life is so much more than that. Thank you Bhaaji and Bhabhi for forever making me feel like the spoilt younger brother. Thank you Praful for giving me an engineer's perspective on basic sciences; from terrace cricket to where we are today, we have come a long way! Thank you to my in-laws, Mumma and Pitaji for their continued support. Last but not the least, thanks to my awesome wife Ananya Rastogi (she hijacked the acknowledgement and added awesome here), who never fails to remind me that she is the first PhD in the family. Thank you for always standing by me.